

**FROM A GARNET INCLUSION TO THE VARISCAN EVOLUTION:
IMPLICATIONS FOR THE POLYMETAMORPHIC HISTORY OF THE
BOHEMIAN MASSIF**

Sorger, D.^{1,2}, Hauzenberger, C.A.¹, Finger, F.³, Linner, M.⁴, Fritz, H.⁵, Sizova, E.¹,
Skrzypek, E.¹, Iglseder, C.⁴, Schorn, S.¹

¹NAWI Graz Geocenter, University of Graz, Universitätsplatz 2, 8010 Graz, Austria

²Present address: Geoscience Center, Georg-August-University Göttingen, Goldschmidtstraße 1, 37077
Göttingen, Germany

³Department of Geography and Geology, University of Salzburg, Hellbrunnerstraße 34, 5020 Salzburg, Austria

⁴Department of Hard Rock Geology, Geological Survey of Austria, Neulinggasse 38, 1030 Vienna, Austria

⁵NAWI Graz Geocenter, University of Graz, Heinrichstraße 26, 8010 Graz, Austria

e-mail: dominik.sorger@uni-goettingen.de

The Central European Variscan orogen consists of a mosaic of various peri-Gondwana terranes, which separated from Gondwana at various times during the Cambrian to Devonian. Later, during the Devonian-Carboniferous they were between the converging continents of Gondwana and Laurussia as the Rheic ocean closed. While the major part of the Bohemian Massif belongs to the so-called Armorican terrane, some eastern parts are assigned to the Avalonian terrane, which amalgamated with the southern margin of Laurussia in the Silurian. The major phase of the regional metamorphism affected the rocks of the Bohemian Massif in the Visean at ~340 Ma and is thought to correspond to the final collision of Avalonia/Laurussia and Armorica/Gondwana (FINGER & STEYRER, 1995; KRONER & ROMER, 2013). Evidence of this predominant metamorphism is typically observed in the Bohemian Massif, while some rocks have remnants of an older metamorphism and/or were affected by a younger metamorphic overprint. The investigated part of the Bohemian Massif can be assigned to the high-grade Moldanubian zone, which is traditionally assigned to the Armorican terrane and is subdivided into several tectonostratigraphic subunits that were juxtaposed into their present relative positions during the Variscan orogeny. The high-grade Gföhl unit overlies both, the Drosendorf and Ostrong units. Although the Drosendorf unit was traditionally assigned to be part of the Armorican terrane, a detrital zircon study revealed zircon ages at ~1.2 Ga, ~1.5 Ga and ~1.8 Ga, which confirms an Avalonian affinity of the Drosendorf unit (SORGER et al., 2020). The youngest detrital zircon generation suggests a Neoproterozoic deposition age of the precursor siliciclastic sediment. These findings are in good agreement with recent zircon studies of orthogneisses from the Drosendorf unit (LINDNER et al., 2020). The area in the south-western part of the Moldanubian zone, which is characterized by a low-pressure–high-temperature (LP–HT) metamorphism associated with granitic plutonism, is referred to as the Bavarian unit. Polyphase garnet growth, remnant mineral inclusions and textural relations in samples from three prominent localities located in the Austrian part of the Bohemian Massif allowed us to decipher three different Variscan metamorphic events: an early Variscan event in the Devonian (event1, ~370 Ma), the predominant metamorphism in the Visean (event2, ~340 Ma), both with collisional P–T characteristics and a Pennsylvanian LP–HT overprint (event3, ~315 Ma). The Devonian event1 can be observed in metapelitic paragneiss from the southern Drosendorf unit, which exhibit two chemically and texturally different garnet generations that provide

evidence of a polymetamorphic evolution. Both garnet generations carry abundant inclusions, the most important are monazite, rutile, kyanite, staurolite (limited to the second garnet generation) and crystallized melt droplets. The latter is indicating a peritectic growth of the host garnet in the presence of a melt phase. Thermodynamic modelling combined with various geothermo- and barometers allow the reconstruction of the complex evolution of two garnet-forming metamorphic events (SORGER et al., 2020). The metamorphic conditions for the first stage of garnet growth are estimated with 0.7–0.8 GPa at 680–700 °C and 0.95–1.10 GPa at 745–785 °C (Fig. 1). A Late Devonian age (373 ± 9 Ma) for this first metamorphic event (event1) was obtained from chemical dating of monazite inclusions in grt1. Generally, monazite has Y- and U-rich core domains that were overgrown by Th enriched domains. The latter may contain inclusions of crystallized melt droplets indicating a peritectic growth of monazite contemporaneous with garnet. Additionally, a significantly older monazite generation (654 ± 17 Ma) enriched in U and Y appears as inclusions in grt1 and can be interpreted as inherited grains of a Cadomian metamorphic event.

Subsequent exhumation after event1 placed these rocks in a shallower position. A second garnet (grt2) started growing in the amphibolite facies reaching peak conditions in the granulite facies with 0.95–1.10 GPa at 745–785 °C (Fig. 1), which are similar to those of the first garnet forming event. Subsequently, the rocks experienced a near isothermal decompression to 0.5–0.8 GPa accompanied by sillimanite and ilmenite growth in the matrix. A Visean age (343 ± 3 Ma) of monazite inclusions in grt2 and matrix grains correlates the second garnet forming event with the predominant metamorphism in the Bohemian Massif (event2). Similar ages are known for the metamorphic peak conditions of the rocks from the adjacent Gföhl unit, which includes high-pressure–ultra-high-temperature (HP–UHT) felsic granulite, orthogneiss and paragneiss. Aluminous paragneiss from the Loosdorf complex (south-eastern Gföhl unit), which constitutes the hangingwall part of the large granulite bodies, provide some new insights on the exhumation history of these high-grade rocks at the end of the Visean metamorphic event (event2). The paragneiss commonly show reaction coronas of complementary cordierite moats and cordierite + spinel symplectites located at former garnet-sillimanite interfaces. Garnets and embedded rutile ± kyanite are reliques of the previous peak assemblage and record the metamorphic conditions of 0.8–1.1 GPa and 770–820 °C. The reaction textures formed in the course of a nearly isothermal decompression (ITD) path at LP–HT of ~ 0.5 GPa and ~ 750 °C. The inferred P–T evolution suggests prograde metamorphism reaching granulite facies metamorphism at lower crustal depth of ~ 35 km subsequently followed by the ITD to the upper/middle crustal level (~ 15 km depth). The P–T evolution emphasizes rapid exhumation of the Loosdorf complex at the hangingwall position of the felsic granulite, which was most likely triggered by the exhumation of the HP–UHT granulite itself. Monazite inclusions in garnet and matrix grains yielded a slightly younger age of ~ 335 Ma. Although ages are overlapping within errors they may indicate the age of the retrograde LP–HT overprint during the exhumation subsequently after the metamorphic peak of event2 at ~ 340 Ma.

The Bavarian unit in the south-western part of the Bohemian Massif is characterized by strong, late-Variscan, LP–HT metamorphism. Rare migmatite varieties hosting garnets record detailed information regarding the regional P–T–t evolution. The garnet porphyroblasts preserve complex three-phase growth zoning and variable mineral inclusions indicative of a polymetamorphic history (Sorger et al., 2018). Garnet cores (grt1) and related inclusions yielded a medium-pressure–medium-temperature (MP–MT) metamorphic peak of 0.85–1.10 GPa at 720–780 °C (Fig. 1). Monazite inclusions in grt1 reveals an age of 340 ± 7 Ma indicating that the garnet cores are remnants of the predominant regional metamorphism (event2).

This first metamorphic stage was followed by a stage of decompression and cooling resulting in a partial resorption of grt1. A second prograde metamorphic stage then caused additional garnet growth, starting at 0.45–0.60 GPa at 580–630 °C (grt2 and inclusions) and leading to

LP-HT peak conditions of 0.55–0.65 GPa and 830–900 °C (grt3 and matrix). Monazite inclusion in grt2 yielded an age of 319 ± 6 Ma, matrix monazite and inclusions in grt3 produced an age of 312 ± 5 Ma, which dates the pervasive LP-HT overprint (event3).

Our petrological and geochronological data suggest that Avalonian and Armoricane terranes had already collided in the late Devonian (event1), as proposed by KRONER & ROMER (2013). However, this is important from the viewpoint of global plate tectonics, as it marks the closure of the Rheic ocean. The final architecture of the Variscan orogen was established considerably later following a further strong collisional phase with regional high-grade metamorphism at ~340 Ma (event2). This was most likely a short-lived tectonic event with HT–HP granulite formation and a rapid exhumation thereafter. In the final stage of the Variscan orogeny some parts of the Moldanubian zone (Bavarian unit) were selectively reheated (event3). The isobaric heating to granulite facies conditions at the middle crustal level point to a significant external heat influx into the middle crust at this stage (e.g. mantle delamination).

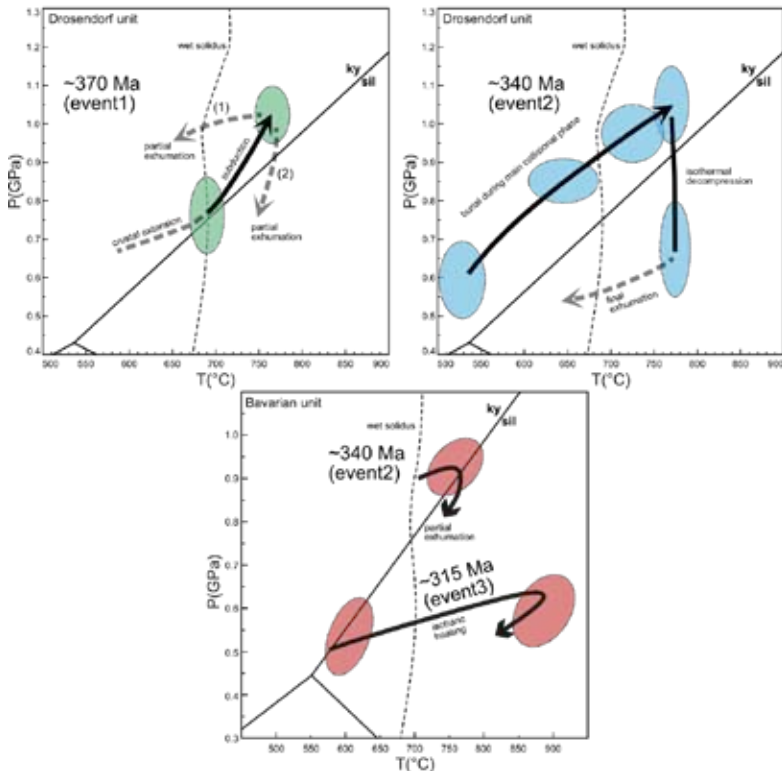


Figure 1: Proposed P–T–t paths for the Late Devonian (event1), the Visean (event2) and the Pennsylvanian (event3) metamorphic events, modified after SORGER et al., 2018, 2020.

FINGER, F., STEYRER, H. P. (1995): Geol. Carpathica, 46, 137–150.

KRONER, U., ROMER, R. L. (2013): Gondwana Res., 24, 298–329.

LINDNER, M., DÖRR, W., REITHER, D., FINGER, F. (2020): Geol. Soc., London, Special Publ., SP503-2019-232.

SORGER, D., HAUZENBERGER, C.A., FINGER, F., LINNÉR, M. (2020): Gondwana Res., 85, 124–148.

SORGER, D., HAUZENBERGER, C.A., LINNÉR, M., IGLSEDER, C., FINGER, F. (2018): J. Petrol., 59, 1359–1382.

CERAMIC INVESTIGATIONS IN THE SYSTEM CaO-Al₂O₃-ZnO

Albertus, M.¹, Kahlenberg, V.¹

¹University of Innsbruck, Institute of Mineralogy and Petrography, Innrain 52, 6020 Innsbruck, Austria
e-mail: max.albertus@studentuibk.ac.at

The ternary system CaO-Al₂O₃-ZnO has been studied since the 1960s with a special focus on the influence of zinc oxide on the properties of the calcium aluminates occurring in Portland cement clinkers (AKATSU et al., 1968). In an investigation by BARBANYAGRE & TIMOSHENKO (1996), single crystals of two different calcium zinc aluminates (Ca₁₄Al₁₀Zn₆O₃₅ and Ca₃Al₄ZnO₁₀, respectively) have been synthesized and their crystal structures and crystallochemical properties have been determined. In recent years, both ternary compounds have seen a revival of interest. After doping with Ti⁴⁺, Ca₁₄Al₁₀Zn₆O₃₅ can be used as an attractive material for phosphor production due to its very good luminescence properties, environmental safety and low-cost components (WU et al., 2019). In addition, the phase offers an extraordinary potential as an optically transparent ceramic material for a wide range of applications. However, previous studies also have shown that one of the major requirements for optical ceramics - sufficient phase purity - has not been achieved yet.

In the course of this investigation, selected synthesis routes aiming on the preparation of phase-pure Ca₁₄Al₁₀Zn₆O₃₅ (C₁₄A₅Z₆) have been evaluated. First, a number of conventional solid-state syntheses were performed using sinter temperatures between 1000 °C and 1250 °C. Qualitative and quantitative phase analyses of the sinter pellets obtained were carried out by means of powder X-ray diffractometry (PXRD). While Ca₁₄Al₁₀Zn₆O₃₅ only occurs in small proportions at temperatures below 1200 °C, sublimation of zinc oxide at higher temperatures results in the formation of zinc-free secondary phases. The highest yield of the target phase (96 wt.-%) could be obtained in the sample fired at 1220 °C (4 x 16 h with intermediate grinding). Furthermore, powder preparations using wet chemical methods based on solution-precipitation as well as sol-gel syntheses were examined. Applying a modified sol-gel process, also known as the Pechini or polymer precursor method, it was possible to obtain a highly reactive amorphous precursor that yielded an almost phase-pure product (98 wt.-%) after a single run of 16 hours at the maximum temperature of 1220 °C. Using this specific precursor, *in-situ* high-temperature PXRD experiments indicate that the sintering temperature can possibly be further reduced to 1150 °C.

AKATSU, K., IKAWA, K., MAEDA, K. (1968): Cem. Assoc. Japan, 22, 40-43.

BARBANYAGRE, V.D., TIMOSHENKO, T.I. (1996): Powder Diff., 12, 22-26.

WU, X., LIU, L., XIA, M., HUANG, S., ZHOE, Y., HU, W., ZHOU, Z., ZHOU, N. (2019): Cer. Internat., 45, 9977-9985.

POLYSTAGE TUNGSTEN MINERALIZATION AT LIENZER SCHLOSSBERG,
EASTERN TYROL, AUSTRIA: EVIDENCE FROM MICRO-TEXTURES AND
LA-ICP-MS ANALYSES OF SCHEELITE

Altenberger, F.¹, Hutter, F.¹, Raith, J. G.¹, Krause, J.², Weibold, J.³, Auer, C.³

¹Montanuniversität Leoben, Chair of Resource Mineralogy, Peter-Tunner-Straße 5, 8700 Leoben Austria

²Helmholtz-Zentrum Dresden-Rossendorf, Helmholtz Institute Freiberg for Resource Technology,

Department of Analytics, Chemnitzer Straße 40, 09599 Freiberg/Saxony, Germany

³Geological Survey of Austria, Department of Mineral Resources, Neulinggasse 38, 1030 Wien, Austria

e-mail: florian.altenberger@unileoben.ac.at

At Lienzer Schlossberg, scheelite mineralization comprises several styles: (1) disseminations in pyrrhotite-dominated massive Fe-Cu sulfide ores, (2) structurally controlled scheelite in a fault zone within altered host rocks, (3) “wallpaper”-like coatings on joints and fractures as well as (4) scheelite in small quartz veinlets. Scheelite has been studied by combining micro-textures visualized by cathodoluminescence (EPMA-CL) with LA-ICP-MS trace element analysis. Mineralization occurs within the contact aureole but also in magmatic rocks of the Oligocene Lienz/Edenwald tonalite intrusion. Host rocks in the contact metamorphic aureole include metapelitic hornfels grading distally into regional metamorphic mica schists and gneisses. Minor marbles, calc-silicate rocks and an up to 3 m thick massive sulfide horizon (FUCHS, 1982) are exposed in abandoned mine workings at Edenwald. Scheelite crystals (Scheelite 1 and 2) were found in the underground workings disseminated in the sulfide layer and in a fault zone associated with strongly altered host rocks. Subsequent stages (Scheelite 3, 4?) are restricted to the tonalitic intrusive rocks. The hypothesis that scheelite mineralization at Lienzer Schlossberg is of magmatic-hydrothermal origin is tested by comparing the scheelite chemistry with geochemical data of the Oligocene tonalite intrusion.

CL revealed internal micro-textures in scheelite which are dominated by oscillatory zoning that reflects fluctuating fluid conditions in hydrothermal systems (POULIN et al., 2018). Continuing hydrothermal activity is indicated by dissolution-replacement and overgrowth textures affecting the primary zonation. The correlation of CL-textures, trace element contents and Eu anomalies ($Eu_A = Eu/Eu^*$) were examined along profiles in scheelite. The distribution of rare earth elements (REE) from Scheelite 1 to 4 comprise convex (i.e., MREE-enriched) fractionation patterns with distinct negative Eu anomalies, which grade into relatively flat REE profiles with variable Eu_A that are replaced by similar flat patterns but lower Σ REE at the outermost rims. In contrast, younger scheelites illustrate a HREE-depleted profile with negative Eu_A .

Scheelite at Lienzer Schlossberg has by far one of the highest Σ REE concentrations in the Eastern Alps but contains minor Mo and the least Sr. High Nb contents and the positive correlation of REE-Eu+Y vs. Nb+Ta suggest that the main exchange vector for REE incorporation in scheelite is via the coupled substitution of $Ca^{2+} + W^{6+} = REE^{3+} + Nb^{5+}$ (GHADERI et al., 1999).

FUCHS, H.W. (1982): Arch. f. Lagerstätt.forsch. Geol. B.-A., 2, 67-70.

GHADERI, M., PALIN, M., CAMPBELL, I.H., SYLVESTER, P.J. (1999): Econ. Geol., 94, 423-438.

POULIN, R.S., KONTAK, D.J., McDONALD, A., McCLENAUGHAN, M.B. (2018): Canad. Mineral., 56, 265-302.

CONTRASTING RARE METAL POTENTIALS IN TWO SOUTHERN ALPINE VEIN DEPOSITS

Angerer, T.¹, Poniewas, T.¹, Profanter, L.¹, Braetz, H.², Tribus, M.¹

¹Institute of Mineralogy and Petrography, University of Innsbruck, Innrain 52, 6020 Innsbruck, Austria

²Geozentrum, Erlangen University, Schlossplatz 4, 91054 Erlangen, Germany

e-mail: thomas.angerer@uibk.ac.at

Investigating rare metal potentials of the Alpine regions is of great importance to progress towards future supply independence. Sphalerite is an important carrier of Co, In, Ga, Ge, and Sb, and we know from the Eastern Alps, that vein deposits roughly host 66 % of the Co, 18 % of the Ga and 4 % of the In resources (MELCHER & ONUK, 2019). Here, we present data of sphalerite (and chalcopyrite) from two contrasting vein deposits in the Southern Alpine basement: the Pfunderer Berg Cu-Zn-Pb-Ag mine near Klausen and the Rabenstein F-Zn mine in the Sarn Valley. Both abandoned mines used to be important pre-industrial, and to some extent post-industrial metal or fluor suppliers.

The Pfunderer Berg mine is a Permian intrusion-hosted vein deposit with a chalcopyrite-sphalerite-galena-sulphosalt paragenesis (KRISMER et al., 2011). The Rabenstein mine is a vein deposit with fluorite-sphalerite paragenesis, probably related to the Periadriatic fault (HEIN et al., 1990).

The two ores show contrasting textures and chemistry of sphalerite, which are primarily related to formation temperature: at Pfunderer Berg high-T ZnS is black and homogeneous and enriched in Fe-Mn-Cd-Cu-Se-Co-In-Sn, while at Rabenstein low-T ZnS is honey-coloured and zoned and enriched in Pb-As-Ag-Sb-Hg-Tl-Ga-Ge. Rare metal medians at Pfunderer Berg are 303, 124, and 187 µg/g for Co, In, and Sn. At Rabenstein medians for Ga, Sb, Ag, and Ge are 383, 203, 85, and 9.1 µg/g. Spot analyses can reach higher values, either related to mineral inclusions (Pfunderer Berg) or to zoning (Rabenstein). Across zoned ZnS grains, co-variations with Fe-content (0.3 to 6 wt.%) or Cu (70 to 5000 µg/g) are related to an evolving hydrothermal pulse. Results demonstrate significant rare metal variations across deposit types, but also complexities of fractionation within given deposits.

HEIN, U., LÜDERS, V., DULSKI, P. (1990): Mineral. Mag., 54, 325-333.

KRISMER, M., VAVTAR, F., TROPPER, P., SARTORY, B., KAINDL, R. (2011): Austr. J. Earth Sci., 104, 36-48.

MELCHER, F., ONUK, P. (2019): BHM Berg- und Hüttenmännische Mh., 164, 71-76.

**CONSTRAINING TIME SCALES OF THE DECOMPRESSION OF
MANTLE ROCKS FROM SECONDARY CHEMICAL ZONING OF GARNET
FROM THE GFÖHL-UNIT, MOLDANUBIAN ZONE**

Asenbaum, R.¹, Racek, M.², Petrishcheva, E.¹, Abart, R.¹

¹Department of Lithospheric Research, University of Vienna, Althanstraße 14, 1090 Vienna, Austria

²Charles University, Praha, Institute of Petrology and Structural Geology,

Albertov 6, 128 43 Praha 2, Czech Republic

e-mail: rene.asenbaum@gmx.at

Up to 100 m sized mafic-ultramafic lenses, considered as mantle fragments, are embedded in felsic granulites of the Gföhl unit, Moldanubian zone, which were incorporated into mid-crustal rocks during the Variscan orogeny. We investigated a garnet-pyroxenite occurrence pertaining to these lenses. The primary mineral assemblage comprises Ca-rich garnet ($X_{\text{Grs}} = 0.4$), kyanite, and Al-rich clinopyroxene ($X_{\text{CaTs}} = 0.23$), indicating pressures of about 1.9 GPa and temperatures of 1100 °C. Towards the margins of the mafic lens, destabilization of these primary mineral assemblages during overprint at lower pressure conditions of about 1.0 GPa is evident. A first decompression phase is represented by sapphirine-spinel-plagioclase symplectites, which presumably replace kyanite and clinopyroxene. A second phase is evident from the partial resorption of garnet by plagioclase and clinopyroxene in the form of "corrosion tubes" that penetrate the garnet in a worm-like fashion. At pressures of about 0.8 GPa and temperatures of about 800 °C, the garnet was partially replaced by plagioclase-orthopyroxene-spinel symplectites at the rim. Along with this, garnet shows a pronounced secondary compositional zoning towards the decompression products. For the sapphirine-spinel-plagioclase symplectites and the plagioclase-clinopyroxene corrosion tubes, the secondary zoning is characterized by a decrease in the Ca content and a simultaneous increase in the Mg and Fe content. Secondary zoning toward the plagioclase-orthopyroxene spinel symplectites shows an increase in the Fe content and a simultaneous decrease in the Mg content with constant Ca content. By fitting a multicomponent diffusion model to the secondary zoning patterns, time scales for the duration of decompression were estimated. These vary, depending on the choice of experimental calibrations of the diffusion coefficients, from a few 1000 to several 100,000 years. Here, the early decompression reactions show the longest time scales of several 100,000 years and are up to five times longer than those obtained from the corrosion tubes and about ten times longer than the late plagioclase-orthopyroxene spinel symplectites. These time scales reflect the duration of the process from the beginning of the decompression reaction until the rocks have cooled below about 700 °C, when the compositional patterns of the garnet were effectively frozen due to increasingly sluggish diffusion towards lower temperatures. In the context of the evolution of the Moldanubian Zone, these time scales are short and indicate rapid transport of mafic-ultramafic lithologies from mantle to intermediate crustal levels and simultaneous integration into a predominantly felsic environment, accompanied by immediate cooling.

TRAPPING OF HETEROGENEOUS FLUIDS

Bakker, R.J.¹

¹Resource Mineralogy, Department of Applied Geosciences and Geophysics, Montanuniversity Leoben,
Peter-Tunner-Straße 5, 8700 Leoben, Austria
e-mail: bakker@unileoben.ac.at

In theory, the formation of a fluid inclusion assemblage from a multi-phase state (i.e. heterogeneous entrainment) is a common process at natural geological conditions. The immiscibility of multi-component fluids may occur at high temperatures and pressures and is not restricted to diagenetic conditions. Specific fluid systems are even immiscible at Greenschist-, Amphibolite-, Blueschist-, and Granulite-facies metamorphic conditions. The identification of a heterogeneous fluid inclusion assemblage in natural rock is a major challenge in fluid inclusion research, and it is expected to be a common phenomenon. There is only little experimental knowledge about the formation of heterogeneous fluid inclusion assemblages. The synthesis of these assemblages has been used in only a few experimental studies to investigate the boundary conditions of fluid immiscibility fields. These studies included the analyses of only a few fluid inclusions (between 1 and 10 per experiment), but do not reveal the variability of the assemblage or systematics on the distribution or deviations of distinct fluid inclusion types. One inclusion is not representative for specific experiments that usually result in a variety of fluid properties. Fluid inclusions are synthesized at approximately 600 °C and 80 MPa, from a 30 mass% NaCl aqueous solution (SR-020) and a 10 mass% NaCl aqueous solution (SR-019). For both experiments, the conditions are within the two-fluid phase field, and both should result in the formation of similar liquid-rich inclusions and similar vapour-rich inclusions, but in different proportions. Due to the unmixing at experimental conditions, two fluids are present in the capsules, i.e. a liquid-like fluid relatively enriched in NaCl (40.42 to 41.40 mass%) and a vapour-like fluid relatively depleted in NaCl (2.41 to 2.71 mass%). The measured dissolution and homogenization temperatures are not consistent with values calculated with the thermodynamic model (Fig. 1). These preliminary results of experiments in the H₂O-NaCl fluid system have illustrated that predicted fluid properties do not correspond to the observed assemblage. Therefore, the processes that are involved during heterogeneous entrainment need to be investigated in greater detail by systematic analyses of entire fluid inclusion assemblages to be able to predict fluid entrainment in natural systems, and to be able to deduce natural trapping conditions from the observed assemblages.

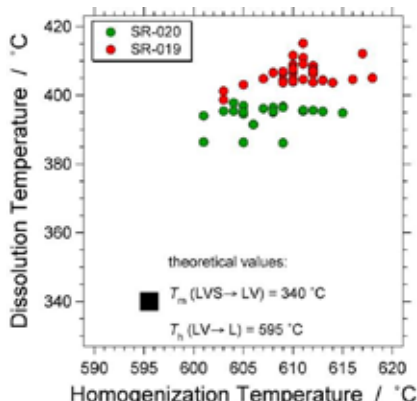


Figure 1. Microthermometric results of liquid-rich fluid inclusions from SR-019 and SR-020. The expected values are illustrated by the black box.

**THE ECCENTRIC CONE MOUNTS DE FIORE, MONTE ROSSI,
MONTE SPAGNOLO, AND THE 2002/03 LAVA FLOW, MT. ETNA:
EVIDENCE FOR MAGMA MIXING**

Bauer, M.¹, Ntaflos, Th.¹, Abart, R.¹, Giacomoni, P.P.², Ferlito, C.³, Coltorti, M.²

¹Department of Lithospheric Research, University of Vienna, Althanstraße 14, 1090 Wien, Austria

²Department of Physics and Earth Sciences, University of Ferrara, Via Savonarola, 9, 44121 Ferrara, Italy

³Department of Biol., Env. and Geol. Sciences, University of Catania, Piazza Università, 2, 95124 Catania, Italy
e-mail: moritz.bauer96@gmail.com

Mt. Etna, located in Sicily, Italy, is Europe's most active volcano and its geodynamic setting and plumbing system have been in the centre of many extensive studies. The 6 stages of eruptive activity from the past to the present are: (1) 'Tholeiitic Stage' between 600-320 ka ago, (2) 'Timpe Stage' 220-110 ka ago, (3) 'Ancient Alkaline Volcanism' 110-65 ka ago, (4) 'Ellittico Stage' 57-15 ka ago, (5) 'Mongibello Stage' from 15 ka ago until 1971, and (6) the 'post -1971 Stage' comprising the volcanic activity since 1971 (CASETTA et al., 2019).

The lava propagating through the Etna plumbing system generated a complex network of sills and dykes and is responsible for the formation of the summit craters and a plethora of eccentric cones that cover the flanks of the volcano.

We studied whole rock and mineral chemistry of the lavas from three eccentric cones (Monte Spagnolo, Mounts de Fiore and Monte Rossi) and the 2002/03 southern flank lava flow. All lavas are trachybasalts with trachytic texture and variable modal composition of olivine, clinopyroxene and plagioclase phenocrysts. The Monte Spagnolo whole rock composition has the most primitive lavas of all the sampled outcrops with Mg# between 55-57.5 and 10.7 wt% CaO, whereas the Monte Rossi lavas are the most evolved ones with a Mg# between 48.3 and 49.3 and a CaO content between 10.44 and 10.48 wt%. Mounts de Fiore and the 2002/03 lava flow are more evolved than the Monte Spagnolo lavas, as they have a Mg# of around 51 to 52. The corresponding CaO concentration is around 11.2 wt% and 10.62 wt% respectively.

Deviating from the trend of the corresponding whole rock composition, the most MgO-rich olivine (Fo = 88.9 %) was found in the Monte Spagnolo lavas. Due to its low NiO content (0.17–0.2 wt%) and high CaO content (0.25–0.26 wt%) this olivine is apparently of magmatic origin. Considering that the olivine, which could be in equilibrium with these lavas, has Fo = 82.2, it is evident that the olivine with Fo=88.9 points to magma mixing with high MgO-rich lavas. The most evolved lavas from Monte Rossi have the lowest Fo-content (Fo = 67–75 %). In conclusion, olivine and pyroxene with inverse zoning and a higher Mg# in the rims than in the cores indicate extensive magma mixing in all locations except for Monte Rossi. These Fo-content differences from core to rim are in the range of 4%.

Monte Spagnolo lavas, compared to the other studied eccentric cones, represent the most primitive magma formed at high temperatures (avg. 1166 °C) and the Monte Rossi lavas the most evolved magma formed at lower temperatures (avg. 1138 °C). In comparison, the lavas of Mounts de Fiore and of the 2002/2003 eruption show a mediate grade of evolvement and average formation temperatures (avg. 1156 °C).

CASETTA, F., GIACOMONI, P.P., FERLITO, C., BONADIMAN, C., COLTORTI, M. (2019): Internat. Geol. Rev., 62, 338-359.

**INVESTIGATING THE EFFECTS OF METAMORPHISM ON THE
SEDIMENT-HOSTED Cu-Co DOLOSTONE ORE FORMATION, NAMIBIA,
USING GEOCHEMISTRY OF COEXISTING IRON-SULFIDES**

Bertrandsson Erlandsson, V.¹, Wallner, D.¹, Ellmies, R.², Melcher, F.¹, Raith, J.G.¹

¹Montanuniversität Leoben, Peter-Tunnerstraße 5, 8700 Leoben, Austria

²Gecko Namibia, Einstein 10, 8912, Swakopmund, Namibia

e-mail: viktor.erlandsson@unileoben.ac.at

The Dolostone Ore Formation (DOF) is a sediment-hosted Cu-Co mineralization in the Kunene Region, northwestern Namibia. The DOF is hosted in Neoproterozoic calcareous siltstones and carbonates of the Ombombo Subgroup (MILLER, 2008). The main ore minerals of the DOF are sphalerite, chalcopyrite, linnaeite, pyrite and pyrrhotite; with subordinate, galena and cobaltite. These sulfides occur in six major mineralization styles: mono-sulfide disseminations, poly-sulfide clusters and nodules, clasts with prominent strain shadows, veins, and the so-called “events”. The “event” mineralization style resemble slump-like structures with both brittle and ductile components, but may also be some sort of crack-seal veins.

Trace element analyses were carried out by LA-ICP-MS to better understand the geochemistry of the sulfides of this sediment-hosted mineralization. Pyrite and pyrrhotite coexist exclusively within the “events”, where euhedral to subhedral pyrite is surrounded by anhedral pyrrhotite. The “event” pyrrhotite is associated with anhedral and intergrown sphalerite, chalcopyrite, and galena. Trace element analyses show that the “event” pyrite is enriched in Cu, As, Sb, Tl, and Pb, compared to the “event” pyrrhotite. Whilst concentrations of elements such as Co, Ni, and Se are relatively similar between the coexisting “event” iron-sulfides.

LARGE et al. (2007) demonstrated that trace elements such as Cu, Zn, Ag, Au, Te, and Pb would be depleted in greenschist facies recrystallized pyrite, compared to the unmetamorphosed pyrite. During metamorphism, the depleted elements would be liberated from the pyrite crystal lattice and form new separate phases, e.g. sphalerite and chalcopyrite. Elements that typically are more tightly incorporated into the crystal lattice of the iron-sulfides (e.g. Co, Ni, and Se) remain at similar concentrations after metamorphism (HUSTON et al., 2017; LARGE et al., 2007). These trends are what we observe in the DOF “event” iron-sulfides. Textural relationships between the “event” pyrite and the pyrrhotite, along with their trace element trends, propose the possibility that early pyrite was a source for Zn, Cu, and Pb that lead to the precipitation of sphalerite, chalcopyrite, and galena that are associated with the pyrrhotite during metamorphism. Preliminary EMPA results indicate that early frambooidal pyrite is enriched in, at least, Zn, suggesting frambooidal pyrite being a possible source of the metals of the DOF mineralization.

- HUSTON, D.L., MERNAGH, T.P., HAGEMANN, S.G., DOUBLIER, M.P., FIORENTINI, M., CHAMPION, D.C. (2017): In: *Ore Geol. Rev.*, 76, 168–210.
LARGE, R.R., MASLENNIKOV, V.V., ROBERT, F., DANYUSHEVSKY, L.V., CHANG, Z. (2007): In: *Econ. Geol.*, 102, 1233–1267.
MILLER, R.M. (2008): *The geology of Namibia. 3 Volumes*, Geol. Surv. Namibia, 1564.

SYSTEMATICS OF FACETED INTERFACES BETWEEN ORIENTED MAGNETITE MICRO INCLUSIONS AND PLAGIOLCASE HOST

Bian, G.¹, Li, C.², Ageeva, O.^{1,3}, Habler, G.¹, Abart, R.¹

¹Department of Lithospheric Research, University of Vienna, Althanstraße 14, 1090 Vienna, Austria

²University of Antwerp, 2020 Antwerp, Belgium

³IGEM RAS, Staromonetnyi 35, 119017 Moscow, Russia

e-mail: rainer.abart@univie.ac.at

Oriented needle- and lath-shaped magnetite (Mt) micro-inclusions in plagioclase (Pl) are robust carriers of natural remanent magnetization. Systematic crystallographic and shape orientation relationships (CORs, SORs) between Mt and Pl may lead to magnetic anisotropy and thus are of pivotal importance for paleomagnetic reconstructions. The unusual needle or lath morphology of the Mt inclusions and their SORs and CORs are due to the alignment of important oxygen layers across the Mt-Pl interfaces that are parallel to the inclusion elongation direction. Typically, the Mt needles are elongated parallel to $Mt\langle 111 \rangle$, and $Mt\{222\}$ is parallel to one of several oxygen layers in Pl, including $Pl(112)$, $Pl(312)$, $Pl(150)$, $Pl(\bar{1}50)$. All these lattice planes have nearly identical d -spacings so that they are coherent across the Mt-Pl interfaces (AGEEVA et al., 2020). This alignment allows one rotational degree of freedom around the needle elongation direction. The rotation is, however, not continuous, but clusters around several specific positions. In this context, the atomic structures of Mt-Pl interfaces are of key interest. We used high angle annular dark field scanning transmission electron microscopy (HAADF-STEM) to determine the atomic structure of the Mt-Pl interfaces of two needles with $Mt\langle 111 \rangle$ parallel to the normal direction to $Pl(\bar{3}12)$. In projections parallel to the needle elongation directions, one inclusion has a hexagonal cross section and, in addition to $Mt\langle 111 \rangle//Pl(\bar{3}12)$, satisfies the relation $Mt\langle 100 \rangle//Pl[\bar{1}4,10,\bar{7}]$. This ensures perfect fit of FeO_6 octahedra of Mt in channels of the Pl crystal structure, which is considered an important match during the nucleation phase and defines the *nucleation orientation*. The other inclusion has a quadrilateral cross section and, in addition to $Mt\langle 111 \rangle//Pl(312)$, satisfies $Mt\{220\}//Pl(150)$, where both planes form facets of the Mt-Pl interface. This is likely the energetically most favourable configuration and defines the *main orientation*. The interface facets can be rationalized based on a modified exact phase boundary model. In nucleation orientation, $Mt\{220\}//Pl(131)$ and $Mt\{220\}//Pl(2\bar{3}4)$. In main orientation, $Mt\{220\}//Pl(112)$ forms the facets or meets $Pl(150)$ with a ratio of 4:3. For the inclusion in nucleation orientation, the elongation direction $Mt\langle 111 \rangle$ deviates by $<1^\circ$ from the normal direction to $Pl(\bar{3}12)$, while in main orientation the deviation is up to $\sim 6^\circ$. The transition from the nucleation to the main orientation corresponds to a two-step rotation: (i) $\sim 6^\circ$ rotation around $Pl(150)n$, (ii) $\sim 30^\circ$ rotation around the inclusion elongation direction. This transition is probably driven by minimizing interfacial energy while keeping the coherent oxygen layers across the Mt-Pl interfaces along the needle elongation direction aligned.

AGEEVA, O., BIAN, G., HABLER G., PERTSEV, A., ABART, R. (2020): CMP, 175(10), 1-16.

FLUID PRODUCTION CONDITIONS MANIFESTED IN MINERAL PRECIPITATES FROM GEOTHERMAL POWER PLANTS

Boch, R.^{1,2}, Kluge, T.³, Szanyi, J.⁴, Leis, A.⁵, Mittermayr, F.⁶, Dietzel, M.¹

¹Graz University of Technology, Institute of Applied Geosciences, Rechbauerstraße 12, 8010 Graz, Austria

²Geoconsult ZT GmbH, Wissenspark Salzburg Urstein, 5412 Puch bei Hallein, Austria

³Karlsruhe Institute of Technology, Inst. of Applied Geosciences, Adenauerring 20b, 76131 Karlsruhe, Germany

⁴University of Szeged, Dept. of Mineralogy, Geochemistry & Petrology, Egyetem u. 2, 6722 Szeged, Hungary

⁵JR-AquaConSol GmbH, Steyrergasse 21, 8010 Graz, Austria

⁶Graz University of Technology, Institute of Technology & Testing of Building Materials,

Inffeldgasse 24, 8010 Graz, Austria

e-mail: ronny.boch@tugraz.at

Fluid circulation and fluid-solid interaction are critical constituents during sustainable and renewable geothermal energy production (heat, electricity) and gas storage (H_2 , CO_2 , CH_4). The occurrence and extent of unwanted processes (scaling, corrosion, plugging) depends on the prevailing natural and technical environmental and fluid production conditions. Differentiated aqueous solutions and gases streaming in subsurface reservoir rocks and boreholes as well as surface infrastructure (pipelines, heat exchangers) lead to successive mineral precipitation and material alteration. This includes mineral (scale) deposits, corrosion products, cements in pore spaces, veins in fractures as well as altered rock and construction materials. Production conditions and potential mineral formation vary across the fluid flow route and with time.

The unwanted mineral precipitates (carbonates, sulfides, sulfates) are originating from the thermal fluid and constitute a chemical-sedimentary archive evolving continuously and/or episodically. Applying some forensic approach (“Scaling Forensics”) an advanced process understanding emerges from the solid deposits. This is based on a steadily growing set of laboratory analytical methods targeting mineralogical, petrographic, chemical, and isotopic compositions. The reconstruction of relevant processes involves the interpretation of indicative minerals and inclusions, crystal growth mechanisms, chemical tracers, and the role of specific interfaces, substrate effects and microbial contributions. Distinct phases and sections of the fluid circuit can further be interrelated by computer based numerical modeling.

Considering novel geochemical tracers, “clumped isotopes” (multiply-substituted isotopologues) in solids (scale deposits, rocks) and gases, hold a highly attractive potential as geothermometer, fluid provenance and evolution tracer and for kinetic effects related to mineral precipitation. In particular, carbonate scales reflecting a broad range of physicochemical growth conditions are promising materials for the evaluation and calibration of the new isotopic tool.

ORE PETROGRAPHIC AND GEOCHEMICAL ANALYSIS OF THE POLYMETALLIC COPPER DEPOSIT WALCHEN NEAR ÖBLARN, STYRIA

Brandner, P.¹, Melcher, F.¹, Onuk, P.², Skrzypek E.²

¹Montanuniversität Leoben, Leoben, Lehrstuhl für Geologie und Lagerstättenlehre, Peter-Tunner-Straße 5,
8700 Leoben, Austria

²Universität Graz, Graz, Austria, Institut für Erdwissenschaften, Universitätsplatz 2, 8010 Graz, Austria
e-mail: brandner.peter@live.at

The stratiform sulfide deposit Walchen is an Fe-rich, polymetallic sedimentary-exhalative mineralization, which occurs in greenschist facies metamorphic sedimentary host rocks. The east-west trending orebodies are located in a transition zone between the Wölz Micaschist complex and the Ennstal phyllite zone. A total of five ore types can be distinguished, i.e. pyrite, pyrrhotite, chalcopyrite, sphalerite impregnation ore, and massive pyrrhotite ore. The main ore minerals, in decreasing order of frequency, are pyrite, pyrrhotite, chalcopyrite, sphalerite, and galena. Minor and trace minerals are arsenopyrite, stannite, Ag-bearing fahlore, boulangerite, bournonite, ullmannite-willyamite, jamesonite, cassiterite, ilmenite, gudmundite, Bi-Sb alloys, and Ag-Au-Hg phases.

The gangue is composed of non-sulfidic minerals with the majority being quartz, alkali feldspar, phyllosilicates and carbonates (dolomite-ankerite, siderite). Monazite and xenotime-group minerals, rutile, ilmenite, uraninite and zircon are accessories. The host rock generally consists of the same minerals except of Fe-rich carbonates. Whereas only minor mineralogical and geochemical differences are found between footwall and hanging wall rocks of the orebody, a significant difference is visible in the trace element contents (i.e. Cr, Ni).

LA-ICP-MS trace element analyses of pyrite, pyrrhotite, chalcopyrite, and sphalerite were evaluated. Pyrite shows a strong accumulation of Co (543 ppm) and As (1099 ppm). Chalcopyrite reveals increased median contents for Ag (190 ppm) and In (51 ppm). In sphalerite Fe (8.4 %), Cd (0.16 %), and In (111 ppm) are accumulated. Preferred accumulation of trace elements in a certain ore type could not be recognized. However, sphalerite and chalcopyrite in massive ore samples (Ph-DE) often show elevated trace element concentrations.

Mineral chemical analyses indicate that the metamorphic overprint of the deposit took place at temperatures of at least 350 °C at pressures around 3.8 kbar. Uranium-lead measurements with the electron microprobe on micro-uraninites from the impregnation ores show a mean age of 93 Ma which is interpreted as the age of the last metamorphic overprint.

**DISTRIBUTION OF CO₂ IN THE LITHOSPHERIC MANTLE BENEATH
NORTHERN VICTORIA LAND (ANTARCTICA): INSIGHTS FROM PETROLOGY,
FLUID INCLUSIONS CHEMISTRY AND X-RAY µCT IN MANTLE XENOLITHS**

Casetta, F.¹, Rizzo, A.L.^{2,3}, Faccini, B.², Ntaflos, T.¹, Lanzafame, G.⁴, Faccincani, L.²,
Mancini, L.⁵, Giacomoni, P.P.², Coltorti, M.^{2,3}

¹Department of Lithospheric Research, University of Vienna, Althanstraße 14, 1090 Vienna, Austria

²Department of Physics and Earth Sciences, University of Ferrara, Via Saragat 1, 44122, Ferrara, Italy

³Istituto Nazionale di Geofisica e Vulcanologia, Sezione di Palermo, Via Ugo La Malfa 153,
90146 Palermo, Italy

⁴Department of Biological, Geological and Environmental Sciences, University of Catania,
Corso Italia 57, 95129 Catania, Italy

⁵Elettra-Sincrotrone Trieste S.C.p.A., s.s. 14 km 163,500 in Area Science Park, 34149 Basovizza, Trieste, Italy
e-mail: cstfrc@unife.it

Modelling the carbon cycle in Earth's deepest reservoirs is crucial for enhancing our comprehension of the evolution of our planet. In fact, geodynamic processes are intimately linked to the storage and mobility of volatiles in the Earth's mantle, as C-O-H species play an important role in driving melt extraction, metasomatism and refertilization. A powerful way to investigate where and how carbon is stored in the deep Earth, and especially in the Sub-Continental Lithospheric Mantle, is the combined application of petrology, fluid inclusions geochemistry and high-resolution imaging techniques to mantle-derived xenoliths.

In the present study, modally and/or chemically heterogeneous mantle xenoliths brought to the surface by Cenozoic lavas in northern Victoria Land (Antarctica) were investigated by means of mineral chemistry, fluid inclusions composition and 3D textural/volumetric characterizations of intra- and inter-granular microstructures performed by X-ray computed microtomography (µCT).

Fluid inclusions are volumetrically abundant in both olivine and pyroxenes, and often associated with inter-granular reaction zones. Olivine-hosted fluid inclusions have the lowest CO₂ concentrations, ranging from 0 to 39 µg(CO₂)/g(sample), while amphibole- and pyroxene-hosted FI are typified by the highest contents [up to 187.3 µg(CO₂)/g(sample)].

X-ray µCT was used to image and quantify the abundance, connectivity, and density of glass/fluid components as well as to speculate about their origin and relationships with the networks of secondary fractures, likely formed during decompression, that sometimes pervade the rocks. In general, glass/fluid components have tetrahedral to prismatic shape and sizes between 2 and 50 µm.

Together with mineral chemistry data and *T-fO₂* models, fluid inclusions chemistry and X-ray µCT results were used to: i) model the storage and distribution of carbon in intra- and inter-granular zones in mantle xenoliths; ii) relate the occurrence/mobility of carbon to the melt extraction and enrichment episodes that affected the Sub-Continental Lithospheric Mantle beneath Antarctica; iii) understand the role played by fluids during the major geodynamic processes.

^{147}Sm - ^{143}Nd SYSTEMATICS FOR TRACING HYDROTHERMAL ALTERATION AND U MOBILIZATION IN PROTEROZOIC JABILUKA UNCONFORMITY-RELATED URANIUM DEPOSIT (NORTHERN TERRITORIES, AUSTRALIA)

Chernonozhkin, S.M.^{1,2,3}, Luais, B.³, Reisberg, L.³, Brouand M.⁴, Cuney, M.², Mercadier, J.²

¹Current address: Chair of General and Analytical Chemistry, Montanuniversität Leoben,
Franz-Josef-Straße 18, 8700, Leoben, Austria

²Université de Lorraine, CNRS, CREGU, GeoRessources Lab, Campus Aiguillettes,

Faculté des Sciences et Technologies, rue Jacques Callot, Vandoeuvre-lès-Nancy, 54506, France

³Centre de Recherches Pétrographiques et Géochimiques (CRPG), CNRS, Université de Lorraine, UMR 7358,
15 rue Notre Dame des Pauvres, Vandoeuvre lès Nancy, 54501, France

⁴Orano Mining, 125 Avenue de Paris, 92320 Châtillon, France

e-mail: stepan.chernonozhkin@gmail.com

Jabiluka unconformity-related U deposit (Alligator Rivers Uranium Field, Northern Territories, Australia) was formed at the unconformity between the Kombolgie sedimentary basin and the Archean-Paleoproterozoic crystalline basement, as a result of percolation of hot U-rich brines. The basement lithologies are characterized by massive hydrothermal alteration linked to these brines, leading coevally to precipitation of U oxides and an illite/chlorite clay alteration. Although the primary mineralization in the form of U oxides should at first glance be easy to date using U-Pb method, this approach is jeopardized by mobilization and loss of Pb and the fact that uraninite is easily dissolved by fluid circulation. U-Pb ages of the uranium minerals provide a broad spectrum of ages with peaks between ca. 1680 - 1300 Ma.

This work revisits the temporal sequence of orogenic events leading to formation of the Jabiluka unconformity-related U deposit using whole rock ^{147}Sm - ^{143}Nd systematics. A series of samples taken from a single drill hole intersecting fresh to hydrothermally altered basement lithologies and the U orebody were investigated. The REE contents and patterns strongly vary with the development of alteration and mineralization, demonstrating that this alteration episode was large enough to isotopically homogenize the ~250 m layer of the basement, such that the ^{147}Sm - ^{143}Nd system can be applied. The petrographic and geochemical features show that the initial mineralogy, with the REE balance largely controlled by monazite, was modified such that clays, phosphate and uranium oxides became the main REE-bearing phases. The ^{147}Sm - ^{143}Nd isotope data demonstrate that U oxides and the hydrothermally altered silicate basement lithologies are formed in a single event. The inferred Sm-Nd age at 1545 ± 27 Ma suggests that this massive alteration episode is not co-eval with the primary U deposition at ca. 1680 Ma, but occurred nearly 100 million years later. The high initial $^{143}\text{Nd}/^{144}\text{Nd}$ shows that Nd evolved in an environment with high Sm/Nd ratio, which could derived from the primary generation of the Jabiluka U oxides, dissolved and re-mobilized ca. 100 Ma after their initial formation.

This work demonstrates therefore the relevance of the application of the Sm-Nd system for studying hydrothermal deposits in context of succession of multiple fluid episodes, and encourages for the development of dedicated applications.

TOWARDS AN ANALYTICAL PROOF OF ORIGIN FOR NATURAL GRAPHITE DEPOSITS

Dietrich, V.¹, Melcher, F.¹, Rantitsch, G.¹

¹Department of Applied Geosciences and Geophysics, Montanuniversität Leoben,
Peter-Tunner-Straße 5, 8700 Leoben
e-mail: valentina.dietrich@unileoben.ac.at

Raw material supply chains are complex systems. They build on the presence of economically mineable mineral commodities that will undergo several steps until they are finally being used as consumer products. Trustworthiness into the transparency of a supply chain is of increasing importance, both to upstream and downstream companies. Any deviation from best-practice and quality standards in mining, processing and production is critically looked by consumers, especially nowadays. Therefore, certification and proof of origin concepts have emerged within the past years, aiming at providing transparency to supply chains (MELCHER et al., 2021).

30 raw materials have been classified as critical by the EU; some of which are particularly relevant for the Green Deal and the digital transformation, including graphite. The classification as a critical raw material is based on the assessment of whether longer interruptions or shortages in supply could have a negative impact on technological progress and economic growth.

In addition to the well-known use of (microcrystalline) graphite in pencils, another very important and currently highly sought-after application of large flake graphite in the electronic industry is in lithium ion batteries and fuel cells. The demand is constantly increasing.

POHL (2020) distinguishes four major deposit types, namely regional metamorphic graphite formed from coal or hydrocarbons; contact-metamorphic graphite formed from sedimentary rock; hydrothermal graphite as a product of magmatic, hydrothermal or volcanogenic processes; and supergene residual deposits. Large-flake graphite can be extracted at a minimum of 3–5 % graphite in rock, whereas fine-grained or microcrystalline graphite ore requires grades >45 %.

The increasing demand for this raw material and the limited market with a small number of players is also accompanied by concerns from industry and consumers about the origin of this raw material. Therefore, different graphite deposits distributed worldwide are included in the present study. The analysis of fingerprints for graphite is favourable in order to check and differentiate between different origins, in particular from African countries (Mozambique, Madagascar, and Zimbabwe), but also from Korea, China and others. Graphites offer several options for an analytical proof of origin, for example the determination of trace elements using ICP-MS and LA-ICP-MS, the $\delta^{13}\text{C}$ isotope ratio by MC-ICP-MS or gas mass spectrometry. Another useful parameter is the degree of graphitization, which is analysed by Raman spectroscopy. Also textural information, such as morphology and grain size, which is assessed by microscopy and scanning electron microscopy are useful parameters for the application of fingerprinting techniques.

MELCHER, F., DIETRICH, V., GÄBLER, H.-E. (2021): Minerals, 11, 461, 1-16.

POHL, W., (2020): Economic Geology: Principles and Practice, 2nd revised edition, Schweizerbart'sche Verlagsbuchhandlung, Stuttgart, Germany.

RADIOMETRIC DATING OF THE MOLYBDENUM DEPOSIT REICHENSPITZE, TYROL

Doppelmayr, D.¹, Melcher, F.¹, Gallhofer, D.², Sorger, D.^{2,3}

¹Lehrstuhl für Geologie und Lagerstättenlehre, Montanuniversität Leoben,
Peter-Tunner Straße 5, 8700 Leoben, Austria

²Institute of Earth Sciences, Universität of Graz, Universitätsplatz 2/II, 8010 Graz, Austria

³Present address: Geoscience Center, Georg-August-University Göttingen,
Goldschmidtstraße 1, Göttingen 37077, Germany
e-mail: frank.melcher@unileoben.ac.at

The occurrence of molybdenum at Reichenspitze in Salzburg and Tyrol is part of the molybdenum ore province Zentralgneis Supersuite in the Tauernfenster. At the Reichenspitze, molybdenite (MoS_2) is restricted to aplitic intrusions in the Zentralgneis. These aplitic granites are also referred to as Reichenspitze granite. Up to now no reliable age of the Reichenspitze granite has been published. In this study, U-Pb zircon dating (LA-ICP-MS) yields a crystallization age of $292.2 \pm 0.68 \pm 3.9$ Ma for the aplitic granites. This puts the Reichenspitze granite directly into relation with the Lower Permian I-Type granitoids of the Zillertal-Venediger-Tux magmatic suite. Geochemical analyses of the aplitic granite show high SiO_2 contents (77 to 79 wt.%), barium contents of 141 to 233 $\mu\text{g/g}$, and rubidium contents of 147 to 171 $\mu\text{g/g}$. Based on low CaO contents (< 1.65 wt.%), a negative barium anomaly (normalized to ocean ridge granites), and high Rb/Sr ratios (up to 5.93), the Reichenspitze granite was previously interpreted as an A-type granite. The analyzed samples of the Reichenspitze granite also show low CaO contents (< 0.8 wt.%), a weak negative barium anomaly, and high Rb/Sr ratios (up to 4.25). However, a $\text{K/Rb} - \text{Rb}$ discrimination diagram indicates a differentiation trend from granites in the Tux Core to the Reichenspitze granite. The Reichenspitze granite is therefore interpreted as a highly differentiated granitoid of the Zillertal-Venediger-Tux magmatic suite. Typological studies of the investigated zircons yield calc-alkaline, highly fractionated magma sources. Crystallization temperatures of 600 to 650 °C are presumed. Additionally U-Pb uraninite dating was carried out in this study. Though the crystallization age of the uraninites could not be precisely determined, the polygenetic zircon grains show younger ages than the published Lower Permian zircon age. The youngest uraninite generation shows consistent ages of 29 ± 5 Ma, which dates the Oligocene Neo-alpine regional metamorphism. Based on the new geochronological data a primary ore formation syngenetic with the intrusion of the Reichenspitze granite is proposed. In the highly fractionated melt, volatile elements (F, Cl) and molybdenum were enriched. This process generated metal-bearing, possibly pneumatolytic fluids which overprinted the host rock and led to metasomatic ore formation. Hydrothermal activity during the Alpine regional metamorphism remobilised the ore, which locally led to molybdenite enrichment as aggregates along shear zones. The Reichenspitze deposit strongly resembles the molybdenum deposit Ackley in Newfoundland, which is also related to aplitic granites in the roof zone of a magma chamber. A genetic relation between the Reichenspitze molybdenum occurrence and the molybdenum deposit Alpeinertscharte/Tyrol dated at 305 Ma (Langthaler et al., 2004) cannot be excluded but calls for further investigations.

LANGTHALER, K., RAITH, J.G., CORNELL, D., STEIN, H., MELCHER, F. (2004): Miner. Petrol., 82, 33-64.

GEOGENIC THALLIUM-EXTREME ENVIRONMENTS: IN WHICH SECONDARY PHASES IS Tl(I) INCORPORATED?

Dorđević, T.¹, Drahota, P.², Kolitsch, U.^{3,1}, Majzlan, J.⁴, Kiefer, S.⁴, Tepe, N.⁵, Hofmann, T.⁵,
Serafimovski, T.⁶, Tasev, G.⁶, Boev, I.⁶, Boev, B.⁶

¹Institut für Mineralogie und Kristallographie, Universität Wien, Althanstraße 14, 1090 Wien, Austria

²Institute of Geochemistry, Mineralogy and Mineral Resources, Faculty of Science, Charles University,
Albertov 6, 128 43 Prague 2, Czech Republic

³Mineralogisch-Petrographische Abteilung, Naturhistorisches Museum, Burgring 7, 1010 Wien, Austria

⁴Institute of Geosciences, Department of Mineralogy, Friedrich-Schiller-Universität, Carl-Zeiss-Promenade 10,
07745 Jena, Germany

⁵Centre for Microbiology and Environmental Systems Science, University of Vienna,
Althanstraße 14, 1090 Wien, Austria

⁶Department of Mineral Deposits, Faculty of Natural Sciences, University “Goce Delčev”-Štip,
Goce Delčev 89, 2000 Štip, North Macedonia
e-mail: tamara.djordjevic@univie.ac.at

Although the oxidation zones of the majority of naturally Tl-rich localities represent a great threat to surrounding ecosystems, they have not been investigated so far in much detail. Since the remediative treatment of highly Tl-contaminated soils depends on the character of the Tl-bearing phases, it is necessary to fully characterize Tl retention through secondary minerals in affected areas, in order to build a sound basis for successful remediation.

In this study we identified Tl reservoirs in waste dumps and soils of the naturally thallium richest locality in the world, the Crven Dol locality (Tl-As-Sb-Au Allchar deposit, North Macedonia). Tl speciation differs to a certain extent from that observed in similar localities, and is reflected by a very well-developed secondary mineralogy. Thallium dissolved during weathering is precipitated mostly as novel poorly crystalline to amorphous thallium arsenates or as dorallcharite (Tl-Fe sulfate). In traces, Tl also appears as a nano-sized Tl(I) oxide (Tl_2O) and as thalliumpharmacosiderite (Tl-Fe arsenate). Furthermore, Tl is accumulated in supergene Mn oxides, pharmacosiderite, and jarosite.

Pore waters contain high aqueous concentrations of Tl (up to 660 µg/L) and As (up to 196 mg/L). Although these concentrations are low with respect to their total concentrations in the solid phase (Tl: 0.07-1.44 wt%; As: 0.72-8.67 wt%), mild extractions mobilized up to 44 % of the total Tl and 23 % of the total As, indicating that a large amount of these toxic elements is only bound weakly (sorption) to solids and can be easily mobilized.

In general, in soil horizons lacking secondary Tl-bearing minerals, Tl(I) adsorption onto micaceous phyllosilicates (mostly illite), followed by Tl(I) and Tl(III) adsorption onto Mn oxides has previously been identified as the dominant Tl retention mechanism (WICK et al., 2018, 2019 and references therein). However, in Tl-extreme environments, when illite and Mn oxides are either absent or exhausted, discrete secondary Tl minerals form and store Tl.

This work was supported by the Austrian Science Fund (FWF) [grant number P 30900-N28 to T. Đorđević].

WICK, S., BAEYENS, B., FERNADES, M.M., VOEGLIN, A. (2018): Environ. Sci. Technol., 52, 571-580.
WICK, S., PEÑA, J., VOEGLIN, A. (2019): Environ. Sci. Technol., 53, 13168-13178.

**THE 4-CENTER 2-ELECTRON BONDED CLUSTER CATIONS
[Ag₃Hg]³⁺ AND [Ag₂Hg₂]⁴⁺**

Effenberger, H.¹

¹Institut für Mineralogie und Kristallographie, Universität Wien, Althanstraße 14, 1090 Wien, Austria
e-mail: herta.silvia.effenberger@univie.ac.at

[Ag₃Hg]³⁺ and [Ag₂Hg₂]⁴⁺ are rare cation complexes. The first evidence was found in tillmannsite, [Ag₃Hg][(V,As)O₄], which was described from an old copper mine of Roua (Alpes-Maritimes, France): space group $\bar{I}\bar{4}$ (SARP et al., 2003). Later on, WEIL et al. (2005) synthesized the V-end member besides the compounds [Ag₂Hg₂]₃[VO₄]₄ and [Ag₂Hg₂]₂[HgO₂][AsO₄]₂ ($\bar{I}\bar{4}2d$ and $P31c$). Just recently, rudabányaite - [Ag₂Hg₂][AsO₄]Cl was found in cavities of siliceous sphaerosiderite and limonite rocks at the Rudabánya ore deposit (Adolf mine area, NE Hungary; $F\bar{4}3c$; EFFENBERGER et al., 2019).

The $M = (\text{Ag}, \text{Hg})$ atoms in all these $[M_4]$ clusters are located at the corners of an empty tetrahedron; the complex is stoichiometric with Ag:Hg = 2:2 or 3:1, respectively. The M atoms are $\sim 1.66 \text{ \AA}$ apart from their vacant centres; thus, the size of the $[M_4]$ tetrahedra corresponds with the arsenate and vanadate tetrahedra. The $M—M$ bond distances of ~ 2.60 to 2.72 \AA suggest predominantly covalent bonding. Order between Ag and Hg atoms is not verified. The M atoms are [6] coordinated by each three M atoms and by three anions. In rudabányaite a partial displacement of the M atoms was observed (about 0.5 \AA). Remarkable is the pronounced one-sided [3] coordination of the Cl⁻ ions in rudabányaite.

Only in [Ag₂Hg₄][XO₄]₂ ($X = \text{P}, \text{As}$) (MASSE et al., 1978; WEIL, 2003) the Ag and Hg atoms are ordered: each two [Ag₂Hg₂] tetrahedra share a common Ag—Ag edge forming an [Ag₂Hg₄]⁶⁺-cluster cation. The shared edge ($\sim 2.85 \text{ \AA}$) is slightly shorter than in native silver but larger than the $M—M$ distance in the [Ag₂Hg₂] complex. The other $M—M$ bond distances are comparable to the $[M_4]$ clusters.

On interest are some crystal chemical, structural, and topological similarities: In kuznetsovite ([Hg₃][AsO₄]Cl, space group $P2_13$; WEIL, 2001) trigonal [Hg₃]⁴⁺ clusters substitute for the larger [Hg₂Ag₂]⁴⁺ metal clusters of rudabányaite; the Cl atom is planar [3] coordinated. – In tillmannsite, two distinct column-like arrangements built solely by [Ag₃Hg]³⁺ cation clusters respectively [(V,As)O₄]³⁻ tetrahedra are running parallel to [001]; alternatingly arranged [Ag₃Hg] clusters and [(V,As)O₄] tetrahedra are verified parallel to <100>. In rudabányaite [Ag₂Hg₂] clusters and [AsO₄] tetrahedra alternate due to the cubic symmetry in all <100> directions.

The dominance of acentric crystal structures in this group of compounds should be noted.

- EFFENBERGER, H., SZAKÁLL, S., FEHÉR, B., VÁCZI, T., ZAJZON, N. (2019): Europ. J. Mineral., 31, 537-547.
- MASSE, R., GUITEL, J.-C., DURIF, A. (1978): J. Solid State Chem., 23, 369-373.
- SARP, H., PUSHCHAROVSKY, D.Yu., MACLEAN, E.J., TEAT, S.J., ZUBKOVA, N.V. (2003): Europ. J. Mineral., 15, 177-180.
- WEIL, M. (2001): Zeitschr. Naturforschung, 56b, 753-758.
- WEIL, M. (2003): Zeitschr. Naturforschung, 58b, 1091-1096.
- WEIL, M., TILLMANNS, E., PUSHCHAROVSKY, D.Yu. (2005): Inorg. Chem., 44, 1443-1451.

GREEN INHIBITORS AGAINST CaCO₃ SCALE DEPOSITS – ON-SITE ASSESSMENT AND TUNING IN TUNNEL DRAINAGES

Eichinger, S.¹, Boch, R.^{1,2}, Leis, A.³, Baldermann, A.¹, Domberger, G.³, Schwab, M.⁴, Dietzel, M.¹

¹Institute of Applied Geosciences, Graz University of Technology & NAWI Graz GeoCenter,
Rechbauerstraße 12, 8010 Graz, Austria

²Geoconsult ZT GmbH, Wissenspark Salzburg Urstein, Urstein Süd 13, 5412 Puch bei Hallein, Austria

³JR-AquaConSol GmbH, Steyrergasse 21, 8010 Graz, Austria

⁴ASFINAG Service GmbH Graz, Fuchsenfeldweg 71, 8074 Graz – Raaba, Austria

e-mail: stefanie.eichinger@tugraz.at

Calcium carbonate scale deposits (CaCO₃ mineral formation from aqueous solution) in groundwater drainage systems are a common and challenging issue, especially if deposition and clogging limit the continuous water transport. The mechanical or chemical removal of such unwanted mineral deposits is highly cost and labor intensive arguing for optimized case-specific and sustainable prevention strategies. In the present study, a novel approach to prevent tunnel drainages from CaCO₃ scale formation was assessed on-site in two selected Austrian road tunnels: The eco-friendly green inhibitor polyaspartate (PASP) was tested and evaluated in order to significantly reduce and modify the (micro)structure and material consistency of the widespread CaCO₃ scale deposits. The application of minor amounts of PASP caused (i) a significant inhibition of CaCO₃ precipitation, (ii) a more porous or even loose consistency (calcareous mud) of the CaCO₃ deposits, and (iii) a shift in CaCO₃ mineralogy from predominant calcite toward metastable aragonite and frequent vaterite formation. Even a very low PASP concentration (few mg PASP L⁻¹) induced a strongly elevated saturation index of calcite up to ~2, i.e. close to the saturation level of ACC (amorphous Ca-carbonate). The upper reasonable dosage level of PASP has to be adjusted by considering the local inhibition requirements and regulative limits, as well as the case-specific microbial activity enabling the consumption of PASP, e.g. by the common iron metabolizing microbial species *Leptothrix ochracea*, which can reduce the effective PASP concentration and thus the anticipated inhibition effect.

COMPOSITION OF GOLD IN THE ROMAN GOLD MINING DISTRICT KARTH, LOWER AUSTRIA

Elmer, S.¹, Lockhoff, N.², Melcher, F.¹, Cech B.³

¹Montanuniversität Leoben, Peter-Tunner-Straße 5, 8700 Leoben, Austria

²Curt-Engelhorn-Zentrum Archäometrie, D6, 3, 68159 Mannheim, Germany

³Independant researcher, Quarngasse 22/3/7, 1100 Wien, Austria

e-mail: simone.elmer@unileoben.ac.at

The Roman mining district Karth is located between Semmering Schnellstraße S6 and Südautobahn A2 southwest of Wiener Neustadt, Lower Austria. It is situated on a wooded plateau in a hilly territory and comprises an area of about 6 km length and 2.5 km width. The terrain shows remarkable formations like tanks and leat channels which are the remains of hydraulic mining of placer gold by the Romans as described by Pliny the Elder (CECH et al., 2013). The placer gold occurs in the Loipersbacher Rotlehmserie (also termed Loipersbach Formation), which is composed of clay and embedded coarse gravel layers (CECH et al., 2019). The data presented were collected as part of a master thesis (ELMER, 2020) in the context of FWF Project P30790-G25 (www.karthgold.com). Morphological investigations of gold particles from Karth using a digital microscope Keyence VHX-6000 based on the classification scheme from YOUNGSON & CRAW (1999) show mainly equant and complex outlines as well as mixed forms, whereas branched particles are unusual. Flattening, rounding and folded edges of the gold particles indicate a distal primary mineralisation, but a statement about the transported distance is not possible. Back-scattered electron images of polished sections using a scanning electron microscope Zeiss EVO MA10 show the zoning of gold with high fineness near the surface, in contrast the interior is rich in Ag; further elements have hardly been detected. Additional LA-ICP-MS analysis at the CEZA Mannheim, Germany, provide trace element data and help to gain more information about the composition of this placer gold. Even though a wide range of elements was analysed, only a few reached the limit of detection. For comparison with placer gold from Mur, Mürz, and Feistritz, core data of Cu, Cd, Sb, and Hg are used as these elements are above the detection limit most frequently. Gold from the different locations contain similar contents of Cu and Sb and therefore do not show cluster to discriminate one from another. In the core areas of Karth gold, Cd is mainly above the detection limit, whereas it is generally below in the comparison samples. Even though the reliability of Hg data by LA-ICP-MS has been discussed (ŽITŇAN et al., 2010) there are significant differences between the data from Karth and the compared rivers. Gold from Karth contains mainly <1000 ppm, in the Mürz values are around 660 ppm, in contrast Feistritz and Mur contain higher contents of Hg that are usually >1000 ppm. Thus, in the data so far the greatest geochemical similarities occur between gold of the Karth and that of the Mürz.

CECH, B., KÜHTREIBER, T. (2013): In: P. SCHERRER (ed.): Römisches Österreich. Graz: Uni-Press Graz Verlag GmbH (Jahresschrift der Österreichischen Gesellschaft für Archäologie, 36, 1–94).

CECH, B., SCHOLGER, R., STREMKE, F., WEIXELBERGER, G. (2019): In: M. FRASS, J. KLOPF, M. GABRIEL (Ed.): Erfinder - Erforscher - Erneuerer. 1. Auflage. Salzburg: Paracelsus (Salzburger Kulturwissenschaftliche Dialoge, 5, 83–114).

ELMER, S. (2020): Masterarbeit. Montanuniversität Leoben, Leoben.

YOUNGSON, J. H., CRAW, D. (1999): Econ. Geol., 94, 615–634.

ŽITŇAN, P., BAKOS, F., SCHMIDRER, A. (2010): Miner. Slovaca, 42, 57–68.

KOLLERITE, $(\text{NH}_4)_2\text{Fe}^{3+}(\text{SO}_3)_2(\text{OH})\cdot\text{H}_2\text{O}$, A NEW SULFITE MINERAL

Ende, M.¹, Effenberger, H.¹, Fehér, B.² Sajó, I.³, Kótai, L.⁴, Szakáll, S.⁵

¹University of Vienna, Institut für Mineralogie und Kristallographie, Althanstraße 14, 1090 Wien, Austria

²Herman Ottó Museum, Department of Mineralogy, Kossuth u. 13, 3525 Miskolc, Hungary

³University of Pécs, Szentágóthai Research Centre, Ifjúság u. 6, 7624 Pécs, Hungary

⁴Institute of Materials and Environmental Chemistry, Hungarian Academy of Sciences, Research Centre for Natural Sciences, Magyar tudósok u. 2, 1117 Budapest, Hungary

⁵University of Miskolc, Department of Mineralogy and Petrology, 3515 Miskolc-Egyetemváros, Hungary

e-mail: herta.silvia.effenberger@univie.ac.at

Sulfite ions are rare constituents of minerals; so far only eight minerals containing $[\text{SO}_3]^{2-}$ groups have been approved by the IMA-CNMNC. During field work in the coal open pit near Köves Hill (Pécs-Vasas, Mecsek Mts., South Hungary) the new mineral kollerite was detected: $(\text{NH}_4)_2\text{Fe}^{3+}(\text{SO}_3)_2(\text{OH})\cdot\text{H}_2\text{O}$, $Cmcm$, $a = 17.803(7)$ Å, $b = 7.395(4)$ Å, $c = 7.096(3)$ Å, $V = 934.2(7)$ Å³, $Z = 4$. Data for structure investigation were collected on a Stoe StadiVari four-circle diffractometer (Dectris Pilatus 300 K pixel detector, MoK α radiation, 100 W air-cooled Incoatec I μ S micro-focus X-ray tube, 50 kV, 1 mA).

The Fe³⁺ ion ($<\text{Fe}^{[6]}-\text{O}> = 1.963(2)$ Å) has site symmetry $2/m$; the atoms S, O1, N, and two of the H atoms belonging to the NH₄ group are located at a mirror plane, the hydroxyl group as well as the O atom belonging to the water molecule (O_w) have site symmetry $m2m$. The water molecules exhibit an orientational disorder with (static or dynamic) half-occupied H atom positions. However, there is no hint for a long-range order. Despite the small size of the crystal used for data collection (6H7H65 μm), the atomic coordinates and isotropic displacement parameter of all H atoms could be refined without any restraints.

$<\text{S}^{[3]}-\text{O}> = 1.538(2)$ Å and O—S—O = 102.71(12) to 104.58(9) $^\circ$ accord with a sulfite group. The $[\text{Fe}(\text{O}_h)_4(\text{O}_h)_2]$ octahedra are corner linked to buckled chains via the O_h atoms and represent the backbone of the $[\text{Fe}(\text{OH})(\text{SO}_3)_2]^{2-}$ chains running parallel to [001]. Similar chain topologies but with $[\text{XO}_4]^{2-}$ tetrahedra instead of the $[\text{SO}_3]^{2-}$ groups are known from the minerals tancoite, sideronatrit, and sideronatrite-2M.

Intercalated between the $[\text{Fe}(\text{OH})(\text{SO}_3)_2]^{2-}$ chains are the water molecules and the ammonium cations. Linkage is achieved by hydrogen bonds only. Despite the loose connection, the (NH₄)⁺ group is ordered and forms clearly defined hydrogen bonds. The N atom of the (NH₄)⁺ cation has a tetrahedral environment: H—N—H and O···N···O are 101.14(11) to 115.24(8) $^\circ$. The bond lengths N—H_n (0.81(3) and 0.90(5) Å), O_h—H_h (0.65(7) Å), and O_w—H_w (0.84(7) Å) are in the range expected for X-ray data. The hydrogen bonds are close to linearity (N/O—H···O = 169(4) / 176(4) $^\circ$). The hydrogen bond lengths in general are relative long emphasising the loose connection of the $[\text{Fe}(\text{OH})(\text{SO}_3)_2]^{2-}$ chains: N—H_n···O is 2.803(4) to 2.958 Å, O_h—H_h···O_w and O_w—H_w···O₂ are 2.747(6) and 3.104(4) Å, respectively. The atomic arrangement accords with the needle-like shape of the crystals: the crystals are elongated parallel to [001], i.e., the direction of the $[\text{Fe}(\text{OH})(\text{SO}_3)_2]^{2-}$ chains.

Two further phases were found at the same locality: $(\text{NH}_4)_2\text{Fe}^{3+}(\text{SO}_3)_6$ is metastable; $(\text{NH}_4)_2\text{Fe}^{2+}(\text{SO}_3)_2$ crystallizes trigonal, $R\bar{3}m$, $a = 5.3879(8)$ Å, $c = 19.980(4)$ Å, $V = 502.3$ Å³.

TWO NEW POLYMORPHS IN THE POOL OF (Li,Sc)-PYROXENE STRUCTURES

Ende, M.¹, Kunit, R.¹, Redhammer, G.J.², Miletich, R.¹

¹ Institut für Mineralogie und Kristallographie, Universität Wien, Althanstraße 14, 1090 Wien, Austria

² Fachbereich Materialforschung und Physik, Universität Salzburg,

Jakob-Haringer-Strasse 2a, 5020 Salzburg, Austria

e-mail: martin.ende@univie.ac.at

Pyroxenes are among the most abundant minerals in the upper mantle. Knowledge of their high-pressure behavior is of particular interest, since phase transitions of pyroxenes are discussed as being responsible for discontinuities in seismic wave propagation (e.g. WOODLAND, 1998). As the compression behavior of pyroxenes does not follow the bulk modulus – unit cell volume relationship for isostructural compounds proposed by ANDERSON & ANDERSON (1970) for isostructural compounds, but strongly depends on chemical compositions (e.g. ENDE et al., 2020), systematic studies seem inevitable to predict their high-pressure behavior. Germanate-analogue phases have already been in the focus early, as the larger Ge atoms were supposed to provide easier access to equivalent high-pressure phases.

In this context in-situ compression studies were conducted on synthetic crystals of α -LiScGe₂O₆ (LSG) orthopyroxenes using Raman spectroscopy as well as single-crystal X-ray diffraction. The purpose of this study is to understand the stability criteria from a structural perspective, any polymorphism, and the mechanisms of the underlying transitions in non-ambient pressure conditions.

In compression studies below 10 GPa on LSG crystals an orthopyroxene- ($\text{OEn-P}b\bar{c}a$) to post-orthopyroxene ($p\text{OEn-P}2_1/c$) transition has been discovered and found to be the second example of this type of transformation (ENDE et al., 2020). However, by a further increase in pressure for the α -phase two more phase transitions were observed between 9.9 and 10.4 GPa as well as around 14 GPa. The first transition was an expected transition from a monoclinic low-clinoenstatite ($\text{LCEn-P}2_1/c$) to a monoclinic high-pressure clinoenstatite ($\text{HP-CEn-C}2/c$) not known for LSG before. Nevertheless, the second transition, visible with Raman spectroscopy and single crystal X-ray diffraction, follows the first transition with only ~ 4 GPa pressure increase and therewith considerably lower pressure as expected. While a structure determination of the first modification was successful using in-situ diffraction data the structure of the second new phase could not be determined reliably even after a quenching from high-P conditions. However, a twinned and still monoclinic new high-pressure clinoenstatite unit cell was found most probably preserving the $C2/c$ space group.

WOODLAND, A.B. (1998): Geophys. Res. Lett., 25, 1241-1244.

ANDERSON, D.L., ANDERSON, O.L. (1970): J. Geophys. Res., 75, 3494-3500.

ENDE, M., MEUSBURGER, J.M., ZEUG, M., SCHEIDL, K.S., REDHAMMER, G.J., MILETICH, R. (2020): Inorg. Chem., 59, 17981-17991.

**SOLID SOLUTION BETWEEN THE TOURMALINE END-MEMBERS
ALUMINO-OXY-ROSSMANITE AND OXY-FOITITE FROM A PEGMATITE IN
HIGH-GRADE METAMORPHIC ROCKS**

Ertl, A.¹

¹Institut für Mineralogie und Kristallographie, University of Vienna, Althanstrasse 14, 1090 Vienna, Austria
e-mail: andreas.ertl@a1.net

Recently, a new tourmaline was described that represents the most Al-rich end-member composition (ERTL et al., 2021). Alumino-oxy-rossmanite, ideally $\square\text{Al}_3\text{Al}_6(\text{Si}_5\text{AlO}_{18})(\text{BO}_3)_3(\text{OH})_3\text{O}$, is an Al-rich oxy-tourmaline from a small pegmatitic body embedded in high-grade metamorphic rocks (amphibolite, biotite-rich paragneiss). This new pink coloured tourmaline was found in a Moldanubian pegmatite (of the Drosendorf Unit) that occurred in a large quarry near the village of Eibenstein an der Thaya, Waidhofen an der Thaya district, Lower Austria. Because of the low mode of associated mica (muscovite), ERTL et al. (2021) assumed that the silica melt, which formed this pegmatite, crystallized under relatively dry conditions, in agreement with the observation that alumino-oxy-rossmanite contains a lower amount of OH than most other tourmalines. These authors also concluded that the significant content of tetrahedrally-coordinated Al reflects the relatively high-temperature conditions (~ 700 °C) inferred for crystallization of this pegmatitic rock. From the same pegmatitic body a dark green Al- and Fe-rich tourmaline was described by ERTL et al. (2004). Based on new Mössbauer interpretations, this tourmaline does not have any tetrahedrally-coordinated Fe^{3+} in contrast to that publication. The amount of Fe^{3+} instead occurs at an octahedral site that is tetrahedrally distorted. Hence, the recalculated formula of the dark green tourmaline is $(\text{Na}_{0.52}\square_{0.47}\text{Ca}_{0.01})(\text{Al}_{1.49}\text{Fe}^{2+}_{0.83}\text{Mn}^{2+}_{0.40}\text{Fe}^{3+}_{0.10}\text{Li}_{0.05}\text{Mg}_{0.05}\text{Ti}^{4+}_{0.03}\text{Mn}^{3+}_{0.02}\square_{0.05})(\text{Al}_{5.90}\text{Mg}_{0.10})(\text{BO}_3)_3[\text{Si}_{5.73}\text{Al}_{0.27}\text{O}_{18}](\text{OH})_3[\text{O}_{0.55}(\text{OH})_{0.31}\text{F}_{0.14}]$. Considering this formula, the components of the dark green tourmaline are 27 mol% alumino-oxy-rossmanite, 16 mol% oxy-foitite, 15 mol% schorl, 11 mol% fluor-tsilaite, 6 mol% dutrowite, 4 mol% foitite, 3 mol% bosiite, 3 mol% oxy-dravite, 2 mol% fluor-elbaite, 2 mol% tsilaite, and 1 mol% fluor-liddicoatite. The sum of these components is 90 mol%. Hence this sample is a complex intergrowth of different endmembers, mainly of the alumino-oxy-rossmanite – oxy-foitite – schorl solid solution. Oxy-foitite, also described from high-grade metamorphic rocks (migmatitic gneisses) by BOSI et al. (2017) fits therefore well into the paragenesis with alumino-oxy-rossmanite.

This work was supported by the Austrian Science Fund (FWF) project no. P 31049-N29.

- BOSI, F., SKOGBY, H., HÅLENIUS, U. (2017): *Europ. J. Mineral.*, 29, 889-896.
 ERTL, A., HUGHES, J.M., PROWATKE, S., LUDWIG, T., LENGAUER, C.L., MEYER, H.-P., GIESTER, G., KOLITSCH, U., PRAYER, A. (2021): *Amer. Mineral.*, 106 (accepted).
 ERTL, A., PERTLIK, F., DYAR, M.D., PROWATKE, S., HUGHES, J.M., LUDWIG, T., BERNHARDT, H.-J. (2004): *Canad. Mineral.*, 42, 1057-1063.

PETROLOGY AND GEOCHEMISTRY OF TRACHYANDESITES AND RHYOLITES FROM BAD GLEICHENBERG, STYRIAN BASIN

Fehleisen, A.¹, Hauzenberger, C.A.¹, Skrzypek, E.¹, Gallhofer, D.¹

¹University of Graz, Universitätsplatz 3, 8010 Graz, Austria

e-mail: anna.fehleisen@edu.uni-graz.at

The volcanic formation of Bad Gleichenberg, localized in the eastern region of the Styrian Basin, is one of the less well studied magmatic formations in the Pannonian Basin System. This occurrence, which nowadays forms the Gleichenberg and Bschaikogel, presents trachyandesites and rhyolites with a calc-alkaline to shoshonitic affinity. A Middle Miocene crystallization age (13 ± 1 Ma) has been determined by K/Ar dating (BALOGH et al., 1990), and is clearly different from the Pliocene alkaline basaltic magmatic formation that characterizes the Styrian Basin. Samples collected from different areas around Bad Gleichenberg were investigated by petrological, mineral chemical and geochemical methods, which allowed to obtain novel information about this volcanic formation. The trachyandesites, which represent the majority of the volcanic rocks, follow a typical magmatic differentiation trend with SiO_2 varying from 57 to 62 wt%. CaO , FeO and MgO decrease with increasing SiO_2 , while Al_2O_3 , K_2O , Na_2O and P_2O_5 increase with increasing SiO_2 . Rhyolites occur in subordinate amounts with SiO_2 contents >71 wt%. Hydrous minerals such as biotite and apatite are commonly found in both magmatic series. The F content is high in biotite and apatite with values up to 2 and 3 wt%, respectively. TiO_2 contents in biotite can be as high as 8 wt%.

Idiomorphic zircons are commonly found in all samples, some with abundant apatite inclusions and visible zircon cores. LA-MC-ICPMS U-Pb zircon dating yielded homogeneous crystallization ages of ~14 Ma for both volcanic rock types. The analyzed zircon cores resulted in exactly the same age as the rims and the homogeneous zircons. The Gleichenberg volcanism and its geochemical characteristics are related to the simultaneous occurring extension and compression in the Styrian/Pannonian Basin caused by the collision of the Adriatic plate with Europe and a subsequent slab retreat. The Gleichenberg formation belongs to a group of related volcanic outcrops in the Western Pannonian Basin System such as the Balatonmária and Bükkalja Volcanic Fields in Hungary.

BALOGH, K., HARALD, L., PÉCSKAY, Z., RAVASZ, CS., SOLTI, G. (1990): MÁFÍ Évi Jel. 1988-ról, 451-468.

U/Pb AGES OF DETRITAL ZIRCONS OF DIFFERENT METASEDIMENTARY COMPLEXES OF THE KORALPE-WÖLZ NAPPE SYSTEM (EASTERN ALPS) - NEW EVIDENCES OF VARYING PROVENANCE AND PROTOLITH AGES BY LA-ICPMS ANALYSES

Frank, N.¹, Hauzenberger, C.A.¹, Skrzypek, E.¹, Schuster, R.², Gallhofer, D.¹,
He, D.³, Kurz, W.¹

¹University of Graz, Graz, NAWI Graz Geocenter, Universitätsplatz 2, 8010 Graz, Austria

²Department of Hard Rock Geology, Geological Survey of Austria, Neulinggasse 38, 1030 Vienna, Austria

³State Key Laboratory of Continental Dynamics, Department of Geology, Northwest University,
Xian, No.229, North Taibai Road, Xi'an City, Shaanxi Province, China
e-mail: nils.frank@edu.uni-graz.at

The Koralpe-Wölz nappe system, as part of the Austroalpine nappe complex, belongs to the crystalline basement of the Eastern Alps and is composed of different metasedimentary complexes with mono-, bi-, or polymetamorphic history (SCHMID et al., 2004; HABLER & THÖNI, 2001; THÖNI & MILLER, 2009). Very little is known about the protoliths of the Koralpe-Wölz nappe system, while the metamorphic conditions for several metamorphic events are very well constrained. This nappe system experienced high grade Eo-Alpine metamorphism during or after Alpine nappe stacking. The different complexes were also affected by Permian high-temperature – low-pressure metamorphism.

Based on U/Pb data of detrital zircons from different metasedimentary complexes, we can give an overview about maximum ages of sediment deposition.

Zircon age spectra of sampled metasediments of three different complexes indicate post-Variscan sedimentation with maximum ages of ~300 Ma (Koralpe / Saualpe), ~330 Ma (Rappold) and ~360 Ma (Millstatt). Zircon ages of the Radenthein complex indicate post-Cadomian sedimentation. The main peaks for zircons of the Koralpe and Saualpe complex show Ordovician and Carboniferous ages. Two samples from Saualpe (Koralpe Complex) have metamorphic rims or crystals and show main zircon age peaks at ~275 Ma which agrees well with the metamorphic “Permian event” (THÖNI et al., 2008). The age spectra for the Rappold, Millstatt, and Radenthein complexes are dominated by Cadomian zircons. Dominating Cadomian zircon ages are detectable at one micaschist sample of the Pohorje massif (Koralpe) as well. One micaschist sample from Saualpe and one micaschist sample from the Pohorje massif (Koralpe) are dominated by zircons with an age of around 90 Ma, recording the Eo-Alpine high-grade metamorphic event.

HABLER, G., THÖNI, M. (2001): J. Metamorphic Geol., 19, 679–697.

SCHMID, S.M., FÜGENSCHUH, B., KISSLING, E., SCHUSTER, R. (2004): Eclogae geol. Helv., 97, 93–117.

THÖNI, M., MILLER, C. (2009): Chem. Geol., 260, 20–36.

THE EFFECT OF FLUORINE ON REACTION RIM GROWTH DYNAMICS IN THE TERNARY CaO-MgO-SiO₂ SYSTEM

Franke, M.G.¹, Joachim-Mrosko, B.¹

¹Institute of Mineralogy and Petrography, University of Innsbruck, Innrain 52f, 6020 Innsbruck, Austria
e-mail: Mees.Franke@uibk.ac.at

Metamorphic corona and reaction rim structures are examples of a net-transfer reaction, where pre-existing mineral phases react to new phases. Growth of these metamorphic structures indicates a change in physical parameters such as pressure and temperature, a change in the chemical composition of the system and/or the presence of volatiles. In particular the effect of volatile components on net-transfer reactions remains is, however, poorly understood. In order to accurately model metamorphic and metasomatic processes and test the potential of natural reaction rims to be used as "geofluidometers", a quantification of the effect of volatiles on reaction-rim growth dynamics is necessary.

In this study, we investigate the effect of fluorine on reaction rim growth dynamics in the ternary CaO-MgO-SiO₂ system. A series of piston cylinder experiments was conducted at P-T conditions of 1000 °C and 1.5 GPa. In each experiment, reaction rims were grown for 20 minutes between a natural wollastonite crystal and MgO powder matrix with the addition of 0 to 10 wt% fluorine. Electron microprobe analyses and Raman spectroscopy were used to analyse the crystalline phases present in the reaction rim.

In the fluorine free system, we produced a monomineralic rim sequence of wo | mer | di | fo | per, complying with phase stabilities at water saturated conditions. As soon as 0.1 wt% fluorine was introduced into the system, humite group minerals (HGMs) and monticellite were stabilised resulting in the multilayer rim sequence wo | mer | mtc | fo + HGMs | per. In experiments with fluorine concentrations >1 wt%, palisades of diopside and cuspidine appear where cuspidine represents the major fluorine sink. Our data show that the addition of fluorine stabilises the fluorine bearing phases cuspidine and HGMs to higher temperatures. Furthermore, results of this study reveal a positive correlation between overall rim thickness and fluorine content. Reaction rim widths increased from 12.50 (146) to 105.49 (185) µm in fluorine free and 10 wt% F experiments respectively.

Our results illustrate the significance of fluorine during net-transfer reactions, where its presence has a strong effect on [I] the overall rim thickness, which increases by 10-fold if 10 wt% F is added to the water saturated system, [II] phase stabilities, where fluorine bearing minerals such as humite group minerals and cuspidine are stabilised, [III] the relative mobilities of the individual components, and as a consequence [IV] the internal rim microstructure. These findings have important implications for reaction rims to be utilized as a potential "geofluidometer" and may allow us to unravel the chemical composition of metasomatic fluids.

**MAGMATIC AND SEDIMENTARY EVOLUTION OF THE NORIC NAPPES
(GREYWACKE ZONE) – THE VARISCAN SLOPING CONTINENTAL MARGIN**

Fritz, H.¹, Nievoll, J.², Gallhofer, D.¹, Hauzenberger, C.A.¹, Gritsch, B.¹, Pfatschbacher, M.¹,
Krenn, K.¹, Karner-Rühl, K.¹

¹University of Graz, Heinrichstrasse 26 and Universitätsplatz 2, 8010 Graz, Austria

²Gumpendorfer Straße 83–85/2/48, 1060 Vienna, Austria

e-mail: harald.fritz@uni-graz.at

Detailed mapping of monotonous (boring) magmatic and sedimentary suites within the Eastern Greywacke Zone allow distinction of four different nappes within the Noric-Tirolic nappe assembly. These are from tectonic bottom to top the Hocheck-, Rossegg-, Steinbach-, and Aschbach nappes. The lowermost Hocheck nappe rests tectonically on slivers of Silbersberg and Veitsch nappes. U/Pb dating of about 600 zircons of magmatic members and of detrital zircons derived from sandstones enable correlation of units across individual nappes. Retrodeformation of the nappe assembly together with definition of different sedimentary facies realms allow a reconstruction of the Ordovician to lower Devonian paleogeography. Highlights of the study include: (1) Magmatism of Blasseneck porphyry type initiated already by c. 480 Ma and continued until c. 445 Ma; all magmatics are calc-alkaline and range from andesite to rhyolite. This documents magmatic pulses from the end of the Cenozoic Orogeny to the opening of the Rheic Ocean. (2) Massive, up to 1000 meter thick porphyries within the Hocheck- and Rossegg Nappes correlate timely with thin layers of tuffs and sills within the Steinbach Nappe. This suggests originally large distances between these nappes and consequently large tectonic transport during Variscan and/or Alpine times. (3) Detrital zircons allow dating of the sandstones within Steinbach- and Aschbach-nappes that range from lower Ordovician to upper Silurian. Sandstones incorporated increasingly lithic components of the collapsing passive continental Gondwana margin. (4) Age correlation together with retrodeformation and definition of facies domains allow reconstruction of this continental margin. The Rad Formation within Hocheck- and Rossegg-nappes is defined, from macrofossils, as shallow marine domain whereas the Stocker Formation of the Steinbach Nappe is, from sedimentary structures, defined as continental slope. The Sommerauer Formation of the Aschbach Nappe contains turbidite interpreted as channel or lobe sediments on the ocean floor.

**COUPLED DISSOLUTION AND CRYSTALLIZATION KINETICS OF
AMORPHOUS AND CRYSTALLINE CALCIUM CARBONATE IN
AQUATIC MEDIA**

Galan, I.¹, Purgstaller, B.¹, Grengg, C.¹, Müller, B.², Dietzel, M.¹

¹Institute of Applied Geosciences, Graz University of Technology, Rechbauerstraße 12, 8010 Graz, Austria

²Institute of Analytical Chemistry and Food Chemistry, Graz University of Technology,

Stremayrgasse 9, 8010 Graz, Austria

e-mail: igalangarcia@tugraz.at

The transformation behaviour of amorphous (ACC) and crystalline calcium carbonate (e.g. vaterite) in aquatic media at high solid/liquid ratio can lead to the formation of so-called ‘calcium carbonate cements’, where reaction kinetics are still less explored. In the present study the dissolution and precipitation processes in the ACC-vaterite-H₂O system were monitored by means of in-situ optical pH sensors and Raman spectroscopy. In addition, solids and liquids were sampled and classically analysed at specific experimental run times. The experimental data were complemented with thermodynamic modelling. The influence of Mg²⁺ ions on the reaction kinetics was assessed in parallel experiments where a 30 mM MgCl₂ solution instead of pure water was used. Vaterite - in the presence of ACC - leads to significantly more cohesive matrixes than aragonite and calcite, which is attributed to the differences in morphology, surface area and dissolution kinetics. The dissolution of vaterite is accompanied by a pH rise and takes place in two stages: (i) immediately after the conversion of ACC to vaterite and (ii) after a period of ~48 hours. In the presence of Mg the formation of vaterite is inhibited and only one dissolution stage, corresponding mostly to the initially added vaterite, is observed after ~30 h. Mg is mostly incorporated into the final calcite and the Mg-containing experiment constant conditions are reached after ~90 h, about 10 hours earlier than using pure H₂O. Time-resolved in-situ technique for pH and solid analyses are suitable and promising tools to further tailor new calcium carbonate based binders.

GEOCHEMICAL AND GEOCHRONOLOGICAL CHARACTERIZATION OF ZIRCON MEGACRYSTS FROM KAWISIGAMUWA CARBONATITE, SRI LANKA

Gallhofer, D.¹, Skrzypek, E.¹, Fernando, G.W.A.R.², Hauzenberger, C.A.¹

¹University of Graz, Graz, Universitätsplatz 2, 8010, Graz, Austria

²The Open University of Sri Lanka, PO Box 21, Nugegoda, Sri Lanka

e-mail: daniela.gallhofer@uni-graz.at

Since *in-situ* dating methods consume large amounts of matrix-matched reference materials, suitable materials are highly sought-after. Ideally, reference materials should have a large volume and be isotopically homogeneous. Here, we present zircon megacrysts from the Kawisigamuwa carbonatite, Sri Lanka, which fulfil these criteria. In this study, we first characterize the crystallinity and composition of the zircon megacrysts. We then present U-Pb isotopic data collected with laser ablation-inductively coupled plasma mass spectrometry (LA-ICPMS) and test the influence of various instrumental settings, primary reference materials, and chemical composition on U-Pb dates.

The Sri Lankan zircon megacrysts have low and variable trace element contents corresponding to zones with distinct cathodoluminescence emission (CL-zones) and are well crystallised (FWHM <5 cm⁻¹). The increasingly darker CL-zones reflect an increase of REE, Th, U, and, to some degree, P, while Hf concentration is inversely correlated with CL-brightness and also seems to be grain-dependant. Very dark CL bands have total REE abundances of more than 100 µg/g, which are associated with high Th/U ratios (2.6-3), low P and Hf contents. Some moderately CL-bright zones are highly enriched in P (>120 µg/g) and show only moderate REE and Hf contents. Phosphorus, REEs, and Al are likely accommodated in the crystal lattice by xenotime-type and berlinitite-type substitutions.

We determined U-Pb ages for four zircon megacrysts. The single zircon dates range from 480-540 Ma. Data show that smaller spot diameters (15 µm, 25 µm) yield a larger scatter of single data, with some of them being markedly younger. Data determined with 35 µm spot size show little variation and commonly overlap within error. The concordant zircon analyses yield a weighted mean ²⁰⁶Pb/²³⁸U age of 529.3 ± 0.4 Ma (internal 2 SE, n = 304/318, MSWD = 3), which is regarded as the best estimate of the (minimum) crystallization age of the zircon megacrysts from the carbonatitic magma.

Our results indicate that the Sri Lankan zircons are probably less suitable as a secondary reference material for LA-ICPMS analysis of trace elements. However, due to their isotopic homogeneity the zircons can be used as secondary reference material for U-Pb dating when an additional TIMS reference age is established.

REACTION OF MgO WITH CARBOXYLIC ACID

Gerger, S.¹, Baldermann, A.¹, Dietzel, M.¹

¹Institute of Applied Geosciences, Graz University of Technology, NAWI Graz Geocenter,
Rechbauerstraße 12, 8010 Graz, Austria
e-mail: sabrina.gerger@tugraz.at

The chemical reaction mechanisms during cast stone formation and in particular the reaction of periclase (MgO) with organic acids are still poorly understood. Therefore, experimental investigations on the reaction of MgO -organo- H_2O castables inferred by type and composition of low temperature MgO_{-l} together with dead-burned MgO_{-d} with citric, malic or acetic acids were carried out. The mineralogy, microstructure and the reactivity of the educts and the precipitates were assessed by XRD, FTIR spectroscopy, sound velocity analyses and scanning electron microscopy. The overall hardening behavior of the reaction product within the MgO -carboxylic acid- H_2O system is strongly influenced by the type and spatial distribution of the distinct acid reacting with the MgO_{-l} . Best hardening performance was observed with citric and malic acid due to the formation of interconnecting Mg-Hcitrate and Mg-malate precipitates, whereas Mg-acetate binding was spatially restricted. Impurities of MgO_{-d} , such as the minerals merwinite $[\text{Ca}_3\text{Mg}(\text{SiO}_4)_2]$, magnesioferrite $[\text{MgFe}^{3+}\text{O}_4]$ or larnite $[\text{Ca}_2(\text{SiO}_4)]$, lead to enhanced hardening by the formation of Ca-Fe-Mg-organo precipitates. Ongoing studies help to better understand the coupled dissolution and precipitation phenomena within the MgO -carboxylic acid- H_2O system. In particular, the stability constants of distinct aqueous complexes and solid phases have to be considered and assessed to develop a conceptual model of the reaction mechanisms and pathways, which are responsible for the hardening process.

ATOM PROBE TOMOGRAPHY OF GEOLOGIC MATERIALS

Gopon, P.^{1,2}, Hofer, C.³, Douglas, J.^{1,4}, Moody, M.², Melcher, F.¹¹Ls. für Geologie und Lagerstättenlehre, Montanuniversität Leoben, Peter-Tunner Straße, 8770 Leoben, Austria²Dept. of Materials, University of Oxford, Parks Road, OX1 3PH, Oxford, UK³Ls. für Stahldesign, Montanuniversität Leoben, Roseggerstrasse, 8770 Leoben, Austria⁴Dept. of Materials, Imperial College London, Royal School of Mines: Exhibition Road, SW7 2AZ, London, UK

As geologists we are often focused on large scale questions, however many of the answers to these questions lie not in describing regional structures but in the proper interpretations of small scale observations. The emerging field of nano-geochemistry has been important in deepening our understanding of a range of geological processes. From a new understanding of the U/Pb system to ore body formation, many of these findings have been elucidated with the aid of the relatively new technique of atom probe tomography (APT; VALLEY et al., 2015; Gopon et al., 2019). APT is a destructive technique that evaporates a sample one atom at a time, in order to digitally reconstruct it (Figure 1). The resultant dataset contains the location and chemical, and isotopic, identity of nearly every atom of the sample in three dimensions to near atomic scale resolution (Figure 1). These datasets are a treasure trove of major, minor, and isotopic chemical information that provides us with an unrivaled view into a materials inner workings.

This talk will introduce the audience to the new technique of APT, challenges of APT, as well as its application or potential application to a select number of geologic systems; namely cosmochemistry, ore geology, and diffusion studies. We will also introduce the cutting edge new APT capability at the University of Leoben, and our current and future research.

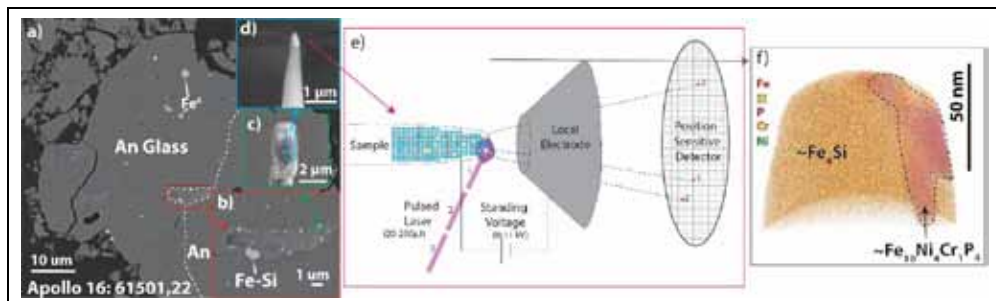


Figure 1. Generalized APT workflow, example from metallic inclusions in Apollo 16 lunar dust. a) BSE image showing sub-micrometer phases of Fe-Si; b) region chosen for a site specific liftout; c) APT specimen prior to the final annular milling step; d) APT specimen after the final annular milling, ready to be put into the atom probe; e) generalized geometry of an APT experiment, the needle shaped sample (from d) on the left; f) reconstruction of the APT needle shaped specimen after the experiment, note that only Si, Cr, and P are shown for clarity.

GOPON, P., DOUGLAS, J.O., AUGER, M.A., HANSEN, L., WADE, J., CLINE, J.S., ROBB, L.J., MOODY, M.P. (2019): Econ. Geol., 114, 1123–1133.

VALLEY, J.W., REINHARD, D.A., CAVOSIE, A.J., USHIKUBO, T., LAWRENCE, D.F., LARSON, D.J., KELLY, T.F., SNOEYENBOS, D.R., STRICKLAND, A. (2015): Presidential Address. Amer. Miner., 100, 1355–1377.

**EOARCHEAN SUBDUCTION-LIKE MAGMATISM
RECORDED IN 3750 MA MAFIC–ULTRAMAFIC ROCKS OF THE
UKALIQ SUPRACRUSTAL BELT (QUÉBEC)**

Grocolas, T.^{1,2}, Bouilhol, P.¹, Caro, G.¹, Mojzsis, S.J.^{3,4,5}

¹Université de Lorraine, CNRS, CRPG, 15 rue Notre Dame des Pauvres BP 20,
54500 Vandœuvre les Nancy, France

²Institute of Earth Sciences, University of Lausanne, Géopolis, 1015 Lausanne, Switzerland

³Origins Research Institute, Research Centre for Astronomy and Earth Sciences,
15-17 Konkoly Thege Miklós Road, 1121 Budapest, Hungary

⁴Department of Lithospheric Research, University of Vienna, Althanstraße 14, 1090 Vienna, Austria

⁵Department of Geological Sciences, University of Colorado, 2200 Colorado Avenue, Boulder,
Colorado 80309-0399, USA

e-mail: stephen.james.mojzsis@univie.ac.at

Our understanding of the nature of crustal formation in the Eoarchean is limited by the scarcity and poor preservation of the oldest rocks, and variable and imperfect preservation of protolith magmatic signatures. These limitations hamper our ability to place quantitative constraints on thermomechanical models (e.g., the stagnant-lid and the active-lid models; FISCHER & GERYA, 2016a, 2016b) for early crustal genesis and hence on the operative geodynamic regimes at that time. The ca. 3.75 Ga Ukaliq supracrustal enclave (northern Québec; CARO et al., 2017) is composed of diverse serpentized ultramafic rocks and amphibolitized mafic schists. The protoliths of the ultramafic rocks are cumulative dunites, olivine-pyroxenites and hornblendites and the mafic amphibolites are basalts to basaltic andesites. Based on major and trace element mineral chemistry and geothermometry, we show the partial preservation of cumulative pyroxenes and amphiboles. Two suites of lavas–cumulates are inferred with a TiO₂-rich, flat rare-earth element pattern-bearing, clinopyroxene-dominated, tholeiitic suite, and a TiO₂-poor, U-shaped rare earth element pattern-bearing, orthopyroxene-dominated, boninite-like suite. Coupled with ¹⁴²Nd isotopic measurements (CARO et al., 2017) and melt modeling, we explored two liquid lines of descent: (i) a water-undersaturated, adiabatic decompression-related, tholeiitic sequence fractionating olivine, clinopyroxene, amphibole, and plagioclase; and (ii) a boninite-like suite documenting the evolution of an initially primitive, flux melting-associated basaltic to andesitic melt at ~0.5 GPa and containing >4 wt% H₂O through fractionation of olivine, orthopyroxene, and amphibole. The large amounts of water required to form near-liquidus amphibole as well as the negative ¹⁴²Nd anomalies in boninitic lavas suggest that a deep fluid carrying the ¹⁴²Nd anomaly played a role in the genesis of the boninitic melts. The simplest way to explain such differentiation sequences and geochemical signatures is the foundering of a Hadean crust in a similar way as modern-style subduction triggering adiabatic decompression generating the tholeiitic melts followed by flux melting producing the ¹⁴²Nd anomaly-bearing boninitic melts.

CARO, G., MORINO, P., MOJZSIS, S.J., CATES, N.L., BLEEKER, W. (2017): Earth Planet. Sci. Lett., 457, 23–37.

FISCHER, R., GERYA, T. (2016a,b): J. Geodyn., 100, 198–214; Gondwana Res., 37, 53–70.

**A U/Pb ZIRCON STUDY ON THE SCHLADMING NAPPE AND ITS
IMPLICATIONS FOR THE PRE-ALPINE EVOLUTION OF THE AUSTROALPINE
BASEMENT**

Haas, I.¹, Kurz, W.¹, Gallhofer, D.¹, Hauzenberger, C.A.¹

¹University of Graz, NAWI Graz Geocenter - Institute of Earth Sciences, Heinrichstraße 26, Graz, 8010, Austria
e-mail: isabella.haas@uni-graz.at

The Schladming Nappe of the Eastern Alps is part of the Silvretta-Seckau Nappe system and is widely built up by pre-Alpine crystalline basement rocks. It consists mainly of paragneisses intruded by subsequently overprinted granites and granodiorites, which are further overlain by a sedimentary cover (quartzite and meta-conglomerate, e.g. Rannach Formation).

Lacking precise geochronological data, the meta-granitoids have so far been assumed to be connected to widely distributed magmatic intrusions related to the Variscan orogeny. To gain insight into the timing of the magmatic emplacement, as well as the tectono-metamorphic history of the Schladming nappe, U-Pb zircon ages were determined by LA-MC-ICPMS. The acquired ages of the meta-granitoids hint at two intrusive events for the main part of the Schladming Nappe: (1) a Cambrian event with zircon $^{206}\text{Pb}/^{238}\text{U}$ mean ages between 494 ± 2 Ma and 498 ± 3 Ma and (2) an Upper Devonian event with zircon mean ages between 353 ± 2 Ma and 371 ± 2 Ma correlating with early Variscan magmatism. Interestingly, an additional Permian-aged intrusion event was found in the SE part of the research area with zircon mean ages between 262 ± 2 Ma and 264 ± 2 Ma. According to the available geological maps these intrusives are part of the Schladming Nappe. However, due to the unclear tectonic contact to the adjacent metapelites of the Wölz Nappe system the actual tectonic position remains debated.

The geochemical data confirms a peraluminous character for all meta-granitoids. The older group has consistently higher SiO_2 values while the Upper Devonian age group has moderate SiO_2 contents but higher amounts of MgO , FeO , and Al_2O_3 as well as Sr and Ba . Additionally, the samples of the Devonian age group can be divided into subgroups, one group reflecting negative Eu-anomalies ($\text{Eu}_N/\text{Eu}^* = 0.44-0.69$) and the other lacking pronounced Eu-anomalies ($\text{Eu}_N/\text{Eu}^* = 0.82-1.08$). The Permian group clearly differs geochemically through partly higher abundance of K_2O , and otherwise shows similarities to the Cambrian age group. While characteristics of the Upper Devonian samples hint at a magmatic arc origin, the oldest and youngest group seem to be linked to a more complex formation.

**THE COLLECTIONS OF THE ARCHIVE OF THE HISTORY OF GEOLOGY
AT THE UNIVERSITY OF VIENNA:
ORGANIZING AND DIGITIZING OF GEOLOGICAL HERITAGE**

Hamilton, M.¹, Nagl, P.²

¹Archiv der Geschichte der Geologie, Institute of Geology, University of Vienna, Althanstraße 14, 1090 Vienna,
Austria

²Department of Lithospheric Research, University of Vienna, Althanstraße 14, 1090 Vienna, Austria
e-mail: Margret.Hamilton@univie.ac.at

The collections of the Geological Institute go back to the initiative of the former head of the Geological Institute Alexander Tollmann (1928-2007). He collected documents from the 1970s at the former institute and transferred them into a separate depot when relocating of the institute in 1995 to the present Geozentrum in the 9th district of Vienna, Althanstraße 14. He arranged and labelled a number of documents.

Many documents of the institute were collected and preserved in various files during the management period of Alexander Tollmann including also his personal records. Thus, there are documents about new acquisitions of the institute and also books about excursions. Partial, but also entire legacies of various geoscientists, were collected in colorful boxes. An interesting part of Eduard Suess's (1831-1914) legacy, the first professor of the Geological Institute, contains a lot of handwritten records. Alexander Tollmann sorted and described a small number and put them into files.

Likewise, part sorted or unsorted legacies were obtained from well-known geoscientists, such as Martha Cornelius-Furlani (1886-1974) and her husband Peter Cornelius (1888-1950). An extensive legacy by Walter Medwenitsch (1927-1992) was found in colorful boxes in an extremely chaotic state. As a side note: there is a beautiful collection of beer mats and even collectors magazines. This gives an indication for the preference of Medwenitsch for beers.

A geological map of the Eastern Alps painted by Leopold Kober (1883-1970) had been restored. Kober named it "Tektonogramm", dated in 1937.

There is also a hammer-collection, hammers of geologists and mineralogists from former times to nowadays given to the Geological Archive.

A large collection of slides with geological content from the legacy of Alexander Tollmann has been preserved. Similarly, many slides of Walter Medwenitsch existed in a disorderly state. In the legacy of Tollmann and Medwenitsch there are a series of photos of geoscientists. These are already sorted and digitized.

A collection of about 1000 pieces of black and white glass photo plates, in excellent condition, are also put into order and digitized. An extensive collection of hammers dating back to the time of Eduard Suess has already been brought into shape.

At the request of the current head of the institute, Prof. Mag. Dr. Bernhard Grasemann, the author took up the task of organizing, systematizing, digitizing, and making accessible this extensive collection in modern archive boxes to the interested audience, professors, and students alike.

**DER EINFLUSS VON ALTERUNGSPROZESSEN AUF DIE RHEOLOGISCHEN
EIGENSCHAFTEN UND CHEMISCHE ZUSAMMENSETZUNG
KOHLENSTOFFHALTIGER TONE**

Hassler, J.¹, Knodt, R.¹, Piribauer, C.¹, Diedel, R.², Häußer, S.²

¹Forschungsinstitut für Anorganische Werkstoffe – Glas | Keramik (FGK), Heinrich-Meister-Straße 2,
56203 Höhr-Grenzhausen, Germany

²Stephan Schmidt KG, Bahnhofstraße 92, 65599 Dornburg, Germany
e-mail: jannis.hassler@fgk-keramik.de

Im Rahmen eines öffentlich geförderten Projektes wird das Alterungsverhalten kohlenstoffhaltiger, keramischer Tone untersucht und die Einflussgröße eines industriell verwendeten Additivs zur Kontrolle von Alterungsprozessen ermittelt. Alterungsprozesse in Tonen führen zu einer Veränderung der chemischen und mineralogischen Zusammensetzung der Tone und so zu (je nach entstehendem Produkt positiven oder negativen) Änderungen der keramischen Verarbeitungseigenschaften. So konnte im Rahmen vorheriger Arbeiten gezeigt werden, dass Huminsäuren, welche selbst Produkte von Oxidations- und Zersetzungsprozessen organischer Materie und somit natürliche Bestandteile von Tonen sind, sich positiv auf die keramischen Verarbeitungseigenschaften auswirken (PIRIBAUER et al., 2020).

Zur Ermittlung der Veränderungen über die Zeit wurde ein kohlenhaltiger Haldenton über einen Zeitraum von 6 Monaten parallel an Luftatmosphäre sowie in einer Klimakammer unter stetiger Atmosphäre zur Alterung gelagert und periodisch auf rheologische Eigenschaften (Viskosität, Trockenbiegefestigkeit (TBF)) und chemische-mineralogische Zusammensetzung (eluierbare Ionen, Leitfähigkeit, Gehalte an C, N und S) untersucht. Zur Erfassung des Einflusses industriell genutzter Additive zur Kontrolle von Alterungsprozessen wurden mit BaCO₃ versetzte Proben analog eingelagert und analysiert. In den mit Additiv versetzten Tonproben ist über den Versuchszeitraum eine stetige Abnahme an eluierbarem Barium so lange zu beobachten, bis die Elementkonzentration im Eluat zum Messzeitpunkt 12 Wochen unterhalb der Nachweisgrenze fällt. In allen untersuchten Proben ist ein Anstieg an löslichem Sulfat über den Versuchszeitraum nachzuweisen, welcher in den Proben ohne zugegebenes Additiv im direkten Vergleich verstärkt und beschleunigt nachweisbar ist. In allen Tonproben sind in Korrelation zu den löslichen Sulfatgehalten verstärkte Löslichkeiten an Ca- und Mg-Kationen zu beobachten. Die mit BaCO₃ versetzten Haldentone verzeichnen in der ersten Hälfte des Versuchszeitraums eluierbare Konzentrationen an Fe- und Al-Ionen, welche unstetig mit der Versuchsdauer abnehmen, bis sie zum Zeitpunkt t = 8 Wochen unterhalb der Nachweisgrenze fallen. Veränderungen an Gehalten von Gesamtschwefel, Stickstoff und Kohlenstoff in den Proben sind über den Versuchszeitraum nicht erkennbar.

Die Haldentone ohne zugegebenes Additiv verzeichnen in Korrelation mit den zunehmenden eluierbaren Anteilen an Sulfat und Erdalkalienten eine Zunahme der Viskosität. Eine Zunahme der TBF ist in keiner der untersuchten Proben über den Versuchszeitraum zu beobachten.

HIGH PRESSURE BEHAVIOUR OF PEARCEITE-POLYBASITE GROUP MINERALS

Hejny, C.¹, Wierer, A.¹, Venturi, A.¹

¹University of Innsbruck, Innrain 52, 6020 Innsbruck, Austria

e-mail: clivia.hejny@unibk.ac.at

Pearceite-polybasite group minerals (PPGM), $[(\text{Ag},\text{Cu})_6(\text{As},\text{Sb})_2\text{S}_7][\text{Ag}_9\text{Cu}\text{S}_4]$, are intriguing materials with Ag^+ fast ion conduction character that have attracted a lot of interest in the recent years. The notation of the chemical formula reflects the fact, that PPGM are composed of two different layers: layer A with general composition $[(\text{Ag},\text{Cu})_6(\text{As},\text{Sb})_2\text{S}_7]^{2-}$ and layer B with general composition $[\text{Ag}_9\text{Cu}\text{S}_4]^{2+}$, whereat layer B is the place where the ionic conductivity takes places (BINDI et al., 2007). The root-name *pearceite* is given to minerals where As is dominant over Sb and the root-name *polybasite* for Sb-dominant phases. In addition, a suffix is attached to the root-name to give crystallographic information on the superstructure variant. Trigonal polytypes with lattice parameters $a \approx 7.5$, $c \approx 12.0$ Å are given the hyphenated italic suffix *-Tac*, trigonal polytypes with lattice parameters $a \approx 15.0$, $c \approx 12.0$ Å have *-T2ac* and monoclinic polytypes with $a \approx 26.0$, $b \approx 15.0$, $c \approx 24.0$ Å, $\beta \approx 90^\circ$ have *-M2a2b2c* as suffix. Depending on the exact chemical composition and disorder of the Ag and Cu atoms within the crystal structure a number of different crystal structures and their temperature-induced phase transitions are known (e.g. BINDI et al., 2006).

In order to test the possibility to use pressure as a switch for superconductivity, i.e. to induce phase transitions from the ionic conduction form to an ordered or partially ordered superstructure form with Ag ions “frozen-up” into fixed atomic positions, in-situ single-crystal diffraction experiments of PPGM have been performed in the diamond anvil cell.

A crystal fragment of pearceite-*Tac*, $\text{Ag}_{13.3}\text{Cu}_{3.8}\text{As}_{1.5}\text{Sb}_{0.4}\text{S}_{11}$, $a = 7.3510(6)$, $c = 11.892(1)$ Å, $V = 556.5(1)$ Å³, $P\bar{3}m1$, from the Clara Mine, Oberwolfbach, Schwarzwald, Germany, shows strong diffuse diffraction features parallel to c^* at ambient conditions that are characteristic for the high temperature fast ion conduction form. On P increase the appearance of additional reflections at $h/2$ and $k/2$ reveals a phase transition to the *T2ac* superstructure between 0.1 and 1.2 GPa (1.2 GPa: $a = 7.3137(5)$, $c = 11.723(4)$ Å, $V = 542.8(2)$ Å³). Diffuse maxima condense within the originally uniform diffuse diffraction features. Furthermore, a number of sharp satellite reflections appear at 1.2 GPa and move between 1.2 and 2.6 GPa (2.6 GPa: $a = 7.2723(4)$, $c = 11.530(3)$ Å, $V = 528.1(1)$ Å³). These features are in accordance with the explanation of a composite modulated structure model for the PPGM superstructures (WITHERS et al., 2008). A crystal of polybasite-*T2ac*, $\text{Ag}_{15.0}\text{Cu}_{1.7}\text{Sb}_{1.8}\text{As}_{0.2}\text{S}_{11}$, $a = 15.1006(5)$, $c = 11.9329(4)$ Å, $V = 2356.5(1)$ Å³, $P321$ (Husky Mine, Elsa, Yukon Territory, Canada) transforms to the *M2a2b2* superstructure variant, $a = 14.785(5)$, $b = 22.643(9)$, $c = 25.48(2)$ Å, $\alpha = 89.94(5)$, $\beta = 90.69(5)$, $\gamma = 89.98(3)$, $V = 8531(9)$ Å³ between 3.5 and 5.4 GPa.

BINDI, L., EVAIN, M., PRADEL, A., ALBERT, S., MENCHETTI (2006): Phys. Chem. Miner., 33, 677-690.

BINDI, L., EVAIN, M., SPRY, P.G., MENCHETTI, S. (2007): Amer. Miner., 92, 918-925.

WITHERS, R.L., NORÉN, L., WELBERRY, T.R., BINDI, L., EVAIN, M., MENCHETTI, S. (2008): Solid State Ionics, 179, 2080-2089.

THERMODYNAMICS OF ALKALI FELDSPAR SOLID-SOLUTIONS DERIVED FROM PARTITIONING EXPERIMENTS

Heuser, D.¹, Ingegneri, F.¹, Lengauer, C.L.², Petrishcheva, E.¹, Abart, R.¹

¹Department of Lithospheric Research, University of Vienna, Althanstraße 14, 1090 Vienna, Austria

²Institute of Mineralogy and Crystallography, University of Vienna, Althanstraße 14, 1090 Vienna, Austria
e-mail: david.heuser@univie.ac.at

Alkali feldspars form a solid-solution between the $\text{NaAlSi}_3\text{O}_8$ (albite) and the KAlSi_3O_8 (K-feldspar) end-members with complete miscibility at temperatures above about 600 °C and a miscibility gap at lower temperatures. Accordingly, alkali feldspar of intermediate composition usually exsolves during slow cooling producing a lamellar intergrowth of more Na-rich and more K-rich alkali feldspar, a microstructure referred to as perthite. The lamellar intergrowth is usually coherent. The strain energy associated with coherent lamellar intergrowth counteracts exsolution. As a consequence, the solvus for coherent exsolution is located at lower temperatures than the “strain free solvus”. Despite being a widespread phenomenon, the quantification of exsolution in alkali feldspar remains challenging due to the chemical and structural variability of alkali feldspars and the complex interplay between non-ideal thermodynamic mixing properties and elastic stress and strain in coherent intergrowth. In this study, four natural gem-quality alkali feldspars including Madagascar Orthoclase ($X_K = 0.95$, where X_K is the K site fraction on the alkali sublattice), Volkesfeld Sanidine ($X_K = 0.85$), Zillertal Adular ($X_K = 0.85$) and Zinggenstock Adular ($X_K = 0.90$) were used for partitioning experiments. Powder XRD revealed monoclinic ($C2/m$) symmetry for Madagascar Orthoclase and Volkesfeld Sanidine, which both have highly disordered Al-Si, and triclinic ($C\bar{1}$) symmetry for Zillertal and Zinggenstock Adular, which both have ordered Al-Si. All four feldspars have very low Ca contents (Ca p.f.u. <0.001), Madagascar orthoclase has an appreciable Fe content (Fe p.f.u. = 0.045), the other three feldspars contain some Ba (Ba p.f.u. = 0.013 (Volkesfeld), 0.015 (Zillertal), 0.010 (Zinggenstock), 0.001 (Madagascar). The Na-K partitioning between the feldspars and a KCl-NaCl salt melt was determined experimentally at 800 °C, 900 °C and 1000 °C. The partitioning curves were used to determine the parameters for an asymmetric Margules-type binary mixing model including their temperature dependence. The obtained Margules parameters were used for calculating the partitioning curves and the coherent and strain free solvi, where the strain energy due to coherent intergrowth was taken from ROBIN (1974). Comparison of the measured and the calculated partitioning curves reveals that the models systematically underestimate the thermodynamic non-ideality of the solid-solution, especially at low temperatures. The triclinic Zillertal Adular exhibits the most non-ideal Na-K partitioning, and the calculated partitioning curves show the strongest deviation from the experimentally observed curves followed in both aspects by the triclinic Zinggenstock Adular. This suggests increasing deviation of the thermodynamic model from the observed relations with increasing degree of non-ideality in the element partitioning. We infer that differences in Al-Si ordering and in the concentrations of minor elements such Ca, Ba, and Fe have substantial influence on the thermodynamics of the solid-solution.

ROBIN, P.-Y.F. (1974): Am. Mineral., 59, 1299–1318.

**PETROLOGICAL CONSTRAINTS ON THE EVOLUTION OF THE
ECCENTRIC CONES MONTE MALETTA, MONTE FRUMENTO,
AND MONTE NUOVO – MT. ETNA**

Hofbauer, B.¹, Ntaflos, T.¹, Abart, R.¹, Giacomoni, P.P.², Coltorti, M.², Ferlito, C.³

¹University of Vienna, Althanstraße 14, 1090 Vienna, Austria

²University of Ferrara, Via Saragat 1, 44122 Ferrara, Italy

³University of Catania, Piazza Università, 2, 95131 Catania, Italy

e-mail: babsi.ho@live.at

Mt. Etna is one of the most pronounced features of the eastern coastline of Sicily, Italy, lying in a complex geodynamic setting; it is situated on the Gela-Catania Foredeep structural domain which lies on the front of the Apenninic-Maghrebian Chain. The volcano covers an area of about 1418 km² and rises approximately 3350 metres above sea level with frequent eruptions from the summit craters. The eruptive activity has been divided according to its age into 6 stages: (1) Tholeiitic Stage active between 600-320 ka ago, (2) Timpe Stage between 220 to 110 ka ago, (3) Ancient Alkaline Volcanism (AAC) between 110 to 65 ka ago, (4) the Ellittico Stage was active between 57 to 15 ka ago, (5) the Mongibello Stage from 15 ka ago until 1971, and (6) the now active “post-1971 Stage” (CASETTA et al., 2020).

Besides the three summit craters there is a plethora of monogenetic cones, referred to as “eccentric cones” all around the edifice of the volcano. We studied three eccentric cones (Monte Maletto, Monte Nuovo, and Monte Frumento) and the 2001 eruption on the south flank of the volcano using mineral and whole rock chemistry. The overall prevalent texture is trachytic and the lavas are trachybasalts with Mg# varying in Monte Maletto between 56-58, in Monte Nuovo between 52-53, and in Monte Frumento between 43-46.

The olivine phenocrysts occur as: (1) diffusive rim/normal zoning (Fo core 57.6-87.5, rim 56-82.8), (2) skeletal (Fo core 68.3, rim 57.8-82.1), and (3) inverse zoning (Fo core 69.3-75, rim 70.2-81.4). The Ni content is generally low (NiO ≤ 0.16 wt%) and correlates positively with the Mg# whereas the CaO content ranges between 0.16 and 0.58 wt% and decreases with increasing Fo content. The most MgO-rich olivine with a Fo of 87.5 was found in Monte Maletto with a core NiO content of 0.16 wt% and CaO content of 0.24 wt% indicating a magmatic origin. The most evolved lavas with Fo = 63.9-69.4 are those of Monte Frumento. Olivine from both, the 2001 eruption and Monte Nuovo show a characteristic inverse zoning. Clinopyroxene exhibit complex zonation patterns of which four can be distinguished: (1) normal zoning with Fe-rich rim, (2) sieve textured core, (3) oscillatory zoning of FeO, MgO, and Al₂O₃, and (4) hourglass zoning. Clinopyroxene from all sample locations plot in the diopside field of the quadrilateral diagram and only a few clinopyroxenes, most notably from Monte Maletto, are plotting in the augite field, albeit only just so. The overall composition of the clinopyroxene ranges between Wo_{42.2}En_{31.1}Fs_{7.7} and Wo_{49.8}En_{47.1}Fs_{20.8}.

The preliminary results suggest that the lavas of the 2001 eruption and Monte Nuovo experienced magma mixing. Furthermore, Monte Maletto lavas represent the most primitive and Monte Frumento the most evolved magma.

THE SPODUMENE PEGMATITES IN DEFEREGGEN (EASTERN TYROL)

Horvat, C.¹, Mali, H.¹

¹Chair of Geology and Economic Geology MUL, Peter-Tunner-Straße 5, 8700 Leoben, Austria
e-mail: christian.horvat@unileoben.ac.at

In the eastern part of the Defereggental valley pegmatites of Permian age (SCHUSTER et al., 2001) occur in the Petzeck-Rotenkogel Complex and the Michelbach Complex of the Koralpe-Wölz and Drauzug-Gurktal Nappe System, respectively. In addition to simple pegmatites, spodumene pegmatites crop out in the area of Poling, Ratzell, Glanzalm, and a newly discovered one at Großer Zunig mountain (HORVAT, 2021). Representing the highly fractionated part of the pegmatite forming melt, spodumene pegmatites are important in understanding the genesis of the Permian pegmatites (KNOLL et al., 2018). Furthermore, a rising economic interest in Li makes spodumene pegmatites a promising target for exploration.

The spodumene pegmatites north and south of the Defereggental valley form predominately concordant dykes in the range of a few meters in thickness and can be followed over several tens of meters at the surface. The Li-pegmatites are mainly composed of quartz, K-feldspar, plagioclase, muscovite, spodumene, tourmaline, and garnet. The sharp contact to the host rock is often characterized by garnet and tourmalinisation. Accessory minerals detected in heavy mineral concentrates and thin sections include apatite, cassiterite, columbite group minerals, monazite group minerals, microlite group minerals, rutile, strüverite, uraninite, native bismuth, an undefined bismuth phosphate mineral, xenotime group minerals, and zircon. Zircon and the columbite group minerals follow a general fractionation trend where Hf and Ta are enriched with respect to Zr and Nb, respectively. Columbite-(Fe) is the main columbite group mineral.

Whole rock analyses of 8 spodumene pegmatite samples yield up to 2.28 % Li₂O with an average grade of 1.12 % Li₂O and 88 ppm Nb and 122 ppm Ta. Certain zones of spodumene pegmatites contain up to 50 vol% of spodumene.

LA-ICP-MS and SEM-EDS measurements were performed on 112 muscovites from a total of 74 simple and spodumene pegmatite occurrences. High trace element contents of Li, Rb, Nb, Sn, Cs, Ta, and Tl in muscovite from spodumene pegmatites point to a high fractionation. However, some muscovites from simple pegmatites in the area also contain significant trace elements, making it likely that certain spodumene pegmatites are “hidden” among the simple pegmatites and additional ones are yet to be discovered in the area.

HORVAT, C (2021): Masterarbeit, Montanuniversität Leoben.

KNOLL, T., SCHUSTER, R., HUET, B., MALI, H., ONUK, P., HORSCHINEGG, M., ERTL, A., GIESTER G. (2018): The Canad. Miner., 56, 489–528.

SCHUSTER, R., SCHARBERT, S., ABART, R., FRANK, W. (2001b): Mitt. Ges. Geol. Bergbaustudenten in Österr., 45, 111–141.

LITHIUM PEGMATITE OF ANATECTIC ORIGIN: A PETROLOGICAL AND GEOCHEMICAL MODEL

Huet, B.¹, Knoll, T.², Schuster, R.¹, Mali, H.³

¹Fachabteilung Kristallingeologie, Geologische Bundesanstalt, Neulinggasse 38, 1030 Wien, Austria

²Fachabteilung Rohstoffgeologie, Geologische Bundesanstalt, Neulinggasse 38, 1030 Wien, Austria

³Department Angewandte Geowissenschaften und Geophysik, Montanuniversität Leoben,

Peter-Tunner-Straße 5, 8700 Leoben, Austria

e-mail: benjamin.huet@geologie.ac.at

Albite-spodumene pegmatite deposits are a valuable source of Li and other rare elements. They are considered to be the product of extreme crystal fractionation of melts or fluids deriving from large fertile granite intrusions. In contrast, none of the ~80 albite-spodumene pegmatite occurrences in the Austroalpine Unit Pegmatite Province (Eastern Alps) are associated with a large fertile granite. Instead, albite-spodumene pegmatite is found at the upper structural level of lithostratigraphic complexes where migmatitic metapelite occurs at the base. Additionally, it is accompanied by simple pegmatite, evolved pegmatite, and relatively small inhomogeneous leucogranite bodies, all Permian in age. Geochronology, metamorphic petrology, field relationships, and geochemistry all converge to the same conclusion: simple pegmatite, leucogranite, evolved pegmatite, and albite-spodumene are products of anatetic melts derived from Al-rich metapelite, at different stages of crystal fractionation. Bulk rock and LA ICP-MS analyses suggest that the source of Li would reside in the Al-rich metapelite (120 ppm Li in average) with staurolite as dominant Li-carrier (up to 2900 ppm Li).

The aim of this contribution is to test if melting of a metapelite could be the origin of albite-spodumene pegmatite. The modelling approach consists in three steps. (1) The proportion of solid phases and melt during prograde melting of an Al-rich metapelite is modelled by thermodynamic forward modelling. The considered P-T conditions of melting (6-7 kbar and <750 °C) are dictated by the Permian metamorphic record in the lithostratigraphic complexes hosting pegmatite. (2) The Li distribution between solid phases and melt is calculated using the modelled phase proportions and Li-partitioning coefficient derived from LA ICP-MS analyses. Different partitioning models are considered in order to account for the different melting scenarios. (3) Crystal fractionation is modelled with mass-balance.

Using conservative parameters and realistic hypotheses, we show that ~7 to ~20 vol% melt containing 200 to 1000 ppm Li can escape the migmatite in case melting is associated with destabilization of staurolite. Subsequent crystal fractionation of the melt with a fractionation degree comprised between 81 and 99% enriches the residual melts to 5,000-10,000 ppm Li. This range corresponds to the Li saturation in felsic melts necessary for crystallizing spodumene. Our model therefore shows that direct transfer of Li from destabilizing staurolite to anatetic melt when a Li-Al-rich metapelite melts for the first time followed by crystal fractionation of the anatetic melt is a realistic genetic process for the formation of the albite-spodumene pegmatites of the Austroalpine Unit Pegmatite Province.

AL INCORPORATION AND DIFFUSION IN NATURAL RUTILE: A GEOTHERMOMETER?

Joachim-Mrosko, B.¹, Konzett, J.¹, Ludwig, T.², Libowitzky, E.³, Stalder, R.¹

¹University of Innsbruck, Institute of Mineralogy and Petrography, Innrain 52, 6020 Innsbruck, Austria

²Heidelberg University, Institute of Earth Sciences, Im Neuenheimer Feld 236, 69120 Heidelberg, Germany

³University of Vienna, Institute of Mineralogy and Crystallography, Althanstraße 14, 1090 Vienna, Austria

e-mail: bastian.joachim@uibk.ac.at

Rutile is one of the most important accessory minerals in igneous and medium- to ultrahigh-pressure metamorphic rocks and is often used as geothermobarometer and geothermometer. This study aims to experimentally investigate the incorporation mechanism and diffusivity of Al and H in natural rutile, thus bridging the gap between elaborate diffusion studies in defined simplified synthetic and complex natural systems.

High-P-T experiments were performed at pressures ranging from 1 bar to 7 GPa, and at temperatures between 1223 and 1373 K. The samples contained natural rutiles extracted from an eclogite that were embedded in a natural metapelitic host rock at fixed $\mu(\text{Al}_2\text{O}_3)$ with Δf_{O_2} buffered to CCO. Based on diffusion profiles of the respective elements in rutile that were analyzed using EPMA and SIMS, the following Arrhenius relations were determined within the experimental temperature range of this study:

$$D_{\text{Al}}^{ru} \left(\frac{\text{m}^2}{\text{s}} \right) = 3.75 \times 10^{11} \exp \left(\frac{-659 \pm 20 \text{ kJ mol}^{-1}}{RT} \right)$$

$$D_{\text{H}}^{ru} \left(\frac{\text{m}^2}{\text{s}} \right) = 3.08 \times 10^{17} \exp \left(\frac{-820 \pm 33 \text{ kJ mol}^{-1}}{RT} \right)$$

EPMA analyses further reveal a complex distribution of oxygen defects at the scale of the diffusion profiles. FTIR analyses indicate that the incorporation of hydrogen is not related to metal impurities. Based on these results, we suggest a complex combination of mechanisms to explain the incorporation of Al and H in natural rutile and its high-pressure polymorphs. This includes (i) the incorporation of Al^{3+} in octahedrally coordinated Ti-sites charge balanced by the formation of oxygen vacancies and (ii) the incorporation of oxygen in interstitial positions charge balanced by hydrogen interstitials.

Al-diffusivities in natural rutile determined in this study are about 8 to 9 orders of magnitude faster than Al-diffusivities in synthetic rutile determined by CHERNIAK & WATSON (2019). Available literature data on the Al content of natural rutiles (e.g., MEINHOLD, 2010) indicate a strong tendency of Al to be returned to coexisting silicates through diffusion in the wake of retrogressive re-equilibration, thus supporting the assumption that Al diffusivities in rutile and its TiO_2 -polymorphs in natural systems are comparatively fast. As a consequence, results of this study question the applicability of the Al-in-rutile geothermobarometer in natural systems.

CHERNIAK, D.J., WATSON, E.B. (2019): Amer. Mineral., 104, 1638-1649.
MEINHOLD, G. (2010): Earth Sci. Rev., 102, 1-28.

**POLYTYPISM AND ALLOTWINNING IN SFCA-III:
KILLING TWO BIRDS WITH ONE STONE**

Kahlenberg, V.¹, Krüger, H.¹, Goettgens, V.S.¹

¹Institute of Mineralogy and Petrography, Innsbruck University, Innrain 52, 6020 Innsbruck, Austria
e-mail: volker.kahlenberg@uibk.ac.at

Silico-Ferrites of Calcium and Aluminum compounds (so-called SFCA's) are major constituents of iron-ore sinters. Concerning their chemical compositions, different types of SFCA compounds can be distinguished. They represent complex solid solutions corresponding to the general formula $M_{14+6n}O_{20+8n}$, where M = Si, Fe, Al, Ca and Mg. The two most frequently observed representatives in industrial sinters are named SFCA (n = 0 or $M_{14}O_{20}$) and SFCA-I (n = 1 or $M_{20}O_{28}$).

A part of the system $CaO-SiO_2-Al_2O_3-Fe_2O_3-MgO$ which is of relevance to iron-ore sintering has been studied in detail. For a bulk composition corresponding to 10.45 wt.-% CaO, 5.49 wt.-% MgO, 69.15 wt.-% Fe_2O_3 , 13.37 wt.-% Al_2O_3 , and 1.55 wt.-% SiO_2 synthesis runs have been performed in air in the range between 1100 and 1300 °C. Products have been characterized using reflected-light microscopy, electron-microprobe analysis and diffraction techniques. At 1250 °C, an almost phase pure material with composition $Ca_{2.99}Mg_{2.67}Fe^{3+}_{14.58}Fe^{2+}_{0.77}Al_{4.56}Si_{0.43}O_{36}$ has been obtained. The novel compound corresponds to the first Si-containing representative of the abovementioned polysomatic series with n = 2 and is denoted as SFCA-III.

Single-crystal diffraction investigations using synchrotron radiation at the X06DA beamline of the Swiss Light Source revealed that the chemically homogenous sample contained both a triclinic and monoclinic polytype. Basic crystallographic data are as follows: triclinic form: $a = 10.3279(2)$ Å, $b = 10.4340(2)$ Å, $c = 14.3794(2)$ Å, $\alpha = 93.4888(12)$ °, $\beta = 107.3209(14)$ °, and $\gamma = 109.6626(14)$ °, $V = 1370.49(5)$ Å³, $Z = 2$, space group $P\bar{1}$; monoclinic form: $a = 10.3277(2)$ Å, $b = 27.0134(4)$ Å, $c = 10.4344(2)$ Å, $\beta = 109.668(2)$ °, $V = 2741.22(9)$ Å³, $Z = 4$, space group $P2_1/n$.

Structure determination of both modifications was successful using diffraction data from the same allotwinned crystal. A description of the observed polytypism within the framework of OD-theory is presented. Triclinic and monoclinic SFCA-III actually correspond to the two possible maximum degree of order structures based on OD-layers containing three spinel (S) and one pyroxene (P) modules (<S₃P>). The existence of SFCA-III in industrial iron-ore sinters has yet to be confirmed. Polytypism, however, is likely to occur in other SFCA-members (SFCA, SFCA-I) relevant to sintering as well, but has so far been neglected in the characterization of industrial samples. Our results shed light on this phenomenon and may therefore be also helpful for better interpretation of the powder diffraction patterns that are used for phase analysis of iron-ore sinters.

**STRUCTURAL SYSTEMATICS OF SFCA-I TYPE SOLID SOLUTIONS
IN THE SYSTEM CaO–Fe₂O₃–FeO–Al₂O₃**

Kahlenberg, V.¹, Krüger, H.¹, Tribus, M.¹

¹Institute of Mineralogy and Petrography, Innrain 52, 6020 Innsbruck, Austria
e-mail: volker.kahlenberg@uibk.ac.at

The present investigation provides - for the first time - a detailed crystallographic analysis on the impact of chemical variations on a compound that is of relevance for the field of applied mineralogy related to the technologically important process of iron-ore sintering.

Effects of Fe ↔ Al substitution on triclinic SFCA-I-type compounds with general formula A₄₀O₅₆ (A: Ca, Al, Fe³⁺, Fe²⁺) have been studied using single-crystal X-ray diffraction. Crystals of sufficient quality and size were synthesized in the temperature range between 1200 and 1300 °C. Six samples with Al/Fe_{Tot}-ratios of 0.127, 0.173, 0.216, 0.310, 0.349, and 0.459, respectively, have been structurally characterized. SFCA-I can be described with a modular approach involving the stacking sequence <PSS> of “P” and “S” modules that can be imagined as being cut from the well-known pyroxene (P) and spinel (S) structure-types. Furthermore, SFCA-I is related to the sapphirine supergroup of minerals.

Within the present solid-solution series the contents in calcium show only minor variations (\approx 6.7 a.p.f.u.). The twenty crystallographically independent tetrahedrally (T) and octahedrally (M) coordinated cation sites exhibit considerable differences concerning the Al-uptake. Indeed, Al is preferentially incorporated into the tetrahedra belonging to the single-chains located in the pyroxene-modules. Ferrous iron, on the other hand, is restricted to one of the T-positions within the spinel-blocks. Most structural aspects, from unit-cell parameters and cell volumes to site occupancies, tetrahedral chain kinking as well as polyhedral distortions are defined by linear or nearly linear trends when plotted against the Al/Fe_{Tot}-ratio.

Analysis of the <T-O> and <M-O> distances showed a complex interplay between the different coordination polyhedra resulting in a contrasting behaviour of these values with positive or negative change rates as a function of composition.

Evaluation of the average chemical strain tensor derived from the sets of lattice parameters for the two limiting compositions of the series indicated that the major contraction with increasing Al-content is perpendicular to the pyroxene- and spinel-modules. Furthermore, the pyroxene-module seems to be more effected when compared with the spinel-block.

There is evidence that the SFCA-I type solid-solution series is limited on both the Al- and Fe-rich sides.

STRUCTURE AND CHEMISTRY OF AEROSOL JET PRINTED GRAPHENE AND CARBON NANOTUBES

Kaindl, R.¹, Gupta, T.², Blümel, A.³, Pei, S.⁴, Hou, P.⁴, Du, J.⁴, Liu, C.⁴, Patter, P.³, Popovic, K.³, Dergez, D.⁵, Elibol, K.², Liu, J.⁶, Eder, D.², Kieslinger, D.⁵, Ren, W.⁴, Waldhauser, W.¹, Bayer, B.C.²

¹JOANNEUM RESEARCH – MATERIALS, Institute for Surface Technology and Photonics,
Leobner Straße 94, 8712 Niklasdorf, Austria

²Vienna University of Technology, Getreidemarkt 9/165, 1060 Vienna, Austria

³JOANNEUM RESEARCH – MATERIALS, Institute for Surface Technology and Photonics,
Franz-Pichler-Straße 30, 8160 Weiz, Austria

⁴Institute of Metal Research, Chinese Academy of Sciences, 72 Wenhua Road, Shenyang 110016, China

⁵ZKW Elektronik GmbH, Samuel-Morse-Straße 18, 2700 Wiener Neustadt, Austria

⁶Chalmers University of Technology, Department of Microtechnology and Nanoscience,
Kemivägen 9, SE 412 96 C, Sweden
e-mail: reinhard.kaindl@joanneum.at

Nanocarbon materials like graphene and carbon nanotubes (CNTs) are promising materials for a number of applications like thermal and electrical interconnects in opto- and high-speed electronics. The direct writing via additive manufacturing technology of aerosol jet printing enables low-cost fabrication, for example by integration into high-throughput roll-to-roll printing processes, rapid customization and prototyping and deposition of several layers on top of each other (PANDHI et al., 2018; ROTHER, 2019).

In this work, the micro- and nano-structure and chemistry of nanocarbon layers on flat silicon and glass and rough aluminium oxide surfaces, printed from inks by aerosol jet, were investigated by light- and scanning electron microscopy, energy-dispersive X-ray spectroscopy, atomic force microscopy, Raman spectroscopy, X-ray diffraction and high-resolution bright-field transmission electron microscopy.

Orientation, arrangement and structural quality of the graphene and CNT aggregates in the printed layers strongly depends upon substrate, ink composition and printing parameter. The investigations demonstrate possible routes to applications mentioned before, on not only flat polished silicon wafers, glass and polymer foils but also on more realistic substrates like rough, surface oxidized aluminium blocks.

PANDHI, T., KREIT, E., AGA, R., FUJIMOTO, K., SHARBATI, M.T., KHADEMI, S., CHANG, A.N., XIONG, F., KOEHNE, J., HECKMAN, E.M., ESTRADA, D. (2018): Sci. Rep., 8, 10842.
ROTHER, M. (2019): Dissertation, Heidelberg University, Germany, 236pp.

SYNTHESIS AND CRYSTAL STRUCTURE OF THALLIUMPHARMACOSIDERITE

Karasalihović, T.¹ Karanović, Lj.², Đorđević, T.¹¹Institut für Mineralogie und Kristallographie, Universität Wien, Althanstraße 14, 1090 Wien, Austria²Laboratory of Crystallography, Faculty of Mining and Geology, Đušina 7, 11000 Belgrade, Serbia

e-mail: tamara.djordjevic@univie.ac.at

Thalliumpharmacosiderite (TPS), $TlFe_4[(AsO_4)_3(OH)_4] \cdot 4H_2O$ (RUMSEY et al., 2014) is a secondary mineral belonging to the pharmacosiderite-group, adopting general formula $AFe_4[(OH)_4(AsO_4)_3] \cdot nH_2O$ ($A = Na^+, K^+, Ba^{2+}$ or H_3O^+). It is a very important sink of both arsenic and thallium in As- and Tl-rich environments.

Single-crystals of TPS, $Tl_{2.5}Fe_4[(AsO_4)_3(OH)_4](OH)_{1.5} \cdot 3H_2O$, have been obtained under mild hydrothermal conditions ($T_{max} = 170$ °C) and were characterized using single-crystal X-ray diffraction (SXRD), infrared, and Raman spectroscopy. TPS crystallizes in the form of yellowish orange, slightly elongated cubes up to 60 µm in size (Fig. 1a) together with scorodite, $FeAsO_4 \cdot 2H_2O$, and/or amorphous arsenic bearing iron oxo-hydroxides (FOH). Ferric iron salts (nitrates and chlorides) and thallium(I) sulfates and/or carbonates led to the precipitation of TPS in the relatively broad pH range from 2-6.

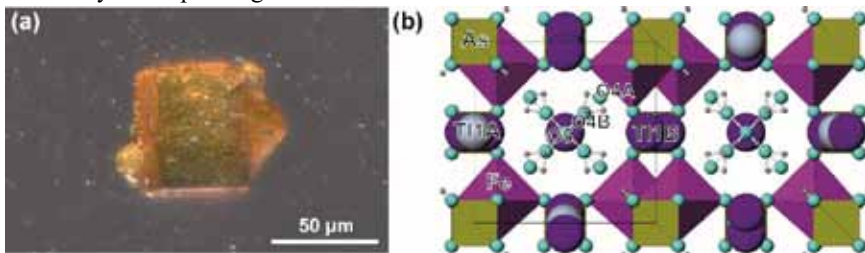


Figure 1. (a) single crystals of TPS; (b) crystal structure of TPS along [001].

TPS is cubic, space group $P\bar{4}3m$ with $a = 7.9645(1)$ Å, $V = 505.214(19)$ Å³, $Z = 1$. Its crystal structure was solved from the SXRD data and refined to $R1 = 0.0156$ for 318 reflections with $I > 2\sigma(I)$. The structure consists of a heteropolyhedral 3D open framework of the pharmacosiderite-type (ZEMANN, 1948) with large channels occupied by 12-coordinated thallium atoms, hydroxyl groups, and water molecules. Besides not fully occupied special $3d$ (Tl1A) site, TPS contains one additional $6g$ (Tl1B) site (Fig. 1b), which is split in two symmetrically equivalent positions close to the Tl1A [$Tl1A-Tl1B = 0.461(3)$ Å], with less than half-occupancy each. Tl is coordinated by eight oxygens from AsO_4 groups and by four statistically distributed O atoms, $\frac{1}{4}$ from water molecule O4A or O4B and $\frac{1}{4}$ from hydroxyl group. Oxygen atom (O5) from hydroxyl group, whose presence is required to maintain charge neutrality, were found in special half-occupied $1b$ position. The discrete hydroxyl group O5H is statistically distributed and bonded to O4 by hydrogen bonding interactions.

**METAMORPHIC EVOLUTION AND GEOCHRONOLOGY OF
VARISCAN REMNANTS IN THE EASTERN ALPS:
THE CRYSTALLINE "SCHOLLEN" IN THE GRAUWACKENZONE**

Karner-Rühl, K.¹, Hauzenberger, C.A.¹, Skrzypek, E.¹, Fritz, H.¹

¹University of Graz, Universitätsplatz 2, 8010 Graz, Austria

e-mail: kevin.karner-ruehl@edu.uni-graz.at

The Eastern Greywacke Zone is composed of three Alpine nappes. From bottom to top these are the Veitsch nappe (Early Carboniferous to Permian molasse), the Silbersberg nappe with the Kaintaleck metamorphic complex and Permian phyllites as cover, and the Noric nappe (Late Ordovician shelf sediments and Permian cover). All units experienced early Alpine metamorphism within the lower greenschist facies which resulted in the formation of ductile shear zones and the appearance of the Kaintaleck Complex as lens-shaped bodies of 10-100 m thickness within the Eastern Greywacke Zone. This work tries to determine the P-T-t path of the Kaintaleck Complex by U/Pb dating and application of geothermobarometric and petrological techniques. Based on whole rock geochemistry, amphibolites and garnet-amphibolites of the Prieselbauer unit and the Frauenberg unit in the area of Bruck/Mur and Kapfenberg, represent tholeiitic basalts with a MORB affinity. The garnet-amphibolites show distinct plagioclase-epidote-rich symplectitic coronas, which are indicative of decompression from possibly eclogite-facies metamorphic conditions. In addition to amphibolites, micaschists and gneisses are exposed in the area, which leads to a classification of the Kaintaleck crystalline unit into mafic and felsic units. The mafic units represent a former ocean, the Paleotethys, whereas the felsic units may derive from a former continental margin. By investigating these units, a geochronological sequence of metamorphic events within the Kaintaleck Complex can be determined.

THE EXCEPTIONAL ICE NUCLEATION ACTIVITY OF ALKALI FELDSPAR IN AIRBORNE MINERAL DUST

Kiselev, A.¹, Keinert, A.¹, Gaedeke, T.¹, Leisner, T.^{1,2}, Sutter, C.³, Petrishcheva, E.³,
Abarth, R.³

¹Karlsruhe Institute of Technology, Karlsruhe, Germany, 76128 Karlsruhe, Germany

²Universität Heidelberg, Heidelberg, Germany, Im Neuenheimer Feld 229, 69120 Heidelberg, Germany

³University of Vienna, Althanstraße 14, 1090 Vienna, Austria

e-mail: rainer.abarth@univie.ac.at

Due to its ubiquitous presence in the Earth's crust, feldspar is an important constituent of airborne mineral dust, where desert dust and volcanic ash are the main contributors. Solid aerosol particles play an important role in the nucleation and growth of ice. The presence of ice particles in the atmosphere has a strong influence on a variety of processes such as radiative heat transfer, precipitation and absorption of trace gases. Some alkali feldspars stand out from other solid aerosol particles due to their particularly high ice nucleation (IN) activity. This phenomenon has been ascribed to structural similarities of the ice (10̄10) prism planes and the (100) planes of alkali feldspar. In this study, this hypothesis is tested by investigating the IN activity of alkali feldspar with a high fraction of surfaces oriented sub-parallel to (100), which were produced by chemically induced fracturing. To this end, K-rich, gem quality alkali feldspar was subjected to cation exchange with an NaCl-KCl salt melt at 850 °C to shift its composition towards the Na-rich side. The associated anisotropic contraction of the crystal lattice produced a system of parallel cracks with close to (100) orientation. Grain mounts of the cation exchanged alkali feldspars were used for droplet freezing assay experiments, which confirmed an increase of the overall density of ice nucleating active sites (INAS) with respect to the untreated feldspar corroborating the view that the particularly high IN activity of some alkali feldspars is due to preferential nucleation of ice on (100) surfaces of the feldspar.

Annealing at 550 °C subsequent to primary cation exchange further enhanced the INAS density and lead to IN activity at exceptionally high temperatures. In nature, parting planes with similar orientation as the chemically induced cracks may be generated in lamellar microstructures resulting from the exsolution of initially homogeneous alkali feldspar, a widespread phenomenon in alkali feldspar known as perthite formation. Perthitic alkali feldspars indeed show the highest IN activity. We tentatively ascribe this phenomenon to the preferential exposure of feldspar crystal surfaces oriented sub-parallel to (100).

MICROSTRUCTURE AND ORIENTATION RELATIONSHIPS OF A GARNET HOST CRYSTAL AND RUTILE INCLUSIONS IN A PEGMATITE FROM THE MOLDANUBIAN ZONE (BOHEMIAN MASSIF, AT)

Kohn, V.¹, Griffiths, T.¹, Abart, R.¹, Habler, G.¹

¹University of Vienna, Vienna, Austria, Althanstraße 14, 1090 Vienna, Austria
e-mail: victoria.kohn@univie.ac.at

An 8 mm sized euhedral spessartine-almandine garnet from a pegmatite in the Moldanubian Gföhl Unit (Bohemian Massif, AT) hosts numerous rutile inclusions. The internal microstructure of garnet is characterized by distinct inclusion and colour zoning; in the optical microscope (OM) a yellowish to brownish coloured garnet core with equant nano- and µm-sized inclusions is observed. The core is rimmed by two colourless, c. 1 mm wide garnet growth zones predominantly parallel to a Grt{110} facet. The main focus of our study is the inner rim. It bares regularly spaced, rutile needles with a total of seven different shape preferred orientations (SPO).

Crystallographic orientation relationships (CORs) between garnet and rutile are known to be complex. In the literature, a total of 11 different CORs have been described from garnet-rutile host-inclusion-systems (GRIFFITHS et al., 2020, and references therein). Based on Electron Backscatter Diffraction (EBSD) data, the vast majority of the inclusions in the inner colourless garnet growth zone belong to one of three COR groups: Two of those groups are linked to the Grt<111> directions: with either the rutile *c*-axis or a rutile <103> direction parallel to Grt<111>. The third COR group has the *c*-axis of rutile parallel to a Grt<100> direction.

Combining the EBSD dataset with OM observations unmasks a correlation between the rutile needle elongation directions in the garnet host crystal and their COR: out of the seven observed SPOs, a set of 4 SPOs exclusively reflect the two COR groups associated with Grt<111>. The 3 remaining SPOs exclusively pertain to the COR group connected to Grt<100>. This interrelation suggests that the crystallographic and shape preferred orientation of rutile needles is governed by the garnet host crystal and potentially gives insight to formation mechanisms.

In addition, the abundance of rutile inclusions having a particular COR varies between microstructurally different garnet zones as follows: in the coloured garnet core, the majority of needles have Grt<111> || Rt<103>. Whereas, in the colourless inner rim Grt<111> || Rt <001> needles are predominant.

Representing work in progress, the new findings in pegmatite garnet contribute to the identification of petrogenetic parameters that influence the development of particular microstructures and textures in the garnet host-rutile inclusion system.

Funding by the Austrian Science Fund (FWF): I4285-N37 is acknowledged.

GRIFFITHS, T.A., HABLER, G., ABART, R. (2020): Amer. J. Sci., 320, 753-789.

REVISION OF THE CRYSTAL STRUCTURE OF RHABDOPHANE-(Ce)

Kolitsch, U.^{1,2}

¹Mineralogisch-Petrographische Abteilung, Naturhistorisches Museum, Burgring 7, 1010 Wien, Austria

²Institut für Mineralogie und Kristallographie, Universität Wien, Althanstraße 14, 1090 Wien, Austria

e-mail: uwe.kolitsch@nhm-wien.ac.at

The crystal structure of rhabdophane, ideally $\text{CePO}_4 \cdot \text{H}_2\text{O}$ according to the current nomenclature, was first reported by MOONEY (1950) using synthetic material (powder precipitate from aqueous solution). On the basis of powder X-ray diffraction data and a trial-and-error approach, she determined a hexagonal atomic arrangement, with the unit-cell parameters $a = 7.07(2)$ and $c = 19.06(5)$ Å, and the space group $P6_222$ (no R -value given). However, she cautioned „The final assignment of the space-group symmetry must follow rather than precede the structure determination.” In fact, an earlier study by her had suggested space group $P3_121$ (MOONEY 1948), and a subsequent study, in which the structure of the Bi analogue was determined from Weissenberg data, led to the formula $\text{BiPO}_4 \cdot 0.5\text{H}_2\text{O}$, space group $P3_121$ (MOONEY-SLATER 1962) and the following conclusion: “In any case, the true space-group symmetry of CePO_4 and of the other hexagonal rare-earth phosphates remains a question for further inquiry.” MOONEY (1948, 1950) also noted the presence of zeolitic water in the channels of the structure „ $[\text{XPO}_4 (0-0.5\text{H}_2\text{O})]$ “ which „is probably necessary to stabilize the structure.” However, the idealised formula $\text{CePO}_4 \cdot \text{H}_2\text{O}$ is given in the subsequent mineralogical literature (including the IMA list of approved minerals), while inorganic-chemical literature generally uses the formula $\text{CePO}_4 \cdot 0.5\text{H}_2\text{O}$.

No modern study of the structure of natural rhabdophane-(Ce) or isostructural members of the rhabdophane group was ever published. The author has reinvestigated the atomic arrangement of rhabdophane-(Ce) using small but sharp, hexagonal, colourless prisms of a Nd- and La-rich specimen from the Clara mine, Black Forest, Germany. The structure solution, based on single-crystal intensity data ($\text{MoK}\alpha$; 293 K) showed the correct space group to be $P3_121$ [Flack x parameter: 0.01(4)], with $a = 7.037(1)$, $c = 6.429(1)$ Å, $V = 275.71(7)$ Å³; $R(F) = 1.68\%$. SEM-EDS analyses of both crystals and crystal fragments adjacent to the studied crystal showed only minor variations of the chemical composition. Refinement of the O(H_2O) site occupancy gave 0.62(2). The bulk structural formula is $\sim(\text{Ce}_{0.41}\text{Nd}_{0.22}\text{La}_{0.16}\text{Ca}_{0.06}\text{Sm}_{0.05}\text{Pr}_{0.05}\text{Eu}_{0.02}\text{Gd}_{0.01}\text{Sr}_{0.01}\text{U}_{0.01})(\text{P}_{0.94}\text{S}_{0.04}\text{As}_{0.2})\text{O}_4 \cdot 0.62(2)\text{H}_2\text{O}$. Rhabdophane-(Ce) is therefore isostructural with its Bi analogue for which a modern multi-technique study gave the formula $\text{BiPO}_4 \cdot 0.67\text{H}_2\text{O}$ (ROMERO et al., 1994). The asymmetric unit of the Clara mine crystal contains one metal, one semimetal and three O sites. Bond lengths of the nine-coordinate (Ce,REE) site range between 2.430(2) and 2.636(3) Å (average: 2.158 Å). The (P,S,As) site shows a bond-length range between 1.524(2) and 1.532(2) Å, with an average of 1.528 Å.

MOONEY, R.C.L. (1948): J. Chem. Phys., 16, 1003.

MOONEY, R.C.L. (1950): Acta Crystallogr., 3, 337-340.

MOONEY-SLATER, R.C.L. (1962): Z. Kristallogr., 117, 371-385.

ROMERO, B., BRUQUE, S., ARANDA, M.A.G., IGLESIAS, J.E. (1994): Inorg. Chem., 33, 1869-1874.

**(Ag_{4.38}Cu_{2.62})_{Σ7.00}AsS₅: A NEW SILVER-COPPER SULPHOSALT
FROM THE BOU AZZER MINING DISTRICT, MOROCCO**

Kolitsch, U.^{1,2}, Topa, D.¹

¹Mineralogisch-Petrographische Abteilung, Naturhistorisches Museum, Burgring 7, 1010 Wien, Austria

² Institut für Mineralogie und Kristallographie, Universität Wien, Althanstraße 14, 1090 Wien, Austria
e-mail: uwe.kolitsch@nhm-wien.ac.at

We have characterised a new silver-copper sulphosalt species from Vein no. 53 ('Filon 53'), Aït Ahmane (Bou Azzer mining district), Zagora Province, Drâa-Tafilalet Region, Morocco, by quantitative electron-microprobe data, a single-crystal structure determination, and reflected-light studies. The new mineral, of which only one specimen is presently known to exist, forms black, elongate pseudo-orthorhombic prisms (up to 0.5 mm in length) with a strong metallic lustre. The crystals show wedge-shaped crystal terminations (similar to löllingite), strong mosaic growth and are arranged in sprays in a void in a white carbonate (probably calcite). The new mineral is intimately associated with tiny dark red, six-sided platelets of earlier crystallised cupropearceite with the empirical formula Ag_{11.39}Cu_{4.67}As_{1.97}S_{10.96} (microprobe data). The black prisms were briefly described, along with preliminary SEM-EDS data, as "UK26 - cupropearceite?" in a collectors' journal (FAVREAU & BARRAL, 2019).

The solution of the structure ($R = 7.6\%$) from single-crystal XRD data (MoK α ; 293 K) unambiguously indicated space group $P2_1/n$ (no. 14), with $a = 7.175(1)$, $b = 13.411(3)$, $c = 10.048(2)$ Å, $\beta = 91.49(3)^\circ$, $V = 966.5(3)$ Å³ ($Z = 4$), with the refined chemical formula (Ag_{4.38}Cu_{2.62})_{Σ7.00}AsS₅, i.e. an Ag:Cu ratio of 1.67. The microprobe data, which were obtained from a spray at the edge of the void, show a lower Ag:Cu ratio (1.48; range: 1.41-1.54). They confirm the complete absence of Sb. Optically, the polished crystals are homogeneous, with no indication of twin lamellae or other anomalies. The associated cupropearceite has a distinctly higher Ag:Cu ratio (2.44).

The asymmetric unit contains seven metal sites, one As site and four S sites. The metal sites comprise three Ag sites, one mixed (Ag_{0.91(4)}Cu_{0.09}) site, one Cu site and two (Cu,Ag) sites with occupancies (Cu_{0.89(3)}Ag_{0.11}) and (Cu_{0.65(3)}Ag_{0.35}). The formula is charge-balanced and no As–As or distinct metal–metal bonds exist. Ag–S bond lengths range between 2.45 and 2.80 Å, while the Cu–S and (Cu,Ag)–S bond lengths show a range between 2.21 and 2.55 Å. The As–S bonds are between 2.23 and 2.26 Å long. The atomic arrangement can be described as a 3D framework composed of metal-S_n ($n = 2-4$) polyhedra and AsS₃ pyramids.

Comparisons will be drawn with chemically related species.

We thank Jean-Pierre Barral for providing the specimen (via Philippe Roth) for analysis.

FAVREAU, G., BARRAL, J.-P. (2019): Le Cahier des Micromonteurs, 145, 3-129 (in French).

REVISIONS OF THE CRYSTAL STRUCTURES OF MATILDITE, AgBiS₂, AND CHRISTITE, TlHgAsS₃

Kolitsch, U.^{1,2}, Topa, D.¹, Giester, G.²

¹ Mineralogisch-Petrographische Abteilung, Naturhistorisches Museum, Burgring 7, 1010 Wien, Austria

² Institut für Mineralogie und Kristallographie, Universität Wien, Althanstraße 14, 1090 Wien, Austria

e-mail: uwe.kolitsch@nhm-wien.ac.at

Results of a crystal-structure determination of matildite (low-temperature form of AgBiS₂) were first reported by GELLER & WERNICK (1959) using synthetic material. On the basis of powder X-ray diffraction data (PXRD) and a comparison with “isostructural” AgBiSe₂ (studied by both single-crystal and PXRD, and using some assumptions), they determined the “most probable space group” to be $\bar{P}\bar{3}m1$, with $a = 4.07(2)$, $c = 19.06(5)$ Å (no R -value given). No detailed study of the structure of natural matildite was ever published. However, for crystals from Canada, HARRIS & THORPE (1969) postulated a doubled a axis, with $a = 8.12$; $c = 19.02$ Å, whereas SHIMIZU et al. (1998) gave $a = 4.0670$, $c = 18.996$ Å for a slightly Se-bearing sample from Japan. We have reinvestigated the atomic arrangement of matildite using well-crystallised material from the Clara mine, Black Forest, Germany (grey, distorted acicular to bladed crystals with a strong metallic lustre). The structure solution, based on single-crystal intensity data (MoK α ; 293 K) showed the correct space group to be $P3_121$ [Flack x parameter: 0.017(11)], with $a = 4.0675(3)$, $c = 18.9570(13)$ Å, $V = 271.62(3)$ Å³; $R(F) = 1.48\%$. Quantitative electron-microprobe data showed the crystals to have a stoichiometric, nearly pure composition, with only trace amounts of Pb present. The asymmetric unit contains one Ag, one Bi, and one S site. Bond lengths are: Ag–S = 2.5263(6) (2 \times), 2.8541(7) (2 \times) Å; Bi–S = 2.6660(6) (2 \times), 2.8543(7) (2 \times), 3.0386(7) (2 \times) Å. The crystal structure is much more distorted than that of the incorrect model from the 1950s.

The crystal structure of synthetic christite, TlHgAsS₃, was first reported by BROWN and DICKSON (1976). They gave space group $P2_1/n$, with $a = 6.113(1)$, $b = 16.188(4)$, $c = 6.111(1)$ Å, $\beta = 96.71(2)^\circ$; $R(F) = 4.4\%$. No structural study of natural material was ever published. Because the reported unit cell looked suspicious ($a \sim c$), we have reinvestigated christite using well-developed crystals from the Jiepaiyu Mine, Shimen deposit, China. Quantitative electron microprobe analysis confirmed the material to be chemically pure. The atomic arrangement was redetermined from single-crystal intensity data (MoK α ; 293 K). It was found to unambiguously have space group $Cmca$, with $a = 8.080(5)$, $b = 9.123(6)$, $c = 16.190(9)$; $R(F) = 6.5\%$. The higher symmetry is also confirmed by a critical analysis of the literature model with the software PLATON, which clearly indicated space group $Cmca$. The crystal faces can all be indexed with simple forms: {010}, {011} and {111}. The asymmetric unit contains one Tl, one Hg, one As, and two S sites (instead of three S sites in the literature model).

BROWN, K.L. & DICKSON, F.W. (1976): Z. Kristallogr., 144, 367-376.

HARRIS, D.C., THORPE, R.I. (1969): Canad. Mineral., 9, 655-662.

GELLER, S., WERNICK, J. H. (1959): Acta Crystallogr., 12, 46-54.

SHIMIZU, M., KATO, A., MATSUYAMA, F. (1998): Resource Geol., 48, 117-124.

ANATECTIC ORIGIN OF PERMIAN PEGMATITES OF THE EASTERN ALPS – EVIDENCE FROM FLUID INCLUSIONS

Krenn, K.¹, Husar, M.¹, Mikulics, A.¹

¹Institute of Earth Sciences Nawi Graz, University of Graz, Heinrichstrasse 26, 8010 Graz, Austria
e-mail: kurt.krenn@uni-graz.at

Fluid inclusions (FIs) and associated solids in host minerals garnet, tourmaline, spodumene, and beryl from five large pegmatite field areas with Permian origin (Radegund, Kor-Saualpe, Millstatt, Polinik, and Bretstein-Lachtal), all located in the Koralpe-Wölz high-pressure nappe system of the Eastern Alps, have been investigated. Although pegmatites suffered intense Eoalpine high-pressure metamorphic overprint during the Cretaceous period, most of the studied samples originate from rock sections with well-preserved Permian magmatic textures. Pegmatite minerals are proposed as having been crystallized under incipient anatetic conditions of their surrounding host rock lithologies and comprise primary FIs with a complex $\text{CO}_2\pm\text{N}_2\pm\text{CH}_4\text{-H}_2\text{O-NaCl-CaCl}_2\pm\text{MgCl}_2$ chemistry. However, the presence of partly exsolved fluids during garnet crystallization in the Kor-Saualpe enables a distinction into two fluid assemblages: assemblage A, defined by coevally entrapped $\text{CO}_2\text{-N}_2$ and $\text{H}_2\text{O-NaCl-CaCl}_2\pm\text{MgCl}_2$ FIs, and assemblage B, characterized by FIs of $\text{CO}_2\pm\text{N}_2\pm\text{CH}_4\text{-H}_2\text{O-NaCl-CaCl}_2\pm\text{MgCl}_2$ chemistry. This suggests a different fluid evolution history in the Kor-Saualpe pegmatites compared to the other pegmatite fields. In the Koralpe, two separately evolved fluids ($\text{CO}_2\text{-N}_2$ and H_2O) entrapped in magmatic garnet domains and experienced subsequent mixing at the solvus. This mixed fluid dominated during tourmaline and spodumene crystallization and entrapped as assemblage B in the form of primary inclusions (cf. KRENN et al., 2021a). At Radegund, Millstatt, Polinik, and Bretstein-Lachtal, fluid assemblage B was the dominant fluid during crystallization of the pegmatite host minerals garnet, tourmaline, and spodumene. Additionally, beryl-hosted FIs from pegmatites of the Polinik pegmatite field consist of assemblage B and can be compared to FIs from beryl host of the Texel pegmatite field in the westernmost areas of the Eastern Alps (KRENN et al., 2021b). Minimum conditions for pegmatite crystallization in the Polinik pegmatite field of ca. 6.3–7.3 kbar in garnet and 5.1–5.9 kbar in beryl as well as 4.5–5.5 kbar in tourmaline of the Kor-Saualpe at 650–750 °C have been constrained by primary FIs that have not been affected by post-entrapment modifications. It is therefore proposed that magmatic/metamorphic fluid interaction dominated during Permian pegmatite formation in a high-grade metamorphic environment: a low-saline aqueous fluid as magmatic constituent mixed with a $\text{CO}_2\text{-N}_2$ -rich fluid that formed as result of partial anatexis with the surrounding host rocks. As potential source for N, mica minerals of the metapelitic host are proposed (cf. KRENN et al., 2021b). The dominance of N in almost all CO_2 -bearing FIs of the studied host minerals of the pegmatite field areas provides further evidence for an anatetic origin of the pegmatites of the Austroalpine basement of the Eastern Alps.

KRENN, K., HUSAR, M., MIKULICS, A. (2021a): Minerals, 11, 638, 1-22.

KRENN, K., KONZETT, J., STALDER, R. (2021b): Canad. Mineral., in press.

FEASIBILITY STUDY ON THE INVESTIGATION OF FORMER POLYCHROME PAINTING ON THE “ROMAN STONES FROM HERNALS”

Krickl, R.¹, Steigberger, E.²

¹Forschungsinstitut Dr. Robert Krickl, Al. Groß G. 42, 2345 Brunn/Geb. / Amundsenstr. 3, 1140 Vienna, Austria

²Bundesdenkmalamt, Abteilung für Archäologie, Kartäuserplatz 1, 3001 Mauerbach, Austria

e-mail: mail@r-krickl.com

In 2003, remarkable Roman stone artefacts were excavated during construction activities in the 17th district of Vienna and thereafter given the name “Römersteine aus Hernals” (“Roman stones from Hernals”). Classified as one of the most important Roman stone finds in the last decades in Austria, they were archaeologically investigated, restored, and put on display by the *Federal Monuments Authority Austria* in Mauerbach Charterhouse (cf. BLESL et al., 2012).

In the course of a feasibility study on the application of noninvasive methods (mainly multispectral imaging in combination with X-ray fluorescence analysis and Raman spectroscopy) in museal environments, the Roman funerary monuments were now investigated on remnants of former polychrome decoration. Aside from visible traces of iron oxide, green earth and carbon black pigments, multispectral imaging could reveal the hitherto unknown presence of abundant Egyptian blue in form of dustsized particles not perceptible by the naked eye (cf. Fig. 1). A very precise localisation was achieved by using the new *CoRL* technique (KRICKL, 2019), thus indicating different usage of this blue pigment: not only as background colour alluding to the sky, but also for depicting metal objects and colourful clothing and, last but not least, as contouring agent for accentuating shadows and plasticity. With few and manageable limitations, the new multispectral methods proved very well suited for the investigation of large stone artefacts in museums, promising new information on materials used in ancient artwork.



Figure 1. Visible (left), infrared luminescence (middle) and *CoRL* (right) image of a side element of a Roman funerary aedicula displayed in Mauerbach Charterhouse, depicting a male servant. White areas in the latter two images indicate the presence of Egyptian blue pigment.

BLESL, C., HEBERT, B., MARIUS, M. (2012): Wiederhergestellt 02 – Römersteine aus Hernals. *Mediterrane Bilder in >Barbarengräbern<*. Bundesdenkmalamt, Wien.

KRICKL, R. (2019): Mitt. Österr. Miner. Ges., 165, 54.

THE CRYSTAL STRUCTURE OF THE NEW MINERAL DEVILLIERSITE
 $\text{Ca}_4\text{Ca}_2\text{Fe}^{3+}\text{O}_4[(\text{Fe}^{3+}\text{Si}_2)\text{O}_{36}]$

Krüger, B.¹, Krüger H.¹, Galuskina, I.O.², Galuskin, E.L.², Vapnik, Ye.³

¹University of Innsbruck, Innrain 52, 6020 Innsbruck, Austria

²Faculty of Earth Sciences, University of Silesia, Będzińska 60, 41-200 Sosnowiec, Poland

³Ben-Gurion University of the Negev, POB 653, Beer-Sheva 84105, Israel

e-mail: biljana.krueger@uibk.ac.at

The crystal structure of the new mineral (IMA 2020-073) devilliersite, $\text{Ca}_4\text{Ca}_2\text{Fe}^{3+}\text{O}_4[(\text{Fe}^{3+}\text{Si}_2)\text{O}_{36}]$, was solved from single-crystal synchrotron data PSI (SLS). Devilliersite, as well as khesinite, $\text{Ca}_4\text{Mg}_2\text{Fe}^{3+}\text{O}_4[(\text{Fe}^{3+}\text{Si}_2)\text{O}_{36}]$ (GALUSKINA et al., 2017), is a VIFe^{3+} -analog of dorrite, $\text{Ca}_4\text{Mg}_2\text{Fe}^{3+}\text{O}_4[(\text{Al}_1\text{Si}_2)\text{O}_{36}]$ (COSCA et al., 1988) and synthetic SFCA (Silico-Ferrite of Calcium and Aluminium) (KAHLENBERG et al., 2019).

The structural formula of minerals of the dorrite–khesinite series can be written as $\text{VII}(\text{Al}_1\text{A}_2)_4\text{VI}(\text{M}_1\text{M}_2\text{M}_3\text{M}_4\text{M}_5\text{M}_6\text{M}_7)_2\Sigma_{12}\text{O}_4[(\text{T}_1\text{T}_2\text{T}_3\text{T}_4\text{T}_5\text{T}_6)_2\Sigma_{12}\text{O}_{36}]$, where A are seven coordinated sites, M are octahedral sites and T are tetrahedral sites (Figure 1). In the structure of devilliersite all of the A -sites are fully occupied by calcium. Further excess of Ca, additional 0.68 atoms, has to be expected at the largest octahedral site $M5$. The remaining scattering power at the $M7$ site is explained by Mg. The octahedral $M1$, $M2$, $M3$, $M4$, and $M6$ sites are dominated by Fe^{3+} , their scattering power was modelled with Fe and Mg, and converged for all sites to ~93% Fe. The $M7$ is a Ti-rich site. Scattering power indicates that the $T4$ site in devilliersite is fully occupied by Si. Occupancy of all other tetrahedral sites was refined as Al vs Fe.

The refined chemical formula is $\text{VII}\text{Ca}_4\text{VI}(\text{Ca}_{1.36}\text{Mg}_{1.33}\text{Fe}_{9.07}\text{Ti}_{0.24})\Sigma_{12}\text{O}_4\text{IV}(\text{Al}_{3.24}\text{Fe}_{6.76}\text{Si}_2)\Sigma_{12}\text{O}_{36}$.

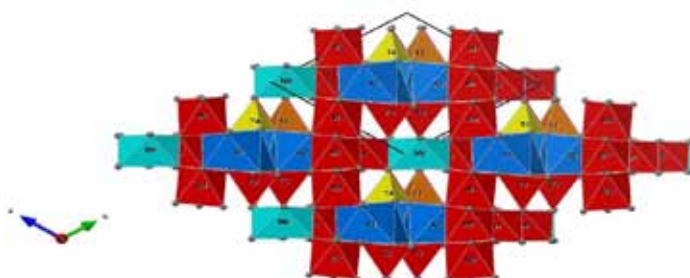


Figure 1. The devilliersite structure, projection on (100): Fe-dominant polyhedra ($M1$, $M2$, $M3$, $M4$, $M6$, $M7$ octahedra and $T2$, $T3$, $T5$, and $T6$ tetrahedra are in red. In blue are 6+1 coordinated pure Ca-polyhedra ($A1$ and $A2$ -polyhedra). The octahedra $M5$, predominantly occupied by Ca (68%) is in light blue colour. Pure Si tetrahedra $T4$ are in yellow. Al-dominant tetrahedra $T1$ have orange colour.

GALUSKINA, I.O., GALUSKIN, E.V., PAKHOMOVA, A.S., WIDMER, R., ARMBRUSTER, T., KRÜGER, B., GREW, E.S., VAPNIK, Y.E., DZIERAZANOWSKI, P., MURASHKO, M. (2017). Eur. J. Miner., 29, 101–116.

COSCA, M.A., ROUSE, R.R., ESSENE, E.J. (1988). Amer. Miner., 73, 1440-1448.

A DEDICATED ELECTRON DIFFRACTOMETER FOR SOLVING CRYSTALLOGRAPHIC CHALLENGES IN MINERALOGY

Lanza, A.E.¹, Hovestreydt, E.¹, Santiso-Quinones, G.¹, Steinfeld, G.¹, Mugnaioli, E.², Gemmi, M.²

¹ELDICO Scientific AG, 5234 Villigen, Switzerland

²Center for Nanotechnology Innovation @NEST, Istituto Italiano di Tecnologia,
piazza S. Silvestro 12, 56127 Pisa, Italy
e-mail: lanza@eldico.ch

While several methods based on Electron Diffraction (ED) are applied in mineralogy since the invention of electron microscopy, the recent development of 3D ED methods has caused a breakthrough into many different fields of science, for the structural determination of micro- and nanocrystalline samples (GEMMI et al., 2019).

Both in natural and synthetic minerals, the structural characterization can be hampered by a too small crystal size, limited sample quantity, presence of spurious phases and by complicated features such as twinning and intergrowth occurring at the submicrometric scales. 3D ED allows to collect complete diffraction datasets from individual nanocrystalline domains, and thus to solve and refine their unknown crystal structures, overcoming the above-mentioned complications (MUGNAIOLI & GEMMI, 2018).

Here we present some examples of mineralogic challenges solved with 3D ED (LANZA et al., 2019; MUGNAIOLI et al., 2020a; MUGNAIOLI et al., 2020b). These complex microcrystalline minerals, showing incommensurate modulations, microtwinning and complex structural rearrangements, all showcase the potential of an electron diffractometer. Our device, developed and optimized exclusively for 3D ED, allows a time-effective, automated and standardized experimental workflow along with user-friendly operability and seamless interaction with the widespread crystallographic software.

- GEMMI, M., MUGNAIOLI, E., GORELIK, T.E., KOLB, U., PALATINUS, L., BOULLAY, P., HOVMÖLLER, S., ABRAHAMS, J.P. (2019): ACS Cent. Sci., 5, 1315-1329.
LANZA, A.E., GEMMI, M., BINDI, L., MUGNAIOLI, E., PAAR, W.H. (2019). Acta Crystal., B75, 711-716.
MUGNAIOLI, E., BONACCORSI, E., LANZA, A.E., ELKAIM, E., DIEZ-GOMEZ, V., SOBRADOS, I., GEMMI, M., GREGORKIEWITZ, M. (2020a); IUCrJ, 7, 1070-1083.
MUGNAIOLI, E., GEMMI, M. (2018): Z. Kristallogr. – Cryst. Mater., 233, 163-178.
MUGNAIOLI, E., LANZA, A.E., BORTOLOZZI, G., RIGHI, L., MERLINI, M., CAPPELLO, V., MARINI, L., ATHANASSIOU, A., GEMMI, M. (2020b): ACS Cent. Sci., 6, 1578-1586.

DIACHRONOUS METAMORPHISM OF CORDIERITE BEARING ASSEMBLAGES
FROM THE WANNI COMPLEX – SRI LANKA

Lechner, N.¹, Hauzenberger, C.A.¹, Skrzypek, E.¹, Masten, M.¹, Sorger, D.¹,
Fernando, G.W.A.R.²

¹University of Graz, Universitätsplatz 2, 8010, Graz, Austria

²The Open University of Sri Lanka, PO Box 21, Nugegoda, Sri Lanka

e-mail: nikolaus.lechner@uni-graz.at

The Sri Lankan basement is subdivided into the Highland Complex (HC), Wanni Complex (WC), and Vijayan Complex (VC) mainly based on Nd-model ages from MILISENDA et al. (1988, 1994) and underwent amphibolite to granulite facies metamorphism during the Pan-African orogeny ~ 600 - 500 Ma ago. While the boundary between VC and HC is well known due to differences in metamorphic grade and a thrust/shear contact, the boundary between the WC and HC is still matter of discussion. The HC probably represents a deeper crustal level than the WC which is overprinted by up to UHT conditions in the central HC (SAJEEV et al., 2010). Parts of the WC may have also experienced UHT conditions but clear evidence is still missing. For this study cordierite bearing garnet-biotite gneisses were collected from the WC/HC boundary area from south-western Sri Lanka. This rock type occurs less frequently compared to the dominant meta-granitoides, garnet-sillimanite gneisses, charnockitic gneisses and basic granulites/amphibolites and are regarded as an own unit. Symplectitic cordierite and biotite growth around garnet indicates decompression by the reaction $\text{Melt} + \text{Grt} + \text{Qtz} + \text{Sil} = \text{Crd} + \text{Sp} + \text{Bt}$. Based on mineral assemblages, textures and EPMA mineral analyses, P-T conditions of 850 ± 50 °C and 6 ± 1 kbar are proposed during metamorphism of the cordierite bearing unit. Recently, WANNIARACHCHI & AKASAKA (2016) and HIRAYAMA et al. (2020) reported metamorphic ages of ~530-540 Ma determined by in-situ monazite and zircon U-Pb dating, respectively. Here, we report additional in-situ EPMA Th-U-Pb monazite ages based on the textural position of the monazite grains: (1) monazite inclusions in garnet yield a weighted mean age of 572 ± 2 Ma, which is interpreted to represent the age of main metamorphism in the HC, which was documented by SAJEEV et al. (2010) with a similar result of 569 ± 5 Ma. They found a metamorphic overprint at approximately 550 Ma (zircon and monazite rims) which is probably also present here, but not well constrained. (2) Monazites in the matrix cluster around 565 ± 3 Ma and 534 ± 2 Ma. The older age is close to the age found in monazites enclosed in garnet and thus represents the age of metamorphism in the HC, while the younger age represents the timing of cordierite formation and the LP/HT metamorphic event seen in southwestern Sri Lanka.

- MILISENDA, C. C., LIEW, T. C., HOFMANN, A. W., KRONER, A. (1988): J. Geol., 96, 608–615.
MILISENDA, C. C., LIEW, T. C., HOFMANN, A. W., KÖHLER, H. (1994): Precambrian Res., 66, 95–110.
SAJEEV, K., WILLIAMS, I. S., OSANAI, Y. (2010): Geology, 38, 971–974.
WANNIARACHCHI, D. N. S., AKASAKA, M. (2016): J. Mineral. Petrol. Sci., 111, 351–362.
HIRAYAMA, E., TSUNOGAE, T., MALAVIARACHCHI, S. P. K., TAKAMURA, Y., DHARMAPRIYA, P. L., TSUTSUMI, Y. (2020): Geol. J., 55, 6147–6168.

CONTRIBUTIONS TO THE CRYSTAL STRUCTURE OF GUÉRINITE FROM THE LAVRION MINING DISTRICT, GREECE

Liebhart, I.¹, Rieck, B.¹, Giester, G.¹

¹Institut für Mineralogie und Kristallographie, Universität Wien, Althanstraße 14, 1090 Wien, Austria
e-mail: gerald.giester@univie.ac.at

Guérinite was first described from samples originating from Schneeberg, Saxony and Richeldorf, Hessia as $\text{Ca}_5\text{H}_2(\text{AsO}_4)_4 \cdot 9\text{H}_2\text{O}$ (NEFEDOV, 1961). The crystal structure was solved on synthetic material only by single-crystal diffraction methods (CATTI & FERRARIS, 1974) in space group $P2_1/n$ with $a = 17.63(1)$, $b = 6.734(3)$, $c = 23.47(2)$ Å, $\beta = 90.6(1)^\circ$. However, these authors discussed several models, favouring a disordered one with two additional, partially occupied calcium sites, leading to the formula $\text{Ca}_5(\text{HAsO}_4)_2(\text{AsO}_4)_2 \cdot 9\text{H}_2\text{O}$.

Recently, during sampling of an arsenic-rich area of the Mine No. 145 at the Lavrion Mining District, Greece, a large number of secondary Ca and Mg arsenates were found. Among them, some specimens were tentatively identified as guérinite. However, the Ca/As-ratio of EMPA-studies did not fit well with published formulas in the literature. The crystals being well-formed (Fig. 1) and of adequate quality enticed the authors to try a full-fledged crystal structure determination of the new material.

Based on single-crystal X-ray data, collected at 200 K, the structure was refined in space group $P2_1/n$ with $a = 17.631(2)$, $b = 6.731(1)$, $c = 23.388(3)$ Å, $\beta = 90.69(1)^\circ$ to $R1 = 0.051$ and the hydrogen-bond system established. The true formula of guérinite turned out to be $\text{Ca}_6(\text{HAsO}_4)_3(\text{AsO}_4)_2 \cdot 10\frac{1}{2}\text{H}_2\text{O}$. It further showed up that there is obviously no type specimen still in existence. The authors therefore propose that guérinite be redefined according to the present results, that the specimen used for our study be termed neotype specimen and the type locality be the Mine No. 145 in the Plaka area of the Lavrion Mining District.



Figure 1. Guérinite, associated with white, needle-like rauenthalite (lower left) and deformed pharmacolite (right) on calcite matrix that is partially covered by tiny marcasite crystals (mainly left of guérinite).

NEFEDOV, E.I. (1961): Mat. All-Union Sci. Res. Geol. Inst., 45, 113-115.
CATTI, M., FERRARIS, G. (1974): Acta Crystallogr., B30, 1789-1794.

**ON A NOVEL PHASE IN THE SYSTEMS K₂O–CaO–SiO₂ —
SOLVING A 90 YEARS OLD RIDDLE**

Liu H., Hildebrandt E., Krammer H., Kahlenberg V., Krüger H., Schottenberger H.

University of Innsbruck, Institute of Mineralogy and Petrography, Innrain 52, A-6020 Innsbruck, Austria
e-mail: volker.kahlenberg@uibk.ac.at

When it comes to the re-use of residual materials such as different types of ashes and slags occurring in industrial combustion, gasification, pyrolysis, and metallurgical processes, the system K₂O–CaO–SiO₂ is of great interest and importance. Revealing the complete picture of all ternary phases as well as detailed crystal structure information on all compounds in the system is of essence for both identification of the phases in technical products and related thermodynamic assessments. In the course of an ongoing research project, we found evidence for the existence of the so-called 2:1:6 phase (K₄CaSi₆O₁₅) and finally proved its presence as a stable material at ambient conditions.

Actually, a compound with composition K₄CaSi₆O₁₅ was first mentioned by MOREY et al. (1930). However, limited by the available analytical tools in the 1930's, the chemical formula was estimated from the initial weight fractions of the educts, i.e. no chemical analysis of the product has been performed. Furthermore, the only other characterization method of the crystals was the determination of their optical properties including measurements of the refractive indices. Though optical features of the crystals served to establish hypotheses concerning the crystal system, neither detailed powder/single-crystal diffraction nor spectroscopic data have been collected.

In the present study, polycrystalline K₄CaSi₆O₁₅ was prepared from (i) solid-state reactions between stoichiometric mixtures of the corresponding oxides/carbonates and (ii) combustion solution synthesis using K- and Ca-nitrates, tetraethyl orthosilicate (TEOS), and glycine (fuel component) as starting reagents. The compound was characterized by powder X-ray diffraction. Differential thermal analysis indicated that K₄CaSi₆O₁₅ melts congruently at about 956 °C. On cooling down from the liquid state, a distinct glass-forming tendency was observed. Single-crystals suitable for further structural investigations were obtained from sinter experiments just below the melting point. Basic crystallographic data are as follows: monoclinic symmetry, space group *Pc*, *a* = 6.9299(2) Å, *b* = 27.3496(9) Å, *c* = 12.2187(4) Å, β = 93.744(3)°, *V* = 2310.86(13) Å³, *Z* = 3. The crystal structure of K₄CaSi₆O₁₅ belongs to the group of interrupted framework silicates with exclusively Q³-units. The tetrahedral network is the first inorganic representative of the so-called *eth*-type (O'KEEFFE et al., 2008) which has been previously observed in metal organic frameworks or molecular structures only. Charge compensation in the structure is achieved by incorporation of potassium and calcium cations, which are coordinated by five to nine oxygen ligands.

MOREY G.W., KRACEK F.C., BOWEN N.L. (1930): J. Soc. Glass Technol., 14, 149-187.
O'KEEFFE M., PESKOV M.A., RAMSDEN S.J., YAGHI O.M. (2008): Acc. Chem. Res., 41, 1782-1789.

GEOCHRONOLOGY AND HIGH-GRADE METAMORPHISM OF THE WANNI COMPLEX, SRI LANKA

Masten, M.¹, Hauzenberger, C.A.¹, Lechner, N.¹, Skrzypek, E.¹, Gallhofer, D.¹,
Fernando, G.W.A.R.²

¹University of Graz, Universitätsplatz 2, 8010 Graz, Austria

²The Open University of Sri Lanka, PO Box 21, Nugegoda, Sri Lanka
e-mail: marcel.masten@edu.uni-graz.at

The assembly of Gondwana in the Neoproterozoic/Early Paleozoic resulted in a number of large-scale orogenic systems. Sri Lanka is located in a central position of the supercontinent and is usually associated with the Mozambique Belt in Eastern Africa, Madagascar and Antarctica. The main geological units of Sri Lanka comprise the (1) Vijayan Complex, which is separated from the (2) Highland Complex by a thrust contact and the (3) Wanni Complex. The boundary between the Wanni and the Highland Complex is poorly defined and a matter of debate. Differences in isotopic model ages were used to separate both units (KITANO et al., 2018; MILISENDÄ et al., 1994). Here, we report new zircon U-Pb ages defining the emplacement age of the igneous precursor rocks as well as the metamorphic overprint. In addition, a detailed petrological study reveals the UHT nature of at least some Wanni metamorphic rocks.

Large areas of the Wanni Complex are covered by migmatitic orthogneisses with occurrences of “arrested” charnockites or displaying potassium metasomatism (COORAY, 1994; KRÖNER et al., 2003). However, charnockitic gneisses, mafic granulites and garnet bearing gneisses and, in the southwestern part, cordierite bearing gneisses and metapelites are frequently found and can be used for constraining the P-T-t history of this complex. P-T conditions of the Wanni Complex obtained from garnet bearing rocks place the metamorphic overprint clearly into the granulite facies and partly into the UHT field with T = 800-1000 °C at 7-9 kbar.

Zircon U/Pb ages obtained from felsic hornblende-biotite gneisses and charnockitic gneisses from different locations of the Wanni Complex show igneous protolith ages of 960-990 Ma. In one sample newly grown metamorphic zircons revealed Cambrian ages that cluster around 530 Ma.

COORAY, P.G. (1994): Precambrian Res., 66, 3–18.

KITANO, I., OSANAI, Y., NAKANO, N., ADACHI, T., FITZSIMONS, I.C.W. (2018): J. Asian Earth Sci., 156, 122–44.

KRÖNER, A., KEHELPANNALA, K.V.W., HEGNER, E. 2003. “Ca” Journal of Asian Earth Sciences 22, 279–300.

MILISENDÄ, C.C., LIEW, T.C., HOFMANN, A.W., KÖHLER, H. (1994): Precambrian Res., 66, 95–110.

CESIUM-ORDERING AND HIGH-PRESSURE BEHAVIOUR IN CESIUM-STUFFED BERYL-TYPE JOHNKOIVULAITE

Milos, S.¹, Ende, M.¹, Gatta, G.D.², Palke, A.C.³, Miletich, R.¹

¹Institut für Mineralogie und Kristallographie, Universität Wien, Althanstrasse 14, 1090 Vienna, Austria

²Dipartimento di Scienze Della Terra, Università Degli Studi di Milano, Via Botticelli 23, 20133, Milano, Italy

³Gemological Institute of America, Inc., The Robert Mouawad Campus, 5345 Armada Drive,
Carlsbad, CA 92008, USA

e-mail: sofija.milos@univie.ac.at

The newly discovered beryl-type mineral johnkoivulaite ($\text{CsBe}_2\text{BMg}_2\text{Si}_6\text{O}_{18}$, space group $P6/mmc$, PALKE et al., 2021) has a discrete structural site for Cs, in some way similar to the related structure of rhombohedral pezzottaite ($\text{Cs}(\text{Be}_2\text{Li})\text{Al}_2\text{Si}_6\text{O}_{18}$; LAURS et al., 2003; ENDE et al., 2021). A striking difference between the two structures is the distinguishable heterovalent substitution (1/3 B^{3+} versus 1/3 Li^+ on the T1 site, and Mg^{2+} versus Al^{3+} on the M site) within the $[\text{T1}^{[4]}_3\text{M}^{[6]}_2\text{Si}_6\text{O}_{18}]$ framework. Despite the different charge distribution within the framework, there is a comparable stoichiometry of one Cs-atom per formula unit. Nevertheless, the overall symmetry is different, and it raises the question of whether the different charge distribution within the framework has a consequence on the extra-framework Cs ordering and if the high-pressure properties of johnkoivulaite are identical or different compared to those reported for pezzottaite (ENDE et al., 2021).

In this context first in-situ compression studies were conducted on a natural single crystal sample originating from the gem deposit of Mogok, Myanmar, using Raman spectroscopy and single-crystal X-ray diffraction. The purpose of this study is to understand the stability criteria from a structural perspective, any polymorphism, and the mechanisms of the underlying transitions in non-ambient pressure conditions. In Raman spectra at ambient conditions johnkoivulaite crystals exhibit no characteristic Raman band in the low-frequency range between 50 and 200 cm^{-1} Raman shift. Such a vibrational band was found for pezzottaite around 111 cm^{-1} and was attributed to Cs-O vibrations (e.g. ENDE et al., 2021). However, at elevated pressure a massive band with its tentative maximum below 50 cm^{-1} shifts from below the lower detection limit (50 cm^{-1}) to higher frequencies within the detectable spectral range. At ~ 6 GPa two new Raman bands evolve at ~ 80 cm^{-1} and ~ 120 cm^{-1} , which indicates a change in Cs-O bonding and related coordination of the Cs site, most likely accompanied by a least local symmetry lowering related to changes in the Cs ordering. First results of X-ray diffraction measurements will be presented to shed light on these potential pressure-induced changes, as compared to the high-pressure behaviour of the related pezzottaite structure.

- PALKE, A.C., HENLING, L.M., Ma, C., ROSSMAN, G.R., SUN, Z., RENFRO, N., KAMPF, A.R., THU, K.,
MYO, N., WONGRAWANG, P., WEERAMONKHONLERT, V. (2021): Amer. Mineral., in press
LAURS, B.M., SKIP SIMMONS, W.B., ROSSMAN, G.R., QUINN, E.P., MCCLURE, S.F., PERETTI, A.,
ARMBRUSTER, T., HAWTHORNE, F.C., FALSTER, A.U., GÜNTHER, D., COOPER, M.A.,
GROBETY, B. (2003): Gems Gemol., 39, 284–301.
ENDE, M., GATTA, D.G., LOTTI, P., GRANDTNER, A., MILETICH, R. (2021): J. Solid State Chem., 293,
121841, 1-11.

MINERALOGICAL ALTERATIONS OF GEOPOLYMERS DOPED WITH METALS UNDER AGGRESSIVE LAB AND SEWER CONDITIONS

Mittermayr, F.¹, Ukraineczyk, N.², Gluth, G. J.G.³, Koraimann, G.⁴, Dietzel, M.⁵, Grengg, C.⁵

¹Institute of Technology and Testing of Building Materials, Graz University of Technology,
Inffeldgasse 24, 8010 Graz, Austria

²Institute of Construction and Building Materials, Technical University of Darmstadt,
Franziska-Braun-Strasse 3, 64 287 Darmstadt, Germany

³Division 7.4 Technology of Construction Materials, Bundesanstalt für Materialforschung und -prüfung (BAM),
Unter den Eichen 87, 12205 Berlin, Germany

⁴Institute of Molecular Biosciences, University of Graz, Humboldstraße 50, 8010 Graz, Austria

⁵ Institute of Applied Geosciences, Graz University of Technology, Rechbauerstraße 12, 8010 Graz, Austria
e-mail: f.mittermayr@tugraz.at

Highly aggressive environmental conditions in wastewater infrastructure can lead to a fast rate of deterioration of concrete sewers. This degradation process is associated with complex biological activities referred to as microbial induced acid corrosion (MIAC). Damage related to MIAC is still an unresolved global challenge with high economic and social relevance. Currently used construction materials in sewers do not withstand long-term requirements, thus raising the demand for more durable alternatives. Options in this context comprise highly durable new materials such as geopolymers and/or reduce or totally inhibit relevant microbes from colonizing concrete surfaces in order to avoid in-situ biogenic sulfuric acid production. In this study we report results and highlight mineralogical and chemical alteration processes from lab test, where samples were immersed in sulfuric acid ($\text{pH}_{\text{stat}} = 2$) and from an on-site testing campaign. After exposure to lab and field conditions geopolymer mortars doped with Cu and Zn metal ions in different concentrations were compared to geopolymer mortars without metal additions, calcium aluminate cement-based mortars and ordinary Portland cement-based mortars. Metal-containing geopolymers performed significantly worse compared to un-doped ones in sulfuric acid tests in the lab. In contrast, geopolymers with small amounts of CuSO_4 additions (~0.1 wt.% Cu per binder) exhibited a much better performance in the field, compared to un-doped materials, due to multiple effects on the microorganisms.

NATURAL ROCKS AS IN-HOUSE CONTROL SAMPLES FOR GEOCHEMICAL ANALYSIS

Nagl, P.¹, Mader, D.¹

¹Department of Lithospheric Research, University of Vienna, Althanstraße 14, 1090 Vienna, Austria
e-mail: peter.nagl@univie.ac.at

All analytical methods are subject to errors, therefore it has to be an analyst's goal to minimize them. Those quality control measurements are not only time consuming but can cause considerable costs by the use of different certified rock reference materials, e.g. for checking repeatability, reproducibility or determining the correctness (deviation from true value). This can be done also by "in-house control samples".

The idea of the present study at the Department of Lithospheric Research of the University of Vienna was to have samples of different rock types available for the geochemical analysis for monitoring analytical processes and also for teaching purposes.

First three different rock types (acid, basic and ultramafic) were selected from Austrian localities where samples were collected in larger amounts. Later the suite was expanded by different carbonates and a quartzite and finally with a silty sediment.

After crushing and homogenization, the samples were split using riffle and rotary sample splitters. Sample preparation and analysis using wavelength dispersive X-ray fluorescence analysis (WDXRF) and integrated neutron activation analysis (INAA) was done according to NAGL & MADER (2019) and MADER & KOEBERL (2009). Very good comparability was approved by randomly selected subsamples.

Comparison of the results of WDXRF and INAA showed, that both types of analysis can complement each other in geochemical whole rock analysis; for a lot of elements both methods show (sometimes very) good accordance.

The whole suite of those eight different in-house control sample types is covering most kinds of rocks investigated at the Department of Lithospheric Research. Those 8 samples can be used for monitoring the processes following the laboratories' SOP and they can be used also for teaching and research purposes.

The analysis using WDXRF is flexible, comparatively quick (especially for major elements), and precise. For some other (trace) elements, preference should be given to the more suitable measurement method, but always with regard to availability and the necessity of a certain method and the cost/benefit ratio.

MADER, D., KOEBERL, C. (2009): Appl. Rad. Isotopes, 67, 2100–2103.

NAGL, P., MADER, D. (2019): SAAGAS 27, abstracts, 48.

GEOCHEMISTRY AND ZIRCON U-Pb GEOCHRONOLOGY OF LATE MESOZOIC IGNEOUS ROCKS FROM SW VIETNAM – SE CAMBODIA

Nong, A.¹, Gallhofer, D.¹, Skrzypek, E.¹, Hauzenberger, C.A.¹

¹University of Graz, Graz, Austria, Universitätsplatz 2, 8010 Graz, Austria
e-mail: christoph.hauzenberger@uni-graz.at

Late Mesozoic volcanic and plutonic rocks are predominantly found in the Dalat zone of southern Vietnam, but smaller volumes also occur in southwesternmost Vietnam and southeastern Cambodia comprising mainly basalt and basaltic-andesite to dacite, and diorite, granodiorite and granite. These igneous rock suites indicate several pulses of magmatism during the late stages of a long-lived convergent margin, where the Paleo-Pacific plate subducted beneath the eastern margin of Asia. The age of the plutonic suites (monzogabbro, monzodiorite, diorite, syenite, granodiorite and granite) is constrained by LA-MC-ICPMS U-Pb zircon dating with 107 to 91 Ma. The associated volcanic suite displays U-Pb zircon ages of 105–95 Ma. Mineral and whole-rock chemistry of volcanic and plutonic rocks is characterized by a calc-alkaline affinity for samples in the Dalat zone and high-K calc-alkaline to shoshonitic affinity for rocks in SW-Vietnam – SE-Cambodia. Mineral characteristics and variation diagrams of selected elements suggest that fractional crystallization dominated during magma differentiation.

A younger magmatic suite (83–75 Ma) is found within the intrusive rocks displaying A-type characteristics. These plutonic bodies comprise fine-grained biotite granites, which are partly fluorite bearing and coarse-grained two-mica granites which are characterized by high contents of HFSEs. Geochemical signatures of these young igneous rocks indicate an extensional tectonic setting, possibly related to basaltic injection/asthenospheric upwelling. This additional heat input is required for partial melting of a dry residual crustal source which resulted from the extraction of subduction-related granitoids at the earlier stage. Geochemical and geochronological results clearly demonstrate that the Late Mesozoic magmatism in southern Indochina can be related to two significant tectonic stages in Indochina and adjacent areas: (1) the Paleo-Pacific subduction (110–90 Ma) and (2) the transitional phase leading to the opening of the East Vietnam Sea/South China Sea (90–75 Ma).

OLIVINE CRYSTAL CHEMISTRY REVEALS THE POSSIBLE TRIGGERING OF THE 2002-2003 Mt. ETNA FLANK ERUPTION

Ntaflos, T.¹, Abart, R.¹, Ferlito, C.², Giacomo, P.P.³, Casetta, F.¹, Coltorti, M.³,
Hauzenberger, C.A.⁴

¹Department of Lithospheric Research, University of Vienna, Althanstraße 14, 1090 Vienna, Austria

²Department of Biological, Environmental and Geological Sciences, University of Catania,
Piazza Universitá 2, 95131 Catania, Italy

³Department of Physics and Earth Sciences, University of Ferrara, Via Saragat 1, 44122 Ferrara, Italy

⁴University of Graz, Universitätsplatz 3, 8010 Graz, Austria
e-mail: theodoros.ntaflos@univie.ac.at

Mount Etna is a stratovolcano with a complex plumbing system. Besides the 3 central summit craters, there are fissure eruptions as well as a large number of eccentric cinder cones located on the flanks around the volcano. We studied the 2002-2003 effusive fissure eruption at 2750 m a.s.l. in the NE flank of the volcano. The rocks are trachybasalts, which were collected directly from the fissure and represent the very last effusive lavas of this eruption. The texture is porphyritic and the mineralogical assemblage is dominated by clinopyroxene phenocrysts with olivine and Fe-Ti oxide inclusions and complex zoning, followed by olivine and plagioclase, which frequently shows cores with sieve texture. The groundmass consists of clinopyroxene, olivine, plagioclase, Ti-Fe oxides and variable amounts of glass. The whole rock Mg# is about 52, the alkali content ($\text{Na}_2\text{O}+\text{K}_2\text{O}$) is close to 5.3 wt%, and the REE abundances (La/Yb) = 20 are lower than those of the typical Mongibello lavas. High precision EPMA analyses of olivine phenocrysts have shown simultaneous occurrence of normal and complex inverse zoning. According to the detailed elemental profiles based on major, minor and trace elements, olivine is divided into three groups: group A with normal zoning, group B with inverse zoning, and group C overgrowth on existing olivine with normal and inverse zoning. The rim to rim compositional profiles in olivine grains of the group A show a remarkably wide plateau with Mg# = 80-83 and Ni = 1000-1700 ppm and a narrow, up to 50 microns wide rim where the Mg# drops to 75-73 and the Ni content to 420 ppm. The olivine from group B is characterized by inverse zoning and has, like group A olivine, a wide compositional plateau but rims with variable thickness. The Mg# at the plateau vary systematically from grain to grain between 69 and 74, whereas the up to 100 microns wide rims show a bell-shaped profile with maximum Mg# between 77 and 79 which, at the very rim in contact with matrix, drops to values similar to those in the corresponding plateau. The Ni-contents at the plateau vary from 100 to 380 ppm and correlate positively with the corresponding Mg#. In the rim, the Ni content increases steeply ranging from 100 to 800 ppm and decreases at the very margin in contact with the matrix to the level of the plateau concentrations. The olivine from group C shows a compositional profile similar to the group A normal zoning and an overgrowth of 50 microns wide rim with a bell shaped Mg# profile, which decreases from 73 in the core to 68 in the rim. It is evident that an ascending magma, which experienced en-route fractional crystallization, mixed with a more mafic magma responsible for the inverse olivine zoning prior to the eruption at relatively shallow depths. The estimated time of the diffusive Fe-Mg exchange between the mafic magma and olivine is very short and ranges from a few days to 100 days. Apparently, the magma mixing is associated with the triggering of the 2002-2003 flank eruption.

**SYNCHROTRON RADIATION MICROTOMOGRAPHIC ANALYSIS
OF A SYNTHETIC TRACHYBASALT:
INSIGHTS INTO TITANOMAGNETITE NUCLEATION MECHANISMS**

Peres, S.¹, Griffiths, A.T.¹, Colle, F.², Iannini Lelarge, S.², Mancini, L.³, Masotta, M.²,
Pontesilli, A.⁴

¹University of Vienna, Vienna, Althanstrasse 14,1090 Vienna, Austria

²University of Pisa, Via Santa Maria 53, 56126 Pisa, Italy

³Elettra-Sincrotrone Trieste S.C.p.A., S.S. 14, 34149 Basovizza, Trieste, Italy

⁴Istituto Nazionale di Geofisica e Vulcanologia, Via di Vigna Murata 605, 00143 Roma, Italy

e-mail: stefano.peres@univie.ac.at

Titanomagnetite (Tmt) and Clinopyroxene (Cpx) commonly form clusters in mafic magmas. Studying the mechanisms of active crystal clustering and the formation conditions of clusters offers important insights into the nature and evolution of volcanic plumbing systems and crystal mushes. 2D images are not sufficient to capture the geometry and true degree of clustering between two phases. To overcome this, we present a phase-contrast synchrotron X-ray microtomographic analysis of Tmt-Cpx clusters in a synthetic trachybasalt sample with 2 wt% H₂O added. The sample is one of a series of isothermal time series experiments, produced in a Quick Press piston-cylinder apparatus at 4 kbar. After 30 minutes of superheating at 1300 °C the sample was cooled to 1150 °C and held for 30 minutes before quenching.

3D X-ray imaging reveals a vertical gradient in crystallinity and in the size of the mineral phases caused by an intrinsic temperature (and thus undercooling) gradient in the experimental apparatus (temperature decreases of approximately 30 °C from bottom to top of the capsule). At the cold end of the capsule, the crystallinity is maximum. The crystal phases are small dendritic Cpx grains (between 100 µm to 300 µm in size) and small anhedral Tmt grains (1 µm to 25 µm in diameter). In the central portion of the sample, the crystallinity is lower but the overall size of Cpx (> 500 µm) and Tmt (skeletal, 80 µm to 150 µm in diameter) increases. The shape of the crystals is less dendritic/anhedral, respectively. In the hot end of the capsule (where the temperature is controlled by the thermocouple), the sample is dominated by glass, and only isolated skeletal Tmt grains crystallized.

Cpx and Tmt grains are clustered together whenever both crystal phases are present. Although large skeletal Tmt grains are more abundant in the central portion while small anhedral Tmt grains dominate the cold end of the sample, the occurrence of the two Tmt morphologies overlaps, and both can be found in contact with the same Cpx grain. The coexistence of two different Tmt grain morphologies and sizes implies two different nucleation mechanisms. Large skeletal Tmt in the bottom (hotter) and central portion of the sample likely crystallized by homogeneous nucleation and probably predated the crystallization of Cpx grains. Smaller, anhedral Tmt crystals, which decorate dendrites in the central to upper (cooler) portion of the sample, probably crystallized by heterogeneous nucleation on already crystallized Cpx grains. In future, EBSD analysis on the sample will assess if crystallographic orientation relationships between Tmt and Cpx in clusters differ depending on Tmt morphology and inferred nucleation mechanism.

DIFFUSION OF CHROMIUM INTO PERICLASE: AN ELECTRON PROBE MICROANALYZER AND PHOTOLUMINESCENCE SPECTROSCOPY STUDY

Pesek, P.R.^{1,2}, Abart, R.², Nasdala, L.¹

¹University of Vienna, Institut für Mineralogie und Kristallographie, Althanstraße 14, 1090 Vienna, Austria

²University of Vienna, Department für Lithosphärenforschung, Althanstraße 14, 1090 Vienna, Austria

e-mail: patrick.pesek@univie.ac.at

The diffusion of chromium in periclase (MgO) was investigated experimentally. To this end, cubic periclase single crystals with polished (100) faces were either coated with, or embedded in, a fine powder of magnesiochromite (MgCrO_4), which served as the Cr source. The samples were annealed at temperatures in the range 1500–1600 °C for 16–96 h under either oxidizing (in air) or reducing (under argon using a graphite crucible) conditions. The annealed samples were investigated with optical and scanning electron microscopy, electron-probe microanalysis and photoluminescence spectroscopy. Depending on the experimental conditions, Cr contents in the range <0.005–0.32 apfu were attained in MgO . Precipitates of magnesiochromite and of metallic Cr were formed under oxidizing and reducing conditions, respectively. For all experiments where the diffusion source was applied as a thin coating, the diffusion profiles show a local maximum of the Cr concentration at a depth of several tens of micrometers below the samples surface. This profile shape is not consistent with the diffusion behavior of chromium under constant boundary conditions and is explained by the successive decomposition of the magnesiochromite (RUTMAN et al., 1968; LEE & SATA, 1978; CHAKRABORTY et al., 2005) and subsequent loss of Cr from the sample surface via the gas phase. The diffusion profiles analyzed in an embedded periclase annealed under oxidizing conditions show inwardly decreasing Cr concentrations, with profiles being approximately linear. This geometry is explained by an increase in the diffusion coefficient with increasing Cr concentration. A diffusion model, in which a linear relationship between the diffusion coefficient and the concentration of chromium was assumed, fits the measurement data reasonably well. Photoluminescence spectroscopy revealed that the luminescent Cr^{3+} is present in different local environments, which is indicated by the shift in relative intensities of one broad- and several narrow-band emissions. The narrow bands tend to increase at low Cr concentrations. The broad band increases at higher Cr-concentrations, which was also observed by CASTELLI & FORSTER (1975). A correlation between the Cr content and the broad-band Cr^{3+} luminescence emission shows a linear increase in the emission with Cr concentration. The emission is saturated at ~1.5 wt% Cr and suppressed by self-quenching at higher Cr concentrations. However, even at higher Cr contents, the concentration of Cr is correlated linearly with the Cr-related light absorption observed in transmission mode.

CASTELLI, F., FORSTER, L.S. (1975): Phys. Rev. B, 11, 920–928.

CHAKRABORTY, D., RANGANATHAN, S., SINHA, S.N. (2005): Metall. Mater. Transactions B, 36, 437–444.

RUTMAN, D.S., SHCHENETNIKOVA, I.L., KELAREVA, E.I., SEMENOV, G.A. (1968): Refractories, 9, 648–652.

LEE, H.L., SATA, T. (1978): Yogyo-Kyokai-Shi, 86(989), 34–40.

THE YOUNGEST PSEUDOTACHYLYTE GENERATION AT THE BASE OF THE SILVRETTA NAPPE AND THE UPPER PLATE DEFORMATION

Pittarello, L.¹, Levi N.², Wegner W.¹, Stehlík H.³

¹Natural History Museum Vienna, Burgring 7, 1010 Vienna, Austria

²University of Vienna, Department of Geology, Althanstraße 14, 1090 Vienna, Austria and

NiMBUC Geoscience OG, Degengasse 41/5, 1160 Vienna, Austria

³Ing. Harald Stehlík, Hagedornweg 2, 1220 Vienna, Austria

e-mail: lidia.pittarello@nhm-wien.ac.at

The seminal work by KOCH & MASCH (1992) presented and investigated the mutual relationship between pseudotachylytes and (ultra)mylonites formed in amphibolites and gneisses at the base of the Silvretta Nappe, Austroalpine Unit (Eastern Alps). As supported by radiometric dating (THÖNI, 1988), KOCH & MASCH (1992) proposed that these structures cyclically formed during the Eoalpine phase (mid Cretaceous), likely in extensional regime, when the Silvretta Nappe was decoupled from its lithospheric roots. The study of new samples collected in the Jamtal, Tyrol (Austria) allowed the discovery of a further step in the deformation history at the base of the Silvretta Nappe. Detailed petrographic investigations revealed the presence of a generation of pseudotachylytes overprinting the previously described pseudotachylytes and mylonites. Compared to the previously described pseudotachylytes, these have not been further deformed under viscous-plastic conditions or epidotized, and have been perfectly preserved, suggesting a more recent and possibly shallower formation. This deformation event might be related to the final subduction of the Penninic Unit in the Paleogene, as also supported by anomalous young ages obtained by dating (THÖNI, 1988) that were not previously considered. The formation of pseudotachylytes in the upper plate in a shallow subduction setting at the base of the Silvretta Nappe recalls the network of pseudotachylytes observed in the Dent Blanche Austroalpine Unit in the Western Alps, also representing the hanging wall of a subduction zone in the Paleogene (MENANT et al., 2018). These authors refer the possible occurrence of multiple shallow earthquakes in mid-crustal environment in the upper plate due to the presence of asperities, such as rigid bodies, “scratching” the base of the upper plate in the subduction zone. In the case of the Silvretta Nappe, such asperities could have been represented by the fragments of the Briançonnais microcontinent within the subducting Penninic Unit. Our work provides further constraints to the tectonic history of the Silvretta Nappe, where the deformation mostly localized along its base over a long time, through several cycles of pseudotachylyte formation, and supports the understanding of brittle deformation localization in the upper plate in subduction environments.

KOCH, N., MASCH, L. (1992): Tectonophysics, 204, 289-306.

MENANT, A., ANGIBOUST, S., MONIÉ, P., ONCKEN, O., GUIGNERD, J.-M. (2018): Earth Planet. Sci. Letters, 487, 84-93.

THÖNI, M. (1988): Jb. Geol. Bundesanstalt, 131, 169-201.

ON THE STRONTIUM INCORPORATION INTO BREDIGITE –
THE SOLID SOLUTION SERIES $\text{Ca}_{7-x}\text{Sr}_x\text{Mg}[\text{SiO}_4]_4$

Salzmann, M.F.G.¹, Prosser, L.¹, Kahlenberg, V.¹

¹Institute of Mineralogy and Petrography, Innsbruck University, Innrain 52, 6020 Innsbruck, Austria
e-mail: volker.kahlenberg@uibk.ac.at

Bredigite (idealized chemical composition $\text{Ca}_7\text{Mg}[\text{SiO}_4]_4$) is a rare mineral that has been described from different petrological settings related to pyrometamorphism (GRAPES, 2011). It has been observed, for example, in contact-metamorphized rocks or in altered carbonate-silicate xenoliths within volcanites based on siliceous limestone-dolomite protoliths. Furthermore, small bredigite grains were repeatedly found in rocks belonging to the famous Hatrurim Complex (Jordan) consisting of products of combustion metamorphism (KAHLENBERG et al., 2019). Apart from being a mineralogical curiosity, bredigite is also of interest for the field of material science and has been intensively studied as a host for rare earth elements for synthesis of new photoluminescent compounds. In addition, research on bredigite included areas as diverse as bioactive ceramics, steelmaking slags or chemical stabilizing of radioactive waste.

So far, only limited information on the cation substitutions in bredigite is available. MOSELEY & GLASSER (1982) found evidence that Ba and Sr can replace Ca. However, no detailed structural investigations have been performed. In the course of an ongoing research project on the cation substitutions in bredigite-type compounds we investigated the potential solid-solution series $\text{Ca}_{7-x}\text{Sr}_x\text{Mg}[\text{SiO}_4]_4$ ($x = 0, 1, \dots, 7$). Samples were prepared by solid-state reactions using pressed pellets prepared from stoichiometric mixtures of the respective oxides/carbonates. The kinetics of the sintering reactions performed in the range between 1275 and 1325 °C was rather sluggish and, therefore, each mix had to be reground and returned to the furnace for at least two times. Progress of the reactions was monitored using PXRD. From the final sinter pellets of each composition crystals of sufficient size and quality could be extracted for single-crystal diffraction experiments. Evolution of the lattice parameters as well as crystal structure analysis proved the existence of a bredigite-type solid solution series in the samples up to $x = 4$. Studies on the Sr/Ca distributions among the six potential cation sites revealed a clear preference of strontium for specific positions.

GRAPES, R. (2011): Pyrometamorphism. 2nd ed. Springer, Heidelberg, Dordrecht, London, New York.

KAHLENBERG, V., GALUSKINA, I., KRÜGER, B., PAULUHN, A., GALUSKIN, E. (2019): Miner. Petrol., 113, 261–272.

MOSELEY, D., GLASSER, F.P. (1982): J. Mater. Sci., 17, 2736–2740.

**PETROGENESIS AND ECONOMIC SIGNIFICANCE OF THE ABU DABBAB
Sn, Ta-BEARING GRANITES FROM THE NORTH ARABIAN-NUBIAN SHIELD**

Sami, M.^{1,4}, Abd El Monsef, M.², Toksoy-Köksal, F.³, Ntaflos, T.⁴, Abart, R.⁴,
Abdelfadil, K.M.⁵

¹Geology Department, Faculty of Science, Minia University, Shalaby Land, Main road, 61519 El-Minia, Egypt

²Geology Department, Faculty of Science, Tanta University, El-Giesh Street, 31111 Tanta, Egypt

³Department of Geological Engineering, Middle East Technical University, Üniversiteler Mahallesi,
Dumlupınar Bulvarı 1/6-133, 06800 Çankaya/Ankara, Turkey

⁴Department of Lithospheric Research, University of Vienna, Althanstraße 14, UZAII, 1090 Vienna, Austria

⁵Geology Department, Faculty of Science, Sohag University, Nasser City Street, 82524 Sohag, Egypt
e-mail: mabrouk.hassan@mu.edu.eg

The Abu Dabbab pluton, which is located in the Central Eastern Desert of Egypt, is one of the most promising Sn, Ta-bearing Neoproterozoic granites in the north Arabian Nubian Shield (ANS). The Abu Dabbab granites are still being explored with their petrogenesis and relationship to Sn, Nb, and Ta mineralization. Mineral chemistry, whole-rock geochemical, and Sr-Nd isotopic data are reported, to constrain their petrogenesis, geodynamic evolution, and economic significance. Geochemically, the Abu Dabbab albite granites are weakly to mildly peraluminous with high SiO₂, alkalis, Nb, Ta, Sn, F, and Ga/Al, but low MgO, CaO, and P₂O₅ contents. They have tetrad-type REE patterns (TE₁₋₃ = 1.8-2.5), strong negative Eu anomalies and extreme depletion in Ba, Sr, P, and Ti, which are characteristics of highly fractionated A-type granites. The isotopic data display positive $\epsilon_{\text{Nd}}(t)$ values (+1.11 to +8.32) and t_{DM2} (0.68-1.13 Ga), suggesting a juvenile magma source of Neoproterozoic age similar to other granitic plutons in the ANS. The granites were formed by partial melting of crustal materials followed by an extensive fractional crystallization and were subsequently affected by late- to post-magmatic fluids during their magmatic evolution. The crystallization of cassiterite and columbite-tantalite may have occurred due to localized saturation and crystallization within trapped intercumulus melt. The granites were formed during the transition from late to post collisional magmatism in the ANS. They are probably related to lithospheric delamination and slab breakoff, which lead to upwelling of asthenospheric magma that provided a continuous flow of volatile-rich fluids and enhanced the fertility of the crustal magma. The strong Ta and Sn enrichments in the granites could be a consequence of crystal melt fractionation and fluid saturation that made the mineralized Abu Dabbab granites of valuable economic significance with promising tonnage of Sn and Ta reserve.

**MINERALOGY AND GEOCHEMISTRY OF THE MICROGRANULAR ENCLAVES
HOSTED BY HIGHLY EVOLVED GRANITES FROM THE
CENTRAL EASTERN DESERT OF EGYPT**

Sami, M.^{1,2}, Ntaflos, T.², Abart, R.², Farahat, E.S.¹, Fathy. D.¹

¹Geology Department, Faculty of Science, Minia University, Shalaby Land, Main road, 61519 El-Minia, Egypt

²Department of Lithospheric Research, University of Vienna, Althanstrasse 14, UZAII, 1090 Vienna, Austria

e-mail: mabrouk.hassan@mu.edu.eg

The genesis of enclaves hosted by highly evolved granites is still a point of dispute, particularly the relative contributions of crustal and mantle sources to the formation of these granites. To address this issue, we report mineralogical and geochemical data for enclaves hosted by fluorite bearing highly fractionated granites from the Central Eastern Desert of Egypt. The majority of the enclaves are circular in shape and have sharp contacts to the host rock. The enclaves have an intermediate silica composition and may be classified as monzodiorite. They consist of biotite, hornblende, plagioclase, quartz, K-felspar, and fluorite as the main mineral phases. Titanite, ilmenite, rutile, and zircon are present as accessory phases. The plagioclases range in composition from oligoclase to labradorite, while biotite and hornblende are classified as Mg-rich minerals. Geochemically, the monzodiorite enclaves have a calc-alkaline and metaluminous character. They contain significant quantities of large ion lithophile elements like Rb and K but are deficient in high field strength elements like Nb, Ta, P, Ti, and U. The studied enclaves are probably formed by partial melting of a metabasaltic to metatontalitic magmatic source. The enclaves represent trapped blebs of intermediate parental magma mixed with felsic melts during their magmatic evolution.

AGE DATING AND GEOCHEMISTRY OF INTRUSIVE IGNEOUS ROCKS IN BOKEO AND LUONG NAMTHA PROVINCES, LAO PDR

Santitharangkun, S.^{1,2}, Hauzenberger, C.A.¹, Gallhofer, D.¹, Phajuy, B.²

¹Karl-Franzens-University Graz, Universitätsplatz 2, 8010 Graz, Austria

²Chiang Mai University, 239 Huay Kaew Road, 50200, Chiang Mai, Thailand

e-mail: srett.santitharangkun@gmail.com

The igneous rocks from the Bokeo and Luong Namtha provinces, northwestern Lao PDR are important for constraining the tectonic evolution Indochina and the closure of the Paleo-Tethys ocean. The investigated area belongs to the Sukhothai zone which is also known as Eastern Granitoid Belt in Thailand and is linked to the Lancangjiang zone in southwestern China. The intrusive rocks in the study area can be separated into two main groups based on geochemical composition: (1) gabbro to diorite group and (2) granitoid group.

(1) The gabbro-diorite group can be further divided into three subgroups: (I) gabbro dike, (II) gabbro, and (III) diorite suites. The mineral assemblage of the gabbro dike suite is plagioclase + clinopyroxene + opaque mineral. The geochemical characteristics of the gabbro dike suite represent a magma derived from a depleted continental lithospheric mantle with contamination from subduction components. The typical mineral assemblage of the gabbro and diorite suites is plagioclase + clinopyroxene + hornblende ± orthopyroxene ± quartz ± biotite + opaque mineral ± apatite and represent melts derived from a subduction setting. The gabbro pluton and diorite suite yielded a zircon U–Pb age of 232.2 ± 3.1 Ma.

(2) The granitoid group can be classified as (I) alkaline-rich granitoid (potassium feldspar rich-granitoid suite), (II) alkaline-poor granitoid (potassium feldspar poor granitoid suite), and (III) cordierite bearing granitoid suite. The alkaline-rich granitoid sample from Bokeo and Luong Namtha provinces yields a zircon U–Pb age of 231.0 ± 3.1 Ma. The samples contained the mineral assemblage quartz + plagioclase + K-feldspar + biotite ± opaque mineral ± apatite ± zircon ± allanite. Most of the alkaline-rich granitoid samples display a well developed negative Eu anomaly which indicates plagioclase crystal fractionation. The primitive mantle normalized diagram proved Nb and Ta negative anomalies. The gabbro and diorite suites represent melts derived from a subduction setting. The alkaline-poor granitoid suite yielded a zircon U–Pb age of 250.8 ± 3.4 Ma, implying that these rocks were generated in a magmatic arc system during the Early Triassic. The alkaline-poor granitoid suite does not display a negative Eu anomaly suggesting no plagioclase crystal fractionation. The cordierite bearing granitoid suite yielded a zircon U–Pb age of 244.4 ± 3.2 Ma. The cordierite bearing granitoid suite displays a narrow range in CaO/Na₂O and a high La_N/Yb_N ratio.

The petrological, geochemical, and geochronological results of this study suggest that the alkaline-poor and cordierite bearing granitoid suite rocks from Bokeo and Luong Namtha provinces represent mainly a volcanic arc setting during the Early Triassic. The gabbro, diorite, and alkaline-rich granitoid suites may be related to a post-collision event following the closure of the Paleo-Tethys during Late Triassic.

H₂O-FLUXED MELTING OF ECLOGITE DURING EXHUMATION: AN EXAMPLE FROM THE ECLOGITE TYPE-LOCALITY, EASTERN ALPS (AUSTRIA)

Schorn, S.¹, Hartnady, M.I.H.², Diener, J.F.A.³, Clark, C.², Harris, C.³

¹NAWI Graz Geocenter, University of Graz, Universitätsplatz 2, 8010 Graz, Austria

²School of Earth and Planetary Sciences, Curtin University, Perth, WA, Australia

³Department of Geological Sciences, University of Cape Town, Private Bag X3, Rondebosch 7701, South Africa
e-mail: simon.schorn@uni-graz.at

Epidote eclogites embedded in paragneisses from the Austrian Eastern Alps host rare, decimetre- to metre-sized planar pegmatitic segregations ('pegmatoids') that consist of a hornblende–plagioclase–epidote–titanite–quartz assemblage. The pegmatoids cut the primary eclogite foliation at a high angle, show abrupt terminations and exhibit numerous microtextures indicating the former presence of melt, whereas the surrounding eclogites and paragneisses lack evidence for dehydration melting. We interpret the pegmatoids as crystallised hydrous melts of intermediate composition derived from a nearby eclogitic source, similar to the eclogite host rock. The host eclogite preserves high-pressure assemblages of garnet–omphacite–epidote–quartz–rutile ± phengite that yield peak P–T estimates of 21 ± 2 kbar and 700 ± 20 °C calculated via pseudosection modelling and Zr-in-rutile thermometry. Subsequent near-isothermal decompression occurred in a closed system under fluid-absent conditions that favoured the preservation of garnet–omphacite assemblages in eclogites. Thermodynamic modelling of the metapelitic country rock indicates that the paragneisses remained fluid-absent during early exhumation, but became fluid-saturated at mid-crustal conditions of 7.5–9 kbar and 680–690 °C. We suggest that, as the metapelites dehydrated, minor aqueous fluid was released and infiltrated the enclosed eclogites along discordant fractures that formed in response to unloading, further facilitated by steep gradients in $\mu\text{H}_2\text{O}$ between the fluid-saturated pelitic country rock and fluid-absent eclogite lenses. Eclogite distal from fluid sources/pathways experienced limited retrogression, whereas localised re-equilibration and H₂O-fluxed melting is inferred for eclogite affected by extensive fluid infiltration. Zr-in-titanite thermometry on crystals from pegmatoids yields a crystallisation temperature of 697 ± 10 °C at 8.5 ± 1.5 kbar, similar to retrograde conditions recorded by the regionally dominant metapelites. Oxygen- and hydrogen isotopic data for eclogite, pegmatoids and paragneiss are consistent with hydrous fluid transfer from paragneisses to eclogites and a low fluid/rock ratio. We suggest that, at conditions that preclude dehydration-melting, even small-scale melting of eclogite requires addition of fluid from a suitable near-field source.

AUTOMATED IDENTIFICATION AND EVALUATION OF MINERALS BY SEM-EDS: MAPS MINERALOGY – THE SIMPLE TOOL FOR COMPLEX ROCKS

Schwarzmueller, S.¹, Phifer, D.¹, Goergen, E.¹

¹Thermo Fisher Scientific, Zwaanstraat 31G/H, Building TR, 5651 CA Eindhoven, The Netherlands

e-mail: stefan.schwarzmueller@thermofisher.com

Automated mineralogy with SEM-EDS has a long-standing history within Thermo Fisher Scientific (legacy FEI). QEMSCAN and the Mineral Liberation Analyzer (MLA) have been used for decades in commercial and scientific applications like mineral exploration and processing, petrology, environmental sciences, archaeology and so on (REID et al., 1984; GOTTLIEB et al., 2000). MAPS MINERALOGY builds on this knowledge in automated mineralogy by providing a higher degree of automation and less manual work to QC the results: Decoupling the backscattered image from EDS enables a submicron SEM image resolution and guarantees preservation of textural details even at coarse EDS resolution. In case several minerals are present within the interaction volume (Figure 1), the “Mixel” technology permits accurate multi-phase mineral ID as well as the quantitative proportions of those phases. The “Mixel” thereby allows deployment of automated mineralogy even on fine-grained or complicated mineral textures and at grain boundaries - areas where other technologies fail to provide accurate results. Minerals are assigned from a database with greater than 4000 entries on an improved classification approach to any rock type with no need for *a priori* knowledge. Users can even modify and create their own solid solutions based on the full database of the end members’ chemistry. The mineral coloring scheme in Maps Mineralogy is dynamic and representative of chemical variance within a mineral. Figure 1 displays a mineral map where the blue phase is dolomite. Variance in the blue shades reflect the amount of Fe distributed in the phase. This makes quick inspection of relative chemical zoning fast and aids targeting additional chemical analysis in other systems (e.g. EPMA). Finally, Maps mineralogy also provides accurate Bulk compositional data that is equivalent to XRF data.

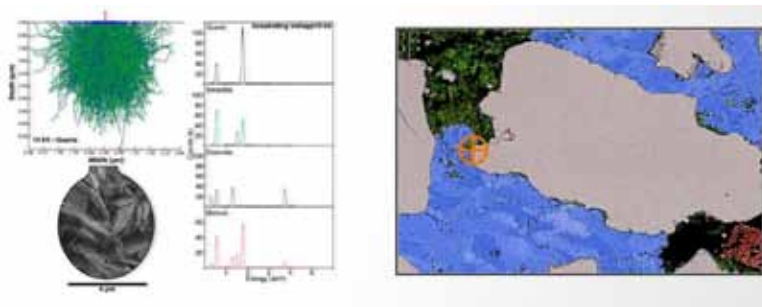


Figure 1. Left: Interaction volume from a mixture of dolomite, smectite and quartz as well as mixed and unmixed (individual contributions) EDS spectra. Right: Point of data acquisition (orange) and assignment of colors and opacity according to database and pre-defined solid solutions.

- REID, A.F., GOTTLIEB, P., MACDONALD, K.J., MILLER, P.R. (1984): In PARK, W.C., HAUSEN, D.M., HAGNI, R.D. (eds): Appl. Miner. (Warrendale, PA: TMS), 191-204.
 GOTTLIEB, P., WILKIE, G., SUTHERLAND, D., HO-TUN, E., SUTHERS, S., PERERA, K., JENKINS, B., SPENCER, S., BUTCHER, A., RAYNER J. (2000): JOM, 52, 24-25.

MANTLE ROCKS IN CONTINENTAL COLLISIONAL OROGENS

Sizova, E.¹, Hauzenberger, C.¹, Gerya, T.^{2,3}, Fritz, H.¹, Faryad, S.W.⁴

¹Institute of Earth Sciences, University of Graz, Universitätsplatz 2/2.Stock, 8010 Graz, Austria

²Institute of Geophysics, ETH-Zurich, Sonneggstrasse 5, 8092 Zurich, Switzerland

³Geology Department, Moscow State University, 119199 Moscow, Russia

⁴Institute of Petrology and Structural Geology, Charles University, Albertov 6, 12843 Prague 2, Czech Republic
e-mail: elena.sizova@uni-graz.at

During the last decades the rising interest for ultrahigh-pressure crustal rocks in the collisional orogens has led the geologists to the detailed investigation of the associated ultramafic rocks, which could be valuable for the reconstruction of the tectonothermal conditions during continental collision. The most intriguing of these rocks are garnet peridotites which are common in the continental collision orogens. Garnet peridotites are typically polymetamorphic rocks appearing as relics (meters to kilometres bodies) within lower-grade ultramafic host rocks (gneisses or granulites) and have concordant to discordant contacts with those (MEDARIS, 1999). The garnet peridotites vary dramatically even within the individual tectonic orogens and propose distinct metamorphic evolution based on their P-T-t paths. The main two groups of these rocks are crustal and mantle peridotites, where the first group represents ultramafic blocks emplaced into the crust prior to subduction event. Based on a series of 2D petrological–thermomechanical numerical experiments we investigated the fate of mantle peridotites incorporated into the subducted continental crust at different continental collision scenarios. We reconstructed the evolution of both crustal and mantle peridotites involved into collision. In the final collisional orogens in the experiments we determined 18 distinct groups of the peridotites based on their P-T-t paths: 12 groups of peridotites from the overriding plate lithospheric mantle and the asthenospheric mantle below, 3 groups of peridotites from the crustal ultramafic blocks (initially emplaced into the later subducting continental crust), and 3 groups among the peridotites from the lithospheric mantle of the subducting plate. The associated crustal material does not necessarily show the same metamorphic evolution showing higher or lower peak metamorphic conditions, meeting with the peridotite markers in most cases during exhumation stage. The determined P-T-t paths for the peridotites cover most of the metamorphic conditions proposed for the natural peridotites from the continental collisional orogens all over the world including those coming from the extreme large depths from the mantle.

MEDARIS, L.G. (1999): Internat. Geol. Rev., 41, 799-815.

**RAMAN SPECTROSCOPIC STUDY OF CARBONACEOUS MATERIAL
AFFECTED BY CONTACT AND REGIONAL METAMORPHIC EVENTS
(RYOKE BELT, SW JAPAN)**

Skrzypek, E.^{1,2}

¹Department of Geology and Mineralogy, Graduate School of Science, Kyoto University,
Kitashirakawa-Oiwakecho, Sakyo-ku, 606-8502 Kyoto, Japan

²Institute of Earth Sciences, NAWI Graz Geozentrum, Petrology and Geochemistry, University of Graz,
Universitätsplatz 2, 8010 Graz, Austria
e-mail: etienne.skrzypek@uni-graz.at

The first- and second-order Raman spectra of carbonaceous material (CM) are explored in metamorphic rocks affected by successive contact and regional metamorphic events (W part of the Ryoke belt, Iwakuni-Yanai area, SW Japan). The area exposes metasedimentary rocks that underwent contact metamorphism before and after the main regional tectono-metamorphic event (DP1). First-order spectra document a decreasing peak area ratio R2 and an increasing temperature T_{CM} towards the south and the surrounding granitoids. Domains with intermediate (535–600 °C) T_{CM} values match the extent of the pre-DP1 contact aureole but also image a so far unrecognized post-DP1 aureole. The axial part of the belt, likely unaffected by granite intrusions, preserves southward increasing T_{CM} from 425 to 660 °C, which is compatible with the regional low-Pressure/high-Temperature gradient described in the area. Second-order spectra show a single S1 band that splits into two peaks (S1- and S1+) whose frequency difference $\Delta S1$ increases stepwise towards the south. The spatial distribution of $\Delta S1$ follows that of the E–W trending regional metamorphic zones.

The splitting of S1 indicates a transition from two-dimensional to three-dimensional CM and occurs at ~500 °C, which seems to be common to all metamorphic belts worldwide. Despite regional metamorphism, CM was also able to record the post-DP1 contact overprint. A discrepancy between first- and second-order Raman parameters suggests that they partly record the influence of different factors; R2 gives an account of thermal events, particularly those related to localized contact metamorphism, whereas $\Delta S1$ potentially yields information on regional variations in heating duration and pressure. This demonstrates the potential of the full Raman spectrum of CM for deciphering the complex thermal history of orogenic systems.

**THE ROLE OF ADDITIVES AND HUMIDITY ON THE TRANSFORMATION OF
AMORPHOUS CALCIUM CARBONATE –
MINERALOGICAL AND MICROSTRUCTURAL EVOLUTION**

Spirk, T.C.¹, Goetschl, K.E.¹, Dietzel, M.¹

¹Institute of Applied Geosciences, Graz University of Technology, Rechbauerstraße 12, 8010 Graz, Austria
e-mail: tina.spirk@student.tugraz.at

Amorphous calcium carbonate (ACC) is one of the seven $\text{CaCO}_3 \cdot n\text{H}_2\text{O}$ ($0 \leq n \leq 6$) solids and due to its high solubility, high specific surface area and porosity of vast interest for the development of advanced materials. The mechanisms and individual pathways of microstructural porosity development during ACC transformation exposed to different humidity-levels have not been sufficiently understood yet.

Therefore, the transformation of four ACC-types, either pure or synthesized with the addition of activated carbon, magnesium chloride or xanthan, was investigated at two distinct humidity levels. The pure and additive containing ACC standard material was stamped into a pellet and exposed to 45 % and 74 % relative humidity (RH) over a period of 28 days.

The addition of xanthan induced a reduction of the vaterite content, activated carbon resulted in an extreme low vaterite content and the presence of Mg^{2+} ions completely inhibited the formation of vaterite. Furthermore, this study highlights that elevated RH favours initial vaterite formation and causes an increase of the mean pore size of the final crystalline product by a factor up to 6.

The findings on porosity evolution during the transformation of ACC can be used to tailor and improve ACC and highly porous CaCO_3 (micro-nano) material designs and syntheses for pharmaceutical and industrial applications.

EFFECT OF SUCROSE AND SEED CRYSTALS ON THAUMASITE AND ETTRINGITE (co)-PRECIPITATION

Steindl, F. R.^{1,2}, Baldermann, A.¹, Galan, I.¹, Mittermayr, F.², Letofsky-Papst I.³, Dietzel, M.¹

¹Institute of Applied Geosciences, Graz University of Technology, Rechbauerstraße 12, 8010 Graz, Austria

²Institute of Technology and Testing of Building Materials, Graz University of Technology,
Inffeldgasse 24, 8010 Graz, Austria

³Institute of Electron Microscopy and Nanoanalysis and Center for Electron Microscopy,
Graz University of Technology, NAWI Graz, Steyrgasse 17, 8010 Graz, Austria
e-mail: florian.steindl@tugraz.at

A particular form of sulfate attack on concrete is the formation of thaumasite, which can cause the destruction of the cement matrix. The influence of ettringite seed crystals on thaumasite formation and the effect of sucrose on the incorporation of Si and carbonate into ettringite were investigated in precipitation experiments using a synthesis protocol adapted from BLANCO-VARELA et al. (2012). The precipitation reactions were monitored regarding the chemical composition, pH, and electrical conductivity of the solutions. The precipitates were examined by infrared spectroscopy, powder X-ray diffraction, and scanning and transmission electron microscopy. The results provide indications for the incorporation of Si and/or carbonate into the ettringite structure during precipitation (Fig. 1). Furthermore, the presence of ettringite seed crystals strongly enhanced thaumasite formation, with seeded experiments yielding significant amounts of precipitate within only 7 days, whereas control experiments without seeds yielded no precipitate within 56 days. The presence of sucrose did not only influence the incorporation of Si and/or carbonate into ettringite, but strongly controlled the crystal morphology of ettringite, causing a shift from acicular crystals to watermelon-shaped balls (Fig. 2). The results provide interesting implications for the formation paths and environmental controls of thaumasite and/or ettringite-thaumasite solid solutions in cementitious materials.

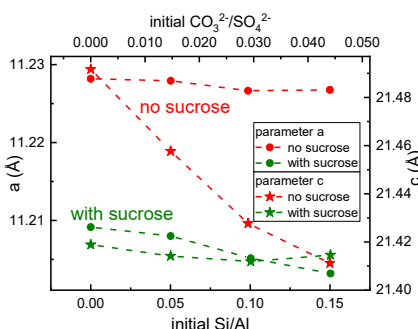


Figure 1. Change of ettringite lattice parameters with increasing $\text{Si}(\text{OH})_4$ and CO_3^{2-} concentrations in the initial solution.

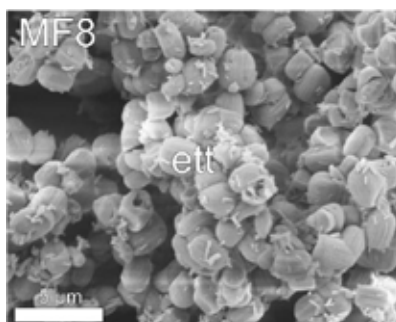


Figure 2. Precipitate of ettringite synthesis after 14 days of reaction, showing "watermelon ettringite".

AN UPDATE ON SECONDARY THALLIUM MINERALS

Steinfeld, A.¹, Đorđević, T.¹, Kolitsch, U.^{2,1}, Nagl, P.³, Tasev, G.⁴, Serafimovski, T.⁴, Boev, I.⁴, Boev, B.⁴

¹Institut für Mineralogie und Kristallographie, Universität Wien, Althanstraße 14, 1090 Wien, Austria

²Mineralogisch-Petrographische Abteilung, Naturhistorisches Museum, Burgring 7, 1010 Wien, Austria

³Department of Lithospheric Research, Universität Wien, Althanstraße 14, 1090 Wien, Austria

⁴Department of Mineral Deposits, University “Goce Delčev”-Štip, Goce Delčev 89, 2000 Štip, North Macedonia
e-mail: tamara.djordjevic@univie.ac.at

In order to gain more knowledge on the environmental behaviour of thallium in As- and Tl-extreme environments, we have chosen the abandoned As–Sb–Tl–Au Allchar deposit (North Macedonia) with unique mineral composition and high thallium grades of the ore. We used X-ray fluorescence analysis (XRFA), powder X-ray diffraction (PXRD), scanning electron microscopy with energy-dispersive spectroscopy (SEM-EDS) and Raman spectroscopy to determine the retention of thallium in secondary minerals of the especially Tl-rich Crven Dol locality in the northern section of the Allchar deposit.

XRFA showed that the mean concentrations of Tl and As in soils adjacent to dumps are 3 g/kg and 59 g/kg, respectively, but can locally, in realgar-rich dumps, rise to extreme values of 11 g/kg for Tl and 166 g/kg for As.

PXRD studies showed that the various solid waste samples are comprised mostly of carbonates (dolomite and calcite), gypsum, quartz, muscovite, kaolinite-group minerals followed by orpiment, realgar, pyrite, marcasite, lorándite ($TlAsS_2$), and various iron and calcium arsenates. Using SEM-EDS and Raman spectroscopy on polished sections, we took a closer look at the secondary minerals formed in the carbonate-buffered environments ($pH = 7\text{--}8$). Besides common arseniosiderite, $Ca_2Fe_3^{3+}(AsO_4)_3O_2 \cdot 3H_2O$, talmessite, $Ca_2Mg(AsO_4)_2 \cdot 2H_2O$, minor thalliumpharmacosiderite, $TlFe_4[(AsO_4)_3(OH)_4] \cdot 4H_2O$, Tl³⁺-bearing scorodite (up to 1.7 at.%), $Fe^{3+}AsO_4 \cdot 2H_2O$, and rare Ca-Mn arsenates, we proved the existence of small (up 100 μm) aggregates of at least five previously unknown secondary thallium phases at the present stage of our studies:

1) Tl– M^{2+} -arsenates with approximate Tl:M:As ratios of (i) ~3:1:1 (Mg- or Ca-dominant with Mg ~ Ca); (ii) 2:1:1 (mainly Mg- oder Mn-dominant); (iii) 1:1:1 (mainly Ca- or Mg-dominant, with major, but variable Fe); (iv) 1:3:2 (strongly Mn-dominant, with apparent Si(?) content). All these arsenates show slightly to distinctly variable ratios of the M^{2+} cations within individual aggregates.

2) Cryptomelane-type Tl-bearing Mn oxides (3.1 to 3.8 at.% Tl), probably closely related to thalliomelane, $Tl(Mn^{4+}_{7.5}Cu^{2+}_{0.5})O_{16}$.

This study provides further evidence of thallium uptake by newly found thallium secondary phases in carbonate-buffered, near-neutral As- and Tl-rich environments and indicates the need for further studies on Tl speciation in As- and Tl-extreme environments.

This work was supported by the Austrian Science Fund (FWF) [grant number P 30900-N28 to T. Đorđević].

GEOCHRONOLOGIE, GEOCHEMIE UND PETROLOGIE EINES TOPAS-FÜHRENDEN ORTHOGNEISES INNERHALB DER „MONOTONEN SERIE“ (OSTRONG EINHEIT, NÖ)

Stockinger, V.¹, Göd, R.¹, Grasemann, B.¹, Linner, M.², Klötzli, U.¹, Abart, R.¹, Slama, J.³

¹Universität Wien, Althanstraße 14, 1090 Wien, Österreich

²Geologische Bundesanstalt, Neulinggasse 38, 1030 Wien, Österreich

³Institute of Geology of the Czech Academy of Sciences,

Rozvojová 269, 165 00 Prag 6-Lysolaje, Tschechische Republik

e-mail: verena.stockinger@univie.ac.at

In den 80er-Jahren wurden weite Teile des österreichischen Anteiles an der Böhmischem Masse in Hinblick auf das Auftreten von Rohstoffen prospektiert (GÖD, 1988), wobei eine spurenhafte Topas-Führung in Gerinnen, die den Ostabhang des Ostrongs entwässern, entdeckt wurde. Die in der gegenständlichen Arbeit untersuchten Orthogneise der Monotonen Serie (Ostrong Einheit, Niederösterreich) wurden als die Quelle dieser Topase nachgewiesen, indem mittels RAMAN-Spektroskopie Topase aus Schwermineralkonzentraten aus den Orthogneisen bestimmt werden konnten. Nach derzeitigem Wissensstand ist dies das einzige Vorkommen Topas-führender Orthogneise innerhalb des gesamten Moldanubikums.

Detaillierte geochemische Untersuchungen der Haupt- und Spurenelemente dieser Gesteine mittels RFA, ICP-MS und Ionenchromatographie ergaben eine Einstufung als Meta-granite oder-rhyolithe mit einem hohen Differenzierungsgrad. Sie besitzen einen hohen SiO₂-Gehalt von 72,8 - 77,3 Gew.%, außerdem ist ein hoher Fluor-Gehalt von bis zu 2760 ppm indikativ und zudem besitzen sie einheitlich einen peraluminösen Charakter. Insgesamt zeigen sich geochemische Ähnlichkeiten einerseits zum Blanik-Gneis (Ostrong Einheit) und andererseits zum Gföhl-Gneis. Die untersuchten Gesteine weisen eine tektonische Überprägung auf und zeigen eine schwache bis gut ausgeprägte Foliation, sowie stellenweise Verfaltungen. Proben, die in der Nähe der tektonischen Grenze der Ostrong zur Drosendorf Einheit genommen wurden, zeigen eine stärkere scherende Deformation mit ausgeprägter mylonitischer Foliation und Streckungslineation. Das Gestein führt durchgehend Sillimanit und jene Proben nahe dieser tektonischen Grenze auch Disthen. Untersuchungen der Mineralchemie mittels Elektronenstrahlmikrosonde zeigen zonierte Plagioklase mit einer Albit-Komponente von etwa 87 – 99 Mol%, die gegen den Korn-Rand zunimmt. In den Proben nahe der tektonischen Grenze der Ostrong zur Drosendorf Einheit tritt Almandin-dominierter Granat auf, der keine Zonierung zeigt und als einphasig charakterisierbar ist. Um das bisher noch unbekannte Alter der untersuchten Orthogneise zu bestimmen, wurde die U-Pb Datierungsmethode an Zirkonen angewandt und dadurch das erste absolute minimale Alter der „Monotonen Serie“ bestimmt. Die Methodik ergab die Alter von $475,3 \pm 0,5$ Ma, $474,8 \pm 1,3$ Ma und $473,5 \pm 0,8$ Ma. Der kurzprismatische Habitus der untersuchten Zirkone deutet darüber hinaus auf eine plutonische und nicht vulkanische Herkunft der Orthogneise hin. Die in dieser Arbeit erzielten Ergebnisse können zum Verständnis der paläogeographischen Position, des tektonischen Aufbaues und der Entwicklung des Moldanubikums beitragen.

GÖD, R. (1988): Zusammenfassende Übersicht über ausgeführte Erzprospektionsvorhaben, dabei eingesetzte Methoden sowie Hoffnungsgebiete im Kristallin der Böhmischem Masse; unveröffentl. Bericht, GBA

**AGE DATING OF DETRITAL ZIRCON AND PETROLOGY OF THE
ENNSTAL PHYLLITE ZONE (EASTERN ALPS)**

Stumpf, S.¹, Skrzypek, E.¹, Stüwe, K.¹

¹University of Graz, Universitätsplatz 2, 8010 Graz, Austria
e-mail: sebastian.stumpf@edu.uni-graz.at

The Ennstal Phyllite Zone is a west-east striking zone paralleling the Enns valley east of Schladming in the Eastern Alps. The affiliation of this area to either the micaschist units of the Koralpe-Wölz nappe system to its south or to the Greywacke Zone to its north is still unclear. In fact, due to the similarities with the phyllites of the Greywacke Zone to the north and the low-grade micaschists in the south, no clear boundary between these units is observable. In order to clear this debate, we present the first U/Pb age dating results and PT-calculations for the Ennstal Phyllite Zone. Samples were taken along multiple north – south striking valleys which transect the Ennstal Phyllite Zone and the northernmost part of the Wölz-Complex. All the samples consist of low-grade metapelite. Detrital zircon grains from pelitic (EA09) and psammitic (SP02) samples in the Ennstal Phyllite Zone were analyzed by laser ablation-inductively coupled plasma- mass spectrometry. In both samples the youngest zircon population yielded dates around 625 Ma, with smaller peaks at ~1000, 2000, 2200 and between 2500 Ma and 2950 Ma. Raman thermometry on carbonaceous material and thermodynamic modelling for garnet-bearing samples in the Ennstal Phyllite Zone and Wölz-Complex do not show any significant difference in peak metamorphic temperature. By gathering the first age and PT data for this area, the correlation of the Ennstal Phyllite Zone with either the Wölz-Complex or the Greywacke Zone can be discussed.

CURVED GROWTH OF CLINOPYROXENE DENDRITES IN A BASALTIC ROCK-PSEUDOFULGURITE

Sutter, C.¹, Habler, G.¹, Abart, R.¹, Griffiths, T.¹, Ferrière, L.²

¹Department of Lithospheric Research, University of Vienna, Althanstraße 14, 1090 Vienna, Austria

²Natural History Museum Vienna, Burgring 7, 1010 Vienna, Austria

e-mail: christoph.sutter@univie.ac.at

Fulgurites are tubular structures generated from rock or soil by lightning strike. They are comprised of vesicular glass and relic as well as newly formed crystals. Pseudofulgurites are similar structures produced by anthropogenic electrical discharge events. During such events, energies of up to 30 MJ are transferred in a fraction of a second, and peak temperatures of 10^5 K are attained at heating rates of several thousand K per second (PASEK & PASEK, 2018). Typically, the target material melts and partially evaporates during such *flash heating*. Subsequently, the material cools very rapidly leading to solidification as glass and to crystallization under extreme undercooling. This results in mineral growth at conditions far from equilibrium, which may lead to peculiar phenomena such as dendritic and curved crystal growth. We studied a pseudofulgurite ($24 \times 15 \times 5$ mm 3) from Maharashtra, India, which was formed in a Deccan Trapp basalt as a result of an anthropogenic high-voltage discharge. The pseudofulgurite has a homogeneous glass matrix of basaltic composition with relics of plagioclase and quartz (partially converted into cristobalite), as well as newly grown clinopyroxene (CPx) with dendritic morphology. Both straight and curved CPx dendrites grew on plagioclase needles, which in turn grew epitaxially on plagioclase relics. The dendrites feature several hierarchical levels of branches and side branches. The main branches grow in the CPx [100] or CPx [001] direction and the first level side branches extend in (001). In the curved dendrites the CPx crystal lattice rotates about [010], while the [100] or [001] growth direction of the main branch is maintained. The lattice rotation is clockwise, when looking down the positive *b* axis. The twisted dendrite has a length up to 100 μm , the rotation is $>180^\circ$ with a radius of 20 μm . This corresponds to an average rotation of almost 2° per μm . Similarly curved growth of CPx dendrites was observed experimentally (HAMMER et al., 2010) and in more recent hitherto unpublished crystallization experiments. We hypothesize that the curved growth is related to the peculiar situation encountered during far from equilibrium crystal growth in a melt. Thereby the morphology of a growing crystal is determined by (*i*) diffusive heat and mass transport in the melt, which favors dendritic growth, and (*ii*) the tendency of the crystal to reduce interfacial energy, which suppresses dendritic morphology. The general tendency of dendrites to propagate towards the most pronounced compositional and thermal gradients would lead to dendritic growth with maximum morphological symmetry. This is, however, not compatible with the monoclinic structure of CPx. The curved growth probably reflects the compromise between growth along crystallographically preferred growth directions and dendrite growth with maximum morphological symmetry.

HAMMER, J.E., SHARP, T.G., WESSEL, P. (2010): Geology, 38, 367-370.

PASEK, M.A., PASEK, V.D. (2018): Miner. Petrol., 112, 185–198.

THE ‘LOUKASTEINE’ FROM THE MORAVIAN KARST – RADIAL CALCITE CONCRETIONS FORMED IN A PLASTIC GEL-LIKE CLAY MEDIUM

Talla, D.¹, Zwicker, J.¹, Peckmann, J.², Nagl, P.³, Filek, T.⁴, Losos, Z.⁵

¹Department of Mineralogy and Crystallography, University of Vienna, Althanstraße 14, 1090 Vienna, Austria

²Institute for Geology, Center for Earth System Science and Sustainability, University of Hamburg,
20146 Hamburg, Germany

³Department of Geosciences, University of Vienna, Althanstraße 14, 1090 Vienna, Austria

⁴Department of Palaeontology, University of Vienna, Althanstraße 14, 1090 Vienna, Austria

⁵Department of Geological Sciences, University of Brno, Kotlářská 2, 61137 Brno, Czech Republic
e-mail: dominik.talla@univie.ac.at

The so-called ‘Loukasteine’ are sedimentary carbonate concretions with radial internal structure occurring in red to whitish sandy clays of the lower Cretaceous Rudice strata in the Moravian karst, Czech Republic. The concretions exhibit disc-shaped morphologies, centred within and aligned parallel to pale sandier strata, with concretion ‘caps’ reaching into surrounding red kaoline clay; the latter apparently having acted as hydraulic seals (cf. SELLÉZ-MARTÍNEZ, 1996). As commonly observed for carbonate concretions, the host sediment, consisting of quartz, kaolinite and muscovite, is cemented by the calcite matrix of the concretions. Most concretions reveal a core without radial structure and well-preserved bedding of the host sediment, indicating pervasive growth due to lower supersaturation of pore fluids during the initial stages of concretion formation. The radial overgrowth, disrupting the original bedding of the host sediment, supposedly reflects an increase in carbonate supersaturation and crystallization pressure, forcing the parent sediment outwards, analogous to the formation conditions of similar concretions at Kettle Point, Canada (WINDER, 1974). Here, the increase of fluid supersaturation even led to the development of calcite crystals on the surface of some concretions. An increase in fluid supersaturation with respect to calcite is also suggested by the systematic increase in carbonate content from the core to the rim of the concretions (45 - 85 wt %, respectively).

Growth experiments in agar gels of varying strength using CaCl_2 and Na_2CO_3 as reagents led to the successful reproduction of radial calcite sphaerolites. Sphaerolites formed both during the initial stages of the reaction and at the end of the experiments, when supersaturation was low enough, with calcite crystals precipitating at high supersaturation.

It is a rare case to find carbonate concretions in such a soft host rock. This circumstance enabled a detailed study of external concretion topologies, even preserving fine striations due to slight variation in stiffness of the surrounding plastic material. The ‘Loukasteine’ represent a mineralogical peculiarity in the Moravian karst. Carbon and oxygen stable isotope analyses are currently underway to elucidate their potential biogenic origin.

SELLÉS-MARTÍNEZ, J. (1996): Earth-Sci. Rev., 41, 177-210.

WINDER, C.G. (1974): University of Western Ontario Faculty of Science Bulletin, 2, 13.

GEOTHERMOBAROMETRIE DER VARISZISCHEN EKLOGITE AUS DEM ÖTZTALKOMPLEX

Tropper, P.¹, Hackhofer, E.¹

¹Institut für Mineralogie und Petrographie, Universität Innsbruck, Innrain 52, 6020 Innsbruck, Österreich
e-mail: peter.tropper@uibk.ac.at

Diese Untersuchung beschäftigt sich mit der Geothermobarometrie, sowie mit der mineralchemischen Charakterisierung von variszischen Eklogiten im Ötztal-Stubai-Kristallin, aus den Lokalitäten Flauerlinger Alm bei Flauerling in der Nähe von Telfs, Längenfeld im Ötztal und Verpeiltal östlich von Feichten im Kaunertal. Die geothermobarometrischen Untersuchungen wurden mittels Granat-Klinopyroxen-Geothermometrie und Thermocalc v.3.21 Average P-T Methode durchgeführt.

Die Eklogite an der Flauerlinger Alm sind durch die Paragenese von Granat + Omphazit + Amphibol + Quarz + Rutil + Klinozoisit + Sympelktit charakterisiert. Dabei repräsentieren die Sympelktite die retrograden Umwandlungen von Omphazit zu Albit, Diopsid und Amphibol. Die Eklogite aus Längenfeld sind charakterisiert durch die Paragenese von Granat + Omphazit + Amphibol + Quarz + Klinozoisit + Kyanit + Sympelktit. Die Eklogite aus Verpei sind charakterisiert durch die Paragenese Granat + Omphazit + Amphibol + Rutil + Quarz + Klinozoisit + Sympelktit. Auch hier erkennt man wieder, dass die Omphazite und auch die Amphibole als Einschlüsse in großen Granatkörnern vorkommen. Die Matrix ist bei diesen Eklogiten völlig symplektitisiert, mit einzeln vorkommenden Omphaziten.

Im Durchschnitt haben die Granate eine Zusammensetzung von etwa 50 % Almandin, 25% Pyrop und 25 % Grossular, die Omphazite bestehen zu etwa gleichen Teilen aus Jadeit und Diopsid-Hedenbergit, mit einer z.T relativ hohen Ägirin-Komponente (Flauerlinger Alm). Bei den Amphiboleinschlüssen in Granat handelt es sich um Taramite, Katophorite, Pargasite (bzw. Ferro-Pargasite) und Sadanagaite. Die retrograd gebildeten Amphibole sind ausschließlich Pargasite. Die Ergebnisse der Granat-Klinopyroxen-Geothermometrie ergaben Werte von 654 ± 37 °C, 597 ± 47 °C und 642 ± 62 °C, jeweils für Flauerling, Verpei und Längenfeld. Unter der Annahme dass $a(\text{H}_2\text{O}) = 1$ ergaben sich für die Average P-T Berechnungen mittlere P-T Bedingungen von 639 ± 32 °C, 21.3 ± 1.9 kbar für Flauerling, 638 ± 28 °C, 23.2 ± 1.6 kbar für Längenfeld und 665 ± 24 °C, 19.3 ± 1.3 kbar für Verpei. Da die P-a(H₂O) Berechnungen ergaben dass $a(\text{H}_2\text{O})$ signifikant von 1 abweicht, stellen diese P-T Bedingungen ein oberes Limit dar.

Betrachtet man die mineralchemischen Daten und die P-T Ergebnisse so kann man vermuten dass die Längenfelder Eklogite im Vergleich zu den Eklogiten von Verpei tiefere Krustenanteile darstellen. Die Eklogite der Flauerlinger Alm liegen hingegen isoliert vor, wobei keine näheren tektonischen Beziehungen zu den beiden anderen Eklogitvorkommen hergestellt werden können. Allenfalls könnten sie auch im Zuge der eoaalpinen Orogenese nach Norden transportiert worden sein.

LOOKING INSIDE EARLY BRONZE AGE SMELTING REMAINS USING MICRO-COMPUTERTOMOGRAPHY

Tropper, P.¹, Kronenbergs, L.¹, Piccolruaz, M.¹, Degenhart, G.², Angerer, T.¹, Keil, J.³

¹Institut für Mineralogie und Petrographie, Universität Innsbruck, Innrain 52, 6020 Innsbruck, Österreich

²Department Radiologie, Medizinische Universität Innsbruck, Anichstraße 35, 6020 Innsbruck, Österreich

³Institut für Archäologie, Universität Innsbruck, Langer Weg 11, 6020 Innsbruck, Österreich

e-mail: peter.tropper@uibk.ac.at

This project deals with the mineralogical and micro-computertomographic (μ -CT) investigation of Early Bronze Age metallurgical remains (slag-tempered ceramics, slag-adherent crucible fragment) from the Buchberg site near Wiesing in the Lower Inn Valley. This archaeological site represents one of the earliest Cu-smelting sites in the Tyrol. The samples were investigated using thin-section microscopy, micro-X-ray fluorescence (μ XRF) as well as electron-probe microanalysis (EPMA) and two fragments were also investigated using μ -CT-analyses. Surprisingly the mineralogical results of the slag-tempered ceramic fragments yield two different sorts of copper such as Cu-Sb-As and Cu-Fe. Also, cassiterite was discovered in a slag temper fragment – until now the use of cassiterite was thought to have begun later as well.

In the crucible sample three different areas were observed based on mineralogical and chemical data: The first area (A) is unmelted and consists mainly of clay minerals and different tempering components. The second area (B) was melted and thus consists of a glass matrix and again temper components. The third area (C) represents the slag crust and consists mainly of high-density metals, clinopyroxenes and a glass matrix. μ XRF reveals an increase in Cu, As, P, and Sb and a decrease in Si from area A (core of the crucible fragment) to area C (slagged rim of the fragment).

The investigations using μ -CT allow the 3-D spatial distribution of high-density particles in the slag temper of the ceramic (Cu-Sb-As- and Cu-Fe-droplets) and crucible (Fe-Sb-Cu-Zn-O phases) fragments. Based upon these data it was possible to calculate the metal and the pore content of the slag crust. These data can then be used for further calculations regarding the efficiency of the Cu-smelting process.

Finally, the results clearly show that the Early Bronze Age ceramics were slag tempered and the slag fragments show that ore minerals used for copper smelting were mostly fahlore-group minerals. The occurrence of cassiterite in one of these Early Bronze Age slag fragments is still puzzling. Moreover, the results show that different additives were used in the Cu-smelting process such as slags, dolomite, quartz, and possibly bone material.

RUTILE PETROCHRONOLOGY AND GEOTHERMOBAROMETRY OF
EO-ARCHEAN METASEDIMENTS FROM
NORTHERN QUEBEC (NUVVUAGITTUQ AND UKALIQ SUPRACRUSTAL BELTS)

Tropper, P.¹, Mojzsis, S.J.², Schmitt, A.K.³

¹ Institute of Mineralogy and Petrography, University of Innsbruck, Innrain 52, 6020 Innsbruck, Austria

² Department of Geological Sciences, University of Colorado, UCB 399, Boulder, CO 80309-0399, USA

³ Institute of Geosciences, Heidelberg University, Im Neuenheimer Feld 236, 69120 Heidelberg, Germany
e-mail: peter.tropper@uibk.ac.at

The world's oldest rocks of demonstrable volcano-sedimentary origin comprise the Archean "supracrustal belts", in which they occur as variably deformed enclaves within ancient metamorphosed granite-granitoid gneiss terranes. The Inukjuak Domain in northern Québec is part of the Archean Minto Block in the northwestern Superior Province of Canada. Eoarchean (ca. 3800-3780 Ma) rocks of the Nuvvuagittuq supracrustal belt (NSB) and the Ukaliq supracrustal belt (USB) are the best known of numerous supracrustal enclaves within this domain. An Eoarchean metamorphic episode has been deduced from zircon depth-profiles, recorded at 3.62 Ga. A Neoarchean event was discerned based on dating of metamorphic zircon, garnet rutile and monazite and yielded $^{207}\text{Pb}/^{206}\text{Pb}$ and Sm/Nd ages ranging from 2.8 Ga to 2.5 Ga. The aim of this study was to provide geothermobarometric constraint on this Neoarchean metamorphic event in the NSB and USB by applying multi-equilibrium geothermobarometry (average PT approach), pseudosection modelling (DOMINO-Theriak) and Zr-in-rutile geothermometry. Two samples are quartz-biotite schists with the mineral assemblage garnet + biotite + muscovite + rutile + quartz \pm plagioclase \pm staurolite \pm kyanite. All samples show extensive retrogression under greenschist-facies metamorphic conditions. The average PT calculations (H_2O -free calculations only) yielded P - T conditions of 590 ± 95 °C and 0.5 ± 0.1 GPa and 610 ± 70 °C and 0.56 ± 0.2 GPa. Pseudosection modelling yielded similar P - T conditions based on the occurrence of garnet + cordierite + biotite. Zr-in-rutile geothermometry yielded 600 ± 30 °C.

From the USB, only one sample, a quartzite interpreted as a quartz-pebble metaconglomerate could be used. The main mineral assemblage is anthophyllite + muscovite + quartz + rutile + zircon. Owing to the pervasive greenschist-facies retrogression of the sample, it was not possible to constrain P - T conditions using phase equilibrium calculations; however, the Zr-in-rutile geothermometer provides a tight constraint on T . Zr contents of rutile range from 407 ppm to 914 ppm and yielded T of 660-730 °C at an assumed pressure of 0.6 GPa. Ion microprobe U-Pb dating of rutile from this sample yielded ages of 2500-2600 Ma, which correlate well with the youngest zircon ages from this sample, consistent with the lower closure T for Zr diffusion in rutile (<600 °C).

The rutile U-Pb ages combined with geothermobarometry show that Neoarchean metamorphism reached upper amphibolite-facies conditions (580-670 °C) in these supracrustal rocks in the northwestern Superior Province of Canada in accordance with previous T estimates and U-Pb zircon ages.

**MINERALOGICAL AND GEOCHEMICAL CHARACTERIZATION OF THE
MAJOR WASTE DUMP OF THE FORMER As-Sb-Cr MINE AT
LOJANE, NORTH MACEDONIA**

Uiblein, S.¹, Đorđević, T.¹, Kolitsch, U.^{2,1}, Nagl, P.³, Drahota, P.⁴, Mihaljević, M.⁴,
Tasev, G.⁵, Serafimovski, T.⁵

¹ Institut für Mineralogie und Kristallographie, Universität Wien, Althanstraße 14, 1090 Wien, Austria

² Mineralogisch-Petrographische Abteilung, Naturhistorisches Museum, Burgring 7, 1010 Wien, Austria

³ Department of Lithospheric Research, Universität Wien, Althanstraße 14, 1090 Wien, Austria

⁴ Faculty of Science, Charles University, Albertov 6, 128 43 Prague 2, Czech Republic

⁵ Department of Mineral Deposits, University “Goce Delčev”-Štip, Goce Delčev 89, 2000 Štip, North Macedonia
e-mail: stefan.uiblein@gmail.com

The As-Sb-Cr mine near Lojane, North Macedonia operated from 1923 to 1979. Despite high concentration of toxic pollutants (As, Sb, Ni), the mine wastes were abandoned without taking any precautions. We present results of the mineralogical and geochemical investigations of a vertical profile (1.50 m) in the center of the major waste dump, located adjacent to a creek. Along the sampled profile (six samples extracted at every 20 cm), the total chemical composition (XRF analyses) is relatively constant for Cr (1771-2915 ppm) and Ni (1718-2959 ppm). For As (10127-48524 ppm) and Sb (4660-12380 ppm), the variations are considerably larger. They are mainly dependent on the amount of the major ore minerals (realgar, stibnite) in the samples. For As, Sb, and Ni, the total concentration correlates with changing sampling level and is lowest in the sample taken next to the surface.

The mineralogy is dominated by quartz, carbonates (dolomite, magnesite), serpentine minerals (lizardite), and layer silicates. The main primary minerals are realgar, stibnite, and Mg-rich chromite. Minor greigite, pyrite, vaesite, violarite, and gersdorffite have also been confirmed. The pH values of the mine waste samples are neutral (6.5-7.7) due to the carbonate buffering that is slowing down the weathering of the sulfides. Chemical extractions in 1 M HCl showed that 20-90 % of As, 10-30 % of Sb, 40-60 % of Ni, and <5 % of Cr was recovered from secondary mineral phases. Mobile fractions were significantly lower (<1.6 % of Sb, <0.8 % of As, <0.4 % of Ni, and <0.002 % of Cr) showing that Cr is almost immobile.

SEM-EDX measurements and Raman spectroscopy showed that the most abundant secondary phases are various arsenates, Fe-oxides, Fe-oxy-hydroxides (FOH), and roméite-group antimonates (RGA). Most of them are fine-grained, more or less poorly crystalline, and inhomogeneous. The FOH contain significant amounts of As (up to 11 at.%), Sb (up to 1.5 at.%), and Ni (up to 1.2 at.%). The major arsenate is scorodite followed by hörnesite and annabergite. The RGA are sinks of Sb (up to 19 at.%) and As (up to 7 at.%).

The mildly oxidizing and temporarily wet conditions under neutral pH indicate that slow weathering of the sulphide phases will continue. Under the present conditions, the confirmed secondary minerals are not ultimate sinks. In particular, As and to a lesser extent Ni and Sb could be re-released into the environment. Therefore, the leaching of contaminants into the groundwater will remain of the highest concern in the future.

This work was supported by the Austrian Science Fund (FWF) [grant number P 30900-N28 to T. Đorđević].

REVEALING THE MINERALOGICAL REASONS FOR DIFFERENCES IN THE LEACHING BEHAVIOUR OF ELECTRIC ARC FURNACE SLAGS

Vollprecht, D.¹, Neuhold, S.¹, Sammer, T.¹, Sorger, C.², Gronen, L.³, Sokol, A.³,
Algermissen, D.³, Schintlmeister, A.⁴, Raith, J.G.¹

¹Montanuniversität Leoben, Franz-Josef-Straße 18, 8700 Leoben, Austria

²Stahl- und Walzwerk Marienhütte GmbH, Südbahnstraße 11, 8020 Graz, Austria

³FEhS-Institut für Baustoffforschung e.V., Bliersheimer Straße 62, 47229 Duisburg, Germany

⁴University of Vienna, Althanstraße 14, 1090 Vienna, Austria

e-mail: daniel.vollprecht@unileoben.ac.at

The mineralogy and leachability of electric arc furnace (EAF) slags has been studied in the last years (NEUHOLD et al., 2019). For a specific EAF slag it has been demonstrated that the leaching of vanadium can be significantly decreased by increasing the SiO₂/FeO ratio by liquid slag treatment which has been explained by the formation of melilite at the expense of wuestite and the subsequent hydration of melilite yielding adsorption sites for vanadium released from its primary spinel host phase (NEUHOLD et al., 2020, SAMMER et al., 2019). However, several research questions such as the mineralogical bonding of fluorine and molybdenum as well as the transferability of the findings regarding mineralogical composition and vanadium leachability could not be answered yet. Therefore, within this study (MiLeSlag 2.0, FFG Bridge, 871269) two novel findings are presented:

- (1) NanoSIMS was applied to identify the mineralogical bonding of fluorine and molybdenum and succeeded in proving the bonding of the former element to spinels and wuestite but failed in case of the latter due to several mass interferences.
- (2) 20 EAF slag samples which were identified as outliers with respect to the total or leachable contents of chromium, vanadium, molybdenum, or fluorine, were investigated in detail with respect to their chemical (XRF, ICP-MS, IC after pyrohydrolytic digestion for fluorine) and mineralogical (XRD) composition. The chemical composition of present mineral phases (EPMA) and the pH-dependent leaching (EN 14429, ICP-MS & IC) were investigated to understand the elemental distribution. Based on this dataset the mechanisms controlling the leaching were modelled using LeachXSTM/Orchestra.

No consistent correlation between distinct chemical or mineralogical features and the leachability of a specific chemical element could be found, i.e. the previously observed inverse correlation between SiO₂/FeO ratio and vanadium leaching seems not to be generally valid. Despite this fact, increasing the SiO₂/FeO ratio in the liquid slag still had the desired effects of decreasing the leachability of four different EAF slags not only of vanadium, but also of molybdenum and fluorine, although the reasons for this are not yet completely understood.

NEUHOLD, S., VAN ZOMEREN, A., DIJKSTRA, J., VAN DER SLOOT, H., DRISSEN, P., ALGERMISSSEN, D., MUDERSBACH, D., SCHÜLER, S., GRIESSACHER, T., RAITH, J., POMBERGER, R., VOLLPRECHT, D. (2019): Minerals, 9, 525, 1-19.

NEUHOLD, S., ALGERMISSSEN, D., DRISSEN, P., ADAMCZYK, B., PRESOLY, P., SEDLAZECK, K.P., SCHENK, J., RAITH, J., POMBERGER, R., VOLLPRECHT, D. (2020): Applied Sci., 10, 2549, 1-17.

SAMMER, T., NEUHOLD, S., VOLLPRECHT, D. (2019): Mitt. Österr. Miner. Ges., 65, 78.

DIE MÖGLICHKEITEN VON MIKRO-COMPUTERTOMOGRAPHIE (μ -CT) AN KORRODIERTEN EISENNÄGELN

Wagner, S.¹, Degenhart, G.², Tropper, P.¹, Töchterle, U.³

¹Institut für Mineralogie und Petrographie, Universität Innsbruck, Innrain 52, 6020 Innsbruck, Österreich

²Department Radiologie, Medizinische Universität Innsbruck, Anichstraße 35, 6020 Innsbruck, Österreich

³Institut für Archäologie, Universität Innsbruck, Langer Weg 11, 6020 Innsbruck, Österreich

e-mail: simon.wagner@student.uibk.ac.at

Eines der größten Probleme der Konservierung- und Restaurierungswissenschaften in der Archäologie stellt der Korrosionsprozess von Eisenobjekten dar. Ausgelöst wird dieser Prozess unter anderem durch den Wechsel der Umweltbedingungen sobald das Objekt von Archäologen freigelegt wird. Durch Redoxprozesse bildet sich an der Metalloberfläche aus dem elementaren Eisen zweiwertiges (Fe^{2+}) und dreiwertiges Eisen (Fe^{3+}). Zum besseren Verständnis der Prozesse wurde mittels Computertomographie die räumliche Verteilung der einzelnen Korrosionsprodukte genauer untersucht. Das bildgebende Verfahren der Computertomographie zählt eigentlich zu einer der wichtigsten radiologischen Diagnosemethoden in der Medizin. Es handelt sich dabei um tomographische Röntgentechnik wobei der Röntgenstrahl durch eine Sammellinse zu einem dünnen Fächer geformt, beim Eintritt in ein Material abgeschwächt und anschließend mithilfe von Detektoren erfasst wird. Mittels geeigneter Computersoftware kann diese Schwächung bildgebend mit unterschiedlichen Grauwerten verarbeitet und dargestellt werden. Die μ -Computertomographie wurde am vivaCT 40 der Firma Scanco Medical AG durchgeführt. Mit einer Auflösung von 10,5 - 76 μ m können damit relativ feine Strukturen aufgelöst und bildlich dargestellt werden. Die computertomographischen Untersuchungen wurden an einem archäologischen Nagel durchgeführt, der in Frischhaltefolie eingewickelt und samt umgebendem Erdreich geborgen wurde. Dadurch sollte es auch möglich sein die gesamte Abfolge der unterschiedlichen Korrosionsschichten beobachten zu können und dadurch ein möglichst vollständiges Korrosionsbild daraus zu generieren. Mittels festgelegter Dichteintervalle ist es möglich, eine räumliche Verteilung des jeweiligen Dichtebereichs zu generieren und dadurch die räumliche Anordnung der unterschiedlichen Korrosionsbereiche zu visualisieren. Es konnten vier markante Korrosionsbereiche innerhalb des Nagels identifiziert werden, die auch mittels Elektronenstrahlmikrosondenanalysen verifiziert werden konnten:

- Reliktisches Eisen: Überreste des ursprünglichen Nagels, die nur noch skelettartig ausgebildet sind. Dieser Bereich entspricht dabei dem „metallic substrate“.
- Hochdichte Korrosionsprodukte (Magnetit, Maghemit): Teile dieses Dichtebereichs findet sich an der Stelle des ehemaligen Nagels, teilweise aber auch über dessen ehemalige Oberfläche hinausgreifend (= dense product layer).
- Niedrigdichte Korrosionsprodukte: Dort treten vor allem Korrosionsprodukte (Fe-hydroxide) auf, die eine deutlich niedrigere Dichte aufweisen. - Eine bereits beginnende Vermischung mit dem umgebenden Boden kann ebenfalls beobachtet werden.
- Anhaftendes Bodenmaterial: Dieser Bereich ist durch die geringsten Dichten gekennzeichnet und besteht größtenteils aus Bodenpartikeln (Muskovit, Feldspat, Quarz). Sowohl die niedrigdichten Korrosionsprodukte und das anhaftende Bodenmaterial entsprechen dem sog. „transformed medium“.

POLYPHASE Co-Cu MINERALIZATION IN THE KUNENE REGION, NAMIBIA

Wallner, D.¹, Bertrandsson Erlandsson, V.¹, Bernegger, S.¹, Raith, J.G.¹, Rantitsch, G.¹,
Melcher, F.¹, Ellmies, R.²

¹Montanuniversität Leoben, Leoben, Peter Tunner Straße 5, 8700 Leoben, Austria

²Gecko Namibia, Einstein 10, 8912 Swakopmund, Namibia

e-mail: daniela.wallner@unileoben.ac.at

Cobalt is a critical metal that is crucial for the future energy transition. Almost two-thirds of the global production (REICHL & SCHATZ, 2021) come from politically unstable countries (DRC, Zambia) in central Africa. Recently discovered sediment-hosted Co-Cu mineralization in the Dolostone Ore Formation (DOF) in the Kunene region, northern Namibia, may become an attractive alternative to these countries. The DOF is hosted within the Neoproterozoic Ombombo Subgroup of the Kaoko Belt in northern Namibia (MILLER, 2008). It has been traced for approximately 30 km in EW direction and dips ca. 60 °N with <1 m to 14 m thickness. The main lithologies are low-grade metamorphosed sediments including pelites, marls and carbonate rocks. The most abundant ore minerals are pyrite, pyrrhotite, chalcopyrite, sphalerite, galena, members of the linnaeite-siegenite series, and cobaltite.

The ore minerals can be found in several mineralization styles: (1) irregular to clustered disseminations, (2) nodules and concretions, (3) synmetamorphic mineralization within pressure shadows, (4) veinlet-hosted mineralization of different generations, and (5) "DOF events", which are distinctive ductile and/or brittle structures showing a complex zoned texture. These mineralization styles can be assigned to four mineralization stages mainly related to the Damaran orogeny (560-550 Ma): Stage I) early stage with frambooidal pyrite, Stage IIa) Co-Fe-Zn-Pb stage with pyrite, pyrrhotite, members of the linnaeite-siegenite series (linnaeite), sphalerite, chalcopyrite, and galena, Stage IIb) Cu-Zn-Fe stage with pyrite, pyrrhotite, cobaltite, linnaeite, sphalerite, and chalcopyrite, Stage III) Cu-Pb-Zn stage with chalcopyrite, galena, sphalerite, and linnaeite, and Stage IV) late stage with jaipurite, members of the linnaeite-violarite series, covellite, pyrite, and magnetite.

Preliminary LA-ICP-MS analyses of sphalerite and chalcopyrite support these paragenetic observations by indicating distinct differences in trace element geochemistry. Sphalerite and chalcopyrite from veins and pressure shadows are significantly enriched in elements such as Ni, Se (and Cd in sphalerite), whilst being depleted in Co, compared to sphalerite and chalcopyrite from the other mineralization styles. Pyrite geochemistry show more complex variations; strongly supporting a multi-stage mineralization model for the DOF.

Raman spectroscopy of carbonaceous material (LÜNSDORF et al., 2017) indicate a formation temperature of 345 ± 32 °C. This overlaps with the regional metamorphic temperature but may indicate either a slightly lower temperature overprint or a higher stress regime in the DOF horizon compared to the surrounding host rock.

LÜNSDORF, N. K., DUNKL, I., SCHMIDT, B. C., RANTITSCH, G., von EYNATTEN, H. (2017): Geostand. Geoanal. Res., 41, 593-612.

MILLER, R. McG. (2008): Geol. Surv., 2nd ed. Windhoek, Namibia.

REICHL, C., SCHATZ, M. (2021): Federal Ministry of Agriculture, Regions and Tourism, 36, Vienna, Austria.

**EVALUATION OF GREEN SCALING INHIBITORS BY
THERMODYNAMIC RATE MODELING**

Wedenig, M.¹, Boch, R.^{1,2}, Leis, A.³, Wagner, H.⁴, Dietzel, M.¹

¹Institute of Applied Geosciences, Graz University of Technology, Rechbauerstrasse 12, 8010 Graz, Austria

²Geoconsult ZT GmbH, Wissenspark Salzburg Urstein, Urstein Süd 13, 5412 Puch bei Hallein, Austria

³JR-AquaConSol GmbH, Steyrergasse 21, 8010 Graz, Austria

⁴ÖBB-Infrastruktur-AG, Streckenmanagement & Anlagenentwicklung, Fachbereich Bautechnik & Tunnelbau,
Europaplatz 2, 8020 Graz, Austria

e-mail: michael.wedenig@tugraz.at

Green technologies are on the rise and not stopping at the gate of tunnel construction sites. So called “green inhibitors” (GI) are eco-friendly, biodegradable organic molecules, which are already applied in many technical fields (oil/gas-industry, industrial and potable water treatment, ...) for scaling reduction (mainly CaCO₃ precipitation) and increasingly used in drainage systems of motor- and railway tunnels. Although, GI's are known to significantly decrease mineral precipitation out of an aqueous solution, their individual inhibition effects are less explored. Therefore, we investigated the functionality and efficiency of aspartic, maleic and acrylic GI products at dosages from 0.5 to 10 mg L⁻¹, using a newly developed rapid and compact test procedure. The GI performance is quantified by combining existing thermodynamic rate models for CO₂-flux and CaCO₃-precipitation. The results showed that (i) the GI performance is independent of the CO₂ degassing rates, (ii) the supersaturation of calcite reaches an upper limit approaching the solubility of amorphous calcium carbonate, and (iii) average efficiencies of 70% up to 100%, and (iv) a delay of crystal nucleation of 3 to 6 times – compared to the control test (no inhibitor) – are observed. Our results also reveal new insights into preferential CaCO₃ polymorph formation: aspartate is suggested to modulate calcite crystallites by serving as a template for predominant vaterite growth. The rate-model aided test procedure provides a compact and rapid tool to assess and quantify GI performances against CaCO₃-scaling to be properly selected and individually tuned.

HIGH-PRESSURE PHASE TRANSITION OF KIESERITE-TYPE $\text{CoSO}_4 \cdot \text{H}_2\text{O}$ AND COMPARATIVE COMPRESSION PROPERTIES OF ISOTYPIC COMPOUNDS $\text{MeSO}_4 \cdot \text{H}_2\text{O}$ ($\text{Me}^{2+} = \text{Mg}, \text{Fe}, \text{Ni}$)

Wildner, M.¹, Ende, M.¹, Meusburger, J.^{1,2}, Kunit, R.¹, Matzinger, P.¹, Talla, D.¹, Miletich, R.¹

¹Universität Wien, Institut für Mineralogie und Kristallographie, Althanstraße 14, 1090 Wien, Austria

²Camborne School of Mines, University of Exeter, Penryn TR10 9FE, Cornwall, UK

e-mail: manfred.wildner@univie.ac.at

The kieserite-type compound $\text{CoSO}_4 \cdot \text{H}_2\text{O}$ has been investigated under hydrostatic pressures up to 10.1 GPa in a diamond anvil cell using single-crystal X-ray diffraction and Raman spectroscopy. The monoclinic α -phase (space group $C2/c$, Fig. 1a) undergoes a second-order ferroelastic phase transition at $P_c = 2.40(3)$ GPa to a triclinic β -phase (s.g. $P\bar{1}$, Fig. 1b). Lattice elasticities derived from fitting third-order Birch-Murnaghan equations of state to the unit-cell volume data yield $V_0 = 354.20(6)$ Å³, $K_0 = 53.0(1.7)$ GPa, $K' = 5.7(1.8)$ for the α -phase and $V_0 = 355.9(8)$ Å³, $K_0 = 45.2(2.6)$ GPa, $K' = 6.6(6)$ for the β -phase.

The most obvious structural feature of the β -phase, and thus a possible driving mechanism of the phase transition, is a partial rearrangement in the hydrogen bonding system (Fig. 1a,b). However, a comparative analysis including the kieserite-type representatives of Mg, Fe and Ni investigated under pressure to date (MEUSBURGER et al., 2019, 2020; ENDE et al., 2020) suggests that the loss of the point symmetry 2 at the otherwise rather rigid SO_4 tetrahedron, allowing symmetrically unrestricted tetrahedral rotations and edge tiltings in the β -phase, could be the actual driving mechanism of the phase transition (Fig. 1b).

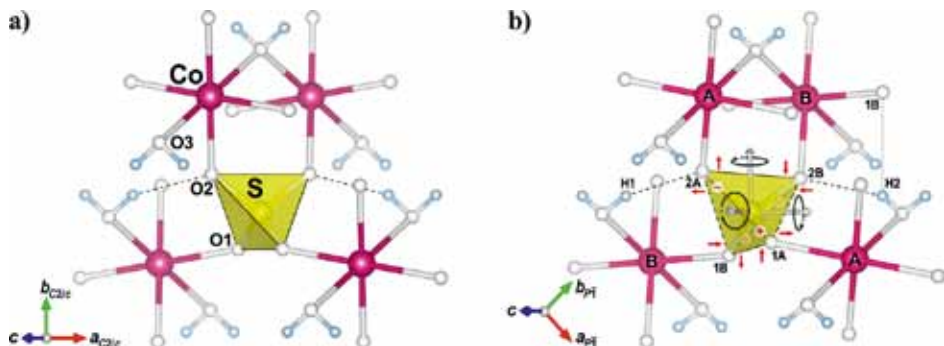


Figure 1. Fragments of the structures of (a) α - $\text{CoSO}_4 \cdot \text{H}_2\text{O}$ (at 10⁻⁴ GPa) and (b) β - $\text{CoSO}_4 \cdot \text{H}_2\text{O}$ (at 4.9 GPa). In (b) the direction of tetrahedral rotations and the sense of edge tiltings relative to the α -phase are indicated.

MEUSBURGER, J.M., ENDE, M., TALLA., D., WILDNER, M., MILETICH, R. (2019): J. Sol. State Chem., 277, 240-252.

MEUSBURGER, J.M., ENDE, M., MATZINGER, P., TALLA., D., MILETICH, R., WILDNER, M. (2020): Icarus, 336, 113459.

ENDE, M., KIRKKALA, T., LOITZENBAUER, M., TALLA., D., WILDNER, M., MILETICH, R. (2020): Inorg. Chem., 59, 6255-6266.